CANADIAN THESES

THÈSES CANADIENNES

NOTICE

The quality of this microfiche is heavily dependent upon the quality of the original thesis submitted for microfilming. Every effort has been made to ensure the highest quality of reproduction possible.

If pages are missing, contact the university which granted the degree.

Some pages may have indistinct print especially if the original pages were typed with a poor typewriter ribbon or if the university sent us an inferior photocopy.

Previously copyrighted materials (journal articles, published tests, etc.) are not filmed.

Reproduction in full or in part of this film is governed by the Canadian Copyright Act, R.S.C. 1970, c. C-30.

AVIS

La qualité de cette microfiche dépend grandement de la qualité de la thèse soumise au microfilmage. Nous avons tout fait pour assurer une qualité supérieure de reproduction.

S'il manque des pages, veuillez communiquer avec l'université qui a conféré le grade.

La qualité d'impression de certaines pages peut laisser à désirer, surtout si les pages originales ont été dactylographiées à l'aide d'un ruban usé ou si l'université nous a fait parvenir une photocopie de qualité inférieure.

Les documents qui font déjà l'objet d'un droit d'auteur (articles de revue, examens publiés, etc.) ne sont pas microfilmés.

La reproduction, même partielle, de ce microfilm est soumise à la Loi canadienne sur le droit d'auteur, SRC 1970, c. C-30.

THIS DISSERTATION HAS BEEN MICROFILMED EXACTLY AS RECEIVED

LA THÈSE A ÉTÉ MICROFILMÉE TELLE QUE NOUS L'AVONS REÇUE

Passive Earth Pressures Behind Retaining Walls For Layered Cohesionless Materials

Radu Solomon

A Thesis

In

The Department

Of

Civil Engineering

Presented in Partial Fulfillment of the Requirements
for the Degree of Master of Engineering at
Concordia University
Montréal, Québec, Canada

March 1986

ISBN 0-315-30603-3

ABSTRACT

Passive Earth Pressures Behind
Retaining Walls For Layered Cohesionless Materials

Radu Solomon

This thesis presents an experimental and theoretical study of the passive earth pressure exerted behind a retaining wall.

The soil was taken as homogeneous and as layered soil. The results are checked against available analytical methods and the proposed one.

The experimental data has compared well with the available theories for homogeneous soils. For the passive earth pressure for layered soil, a new theoretical model was developed and agreed well with the experimental data.

It was found that in the case of layered sand, for the case of a strong layer overlying a weak layer of sand, the value of the passive earth pressure is less than that for the homogeneous strong sand, while for the case of a weak layer overlying a strong layer of sand, the value of the passive earth pressure is very close to that of the homogeneous weak sand.

ACKNOWLEDGEMENTS

I wish to express my sincere gratitude to Dr. A.M. Hanna under whose direct supervision and able guidance the present investigative study has been carried out.

I am deeply indebted to Mr. Joseph Zilkha for his assistance to set-up the equipment and running it during the experiments.

Thanks to Nagib Gergis who helped with drawing charts and tables.

Finally, I am indebted to my wife Ioana and my parents for their constant encouragements.

TABLE OF CONTENTS

LIST OF SYMBOLS

τ	=	Shear Stress
c	=	Cohesion
σ	=	Normal Stress
ϕ	=	Angle of Internal Friction
P_p	=	Passive Earth Pressure
γ	=	Unit Weight of Soil
γ_w	=	Unit Weight of Water at 4^oC
δ	=	Angle of Friction of Sand against the Wall
e_{max}	=	Maximum Void Ratio
e_{min}	=	Minimum Void Ratio
e	=	Void Ratio of Soil Deposit
G	=	Specific Gravity of Solid Particles
H	=	Weight of Wall
k_p	=	Coefficient of Passive Earth Pressure
R.D.	=	Relative Density
W	=	Weight of Materials

P_f = Frictional Resistance Value

λ = Parameter Coefficient

r = Generating Radius of a Spiral

r_o = First Radius of the Spiral

θ = Angle of Spiral between First Radius of Spiral and the Line on which the Center of the Spiral lies

P_d, P_R = Passive Earth Pressure according to Rankine

R = Reaction of Forces

α_w = Angle between Tangent to the Spiral and the Horizontal at the Foot of the Retaining Wall

E = Horizontal Force on Slice of Soil

dE = Increment of Horizontal Force on Slice of Soil

X = Vertical Shear Force on Slice of Soil

dX = Increment of Vertical Shear Force on Slice of Soil

L_w = Arm of the Weight Force with Respect to the Origin of the Spiral

Ld = Arm of the Passive Earth Pressure according to Rankine with Respect to the Origin of the Spiral

Lp = Arm of the Passive Earth Pressure with Respect to the Origin of the Spiral

LIST OF FIGURES

Page

Page

LIST OF TABLES

CHAPTER 1

INTRODUCTION

1.1 Preface

Earth pressure problems have intrigued and challenged engineers for a very long time and they still occupy a place of high importance in the field of soil mechanics. Recently, another problem surfaced in this domain, that of layered soils. The problem of layered soils arises, for example, while building a retaining wall along the shores of a river, or when constructing a bridge whose abutments rest on one type of soil and backfill material is of a different density, like in Figure 1.1.

Due to the fact that the fill material cannot interact with the existing soil and therefore homogeneity for the material behind the wall cannot be achieved by duplication of the lower layer the problem is developing into a layered soil problem rather than an homogeneous one as it is presently treated.

1.2 Research Objectives

The objective of this thesis is to study the effect of layered soils on the passive earth pressure behind a retaining wall. Specifically:

a) to conduct model testing on a retaining wall,

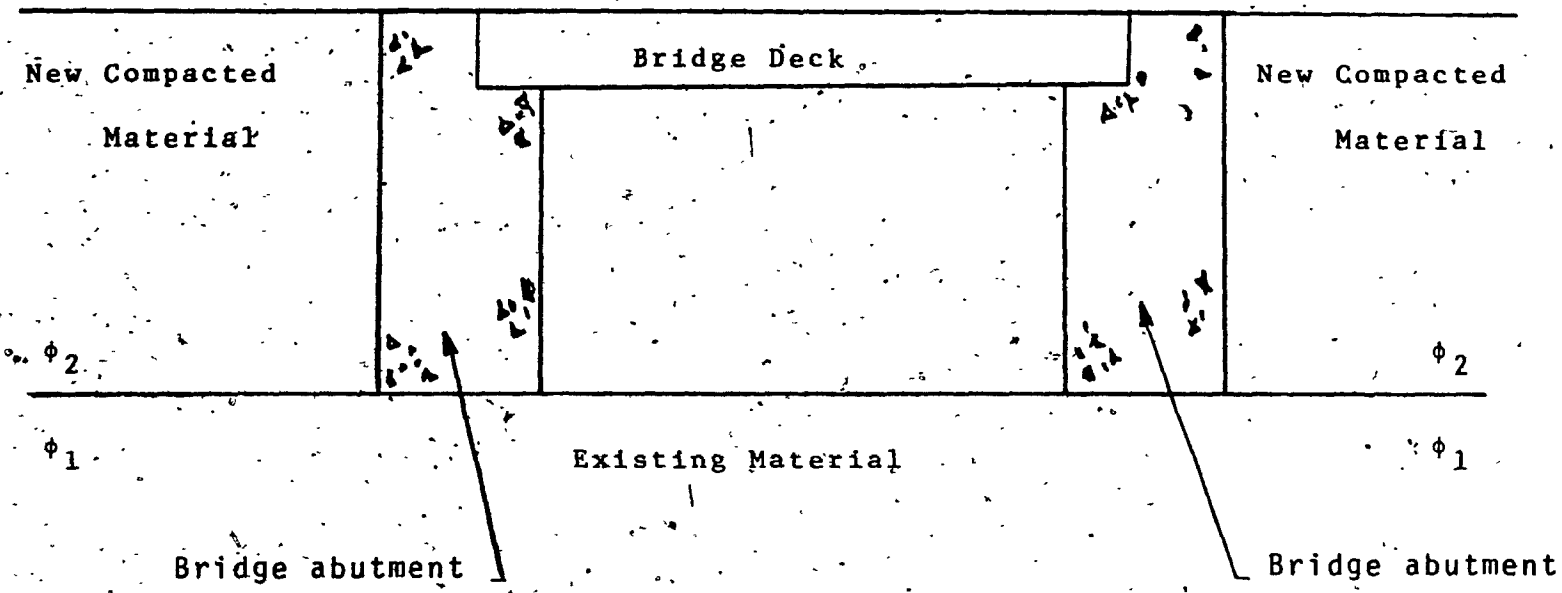

Figure 1.1: Bridge abutments resting on existing soil and retaining new soil

b) to compare the test results for the passive earth pressure for homogeneous sand with available theories for homogeneous sand,

c) to develop a new theoretical model for determining the passive earth pressure for the layered sand behind a retaining wall.

A review of the classical theories for passive earth pressure for homogeneous soils is given in Chapter 1.

A description of the test apparatus, the test procedure and the soil properties is given in Chapter 2. The test results are presented in Chapter 3. The analysis of results and the discussion is presented in Chapter 4 and conclusions are presented in Chapter 5.

1.3 LITERATURE REVIEW

1.3.1 General

The problem of earth pressures is of a long time nature, as people questioned the forces behind wall failures or other retaining structures from the times when they were building fortifications, temples, etc.

Of course, at the time the problem was not perceived as due to soil, but mostly due to the structure, and it was therefore reinforced many times more than needed, resulting in amazing structures such as walls 10 feet to 20 feet wide.

Later on, with the development of the exact sciences, the scolars started to examine the problem from the theoretical and experimental view and later, as data was gathered and exchanged, past experience began to play a role in the solving of the problem.

All the three approaches are continued nowadays and every year, there is at least one paper on the determination of earth pressures.

1.3.2 Historical Outlook

In 1720, Belidore, a French man, was the first to record the results of the experimental work he performed. He reached the conclusion that the surface of rupture behind a retaining wall was on a slope of 1:1. That was later modified by Mayniel, in 1808, to a slope of 2:4 to 3:1, even though the natural slope of the material was 1:1.

In 1776, Coulomb was the first to supply a mathematical relation for calculating the earth pressures. In 1785 Gauthey succeeded in measuring the earth pressures at five different depths showing that indeed the pressure was increasing with depth. He also managed to show that at a certain depth below the retaining structure, the earth pressure does not affect the retaining structure.

In 1857, Rankine found a mathematical solution using an entirely different approach than Coulomb. In 1905, in Germany, Müller-Breslau tried to check experimentally Coulomb's assumptions. He concluded that the point of application of the resultant was somewhere between 0.33 and

0.36 of the height of the wall, if there was no surcharge.

Since 1910, the development of the different theories of plasticity was emphasized by Saint Venant (1871), Von Mises (1913), Prandtl (1920, 1927), Nadai (1929) and Odquist (1934). These theories were generally developed for metals but were modified to extend to problems of earth pressures.

In 1927, Fellenius, assuming a circular rupture line was able to make a simple analysis for frictionless soil because the unknown stresses do not enter into the moment equation about the center of the circle. In 1935 and 1940, Rendulic succeeded in determining the general relation between the magnitude of the earth pressures on a smooth vertical wall and the location of the pressure center. Ohde in 1938 and 1948 derived the distribution of earth pressure on a retaining wall. In 1943, Peck found that for cohesive soils the distribution of the pressure was non-hydrostatic. In 1953 B. Hansen proposed a new method for calculation of earth pressures which is applicable to most problems in practical engineering. It was based on the equilibrium principle by which the unknown forces are determined by the statical equilibrium conditions of the structure and the soil mass.

Recently, many scientists and engineers have turned to monitoring actual field conditions and developing theories or amendments to existing theories based on the data collected.

A more indepth look at the main theories follows:

1.3.3 Coulomb's Theory

In 1776 Coulomb supplied for the first time a mathematical solution for the calculation of the earth pressures acting on a retaining structure. He based his analysis on the following assumptions:

- that the failure surface was a plane and
- that the thrust on the wall acted in some known direction.

After the above two assumptions are made, the resultant thrust on the wall could be determined by statics.

Coulomb's mathematical relation: $\tau = c+\sigma\tan\phi$

is also known as the law of shearing resistance.

The principle behind his method consists of considering an earth wedge bounded by the surface, the wall and a straight rupture line through the foot of the wall. By projecting all forces (acting upon this wedge) onto a line making an angle $\emptyset$ with the rupture line, he was able to obtain the critical failure plane, which yielded the minimum value of P_p (see Figure 1.2).

1.3.4 Rankine's Theory

In 1857, Rankine approached the earth pressure problem from an entirely different point of view. He considered the case of a semi-infinite cohesionless earth mass with a sloping surface and assumed the whole earth mass to be in a state of failure. Thereupon, he showed that the two systems of straight parallel lines, intersecting at angles

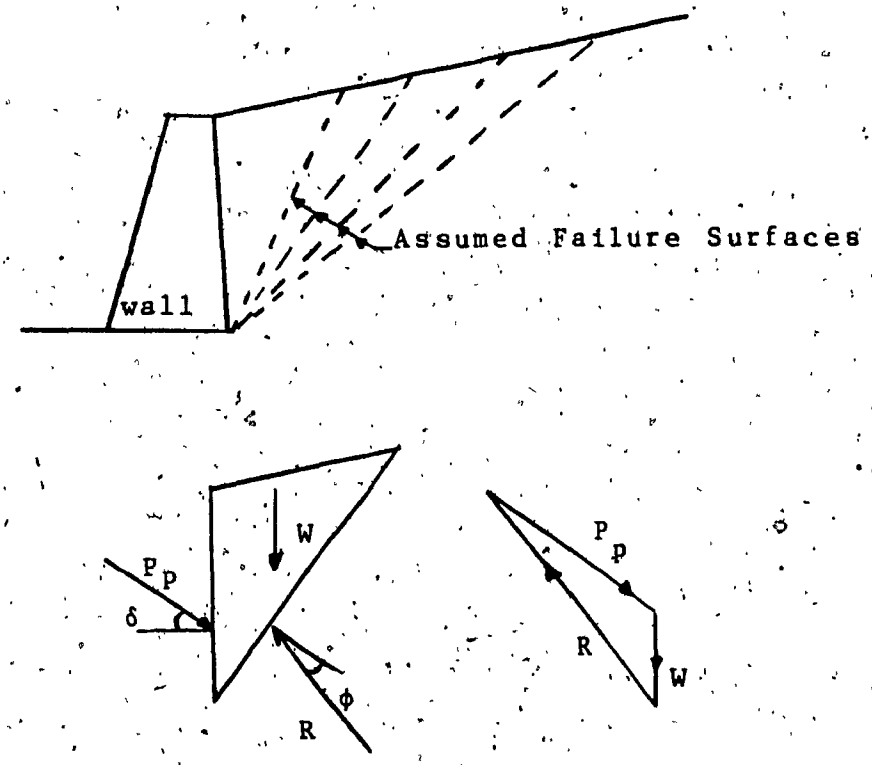

Figure 1.2: Passive earth pressure calculated using Coulomb's Method

of $90 \pm \phi$ formed the rupture line (see Figure 1.3).

On a smooth retaining wall, Rankine's passive earth pressure is

$$P_p = (1/2)\, k_p\, \gamma\, H^2,$$

where: $k_p = \tan^2 (45 + \phi/2)$

γ = Initial unit weight of the soil

H = Height of the wall

P_p = Passive force on the retaining wall

1.3.5 Terzaghi's Theory

In 1941 Terzaghi adopted an alternate method for predicting the passive earth pressure using Rendulic's logarithmic spiral as the surface of sliding. A moment equilibrium condition for the soil wedge in front of a wall was studied by taking the moment of all forces about the center of the logarithmic spiral. Utilizing a trial and error procedure, the rupture surface giving the minimum passive resistance was obtained (see Figure 1.4).

1.3.6 Recent Work

In the previously discussed earth pressure theories, the relationship between the direction of wall movement and the change in wall friction angles is rarely discussed.

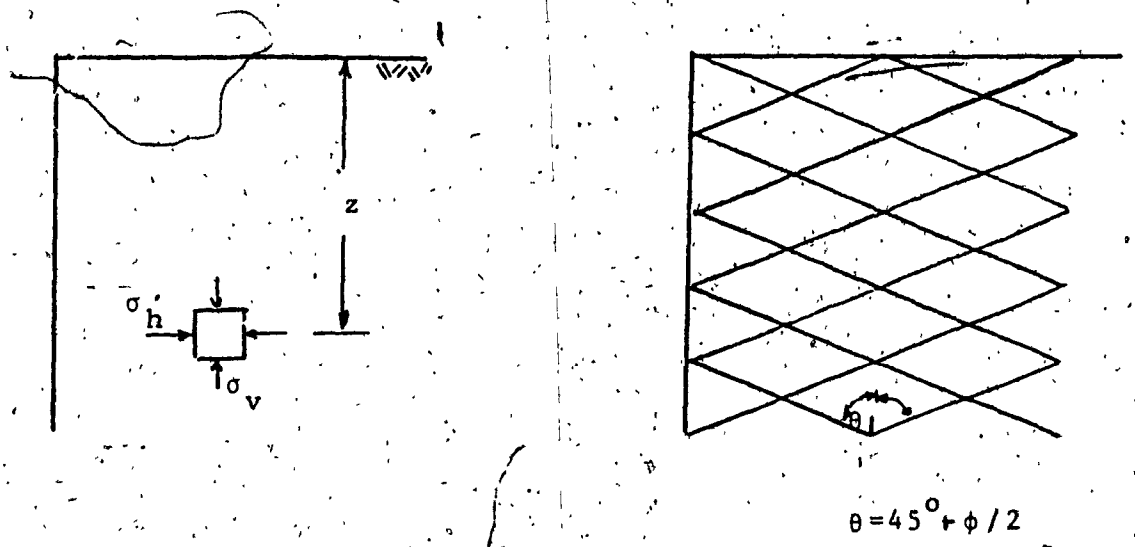

Figure 1.3: Passive Rankine State of Vertical Wall

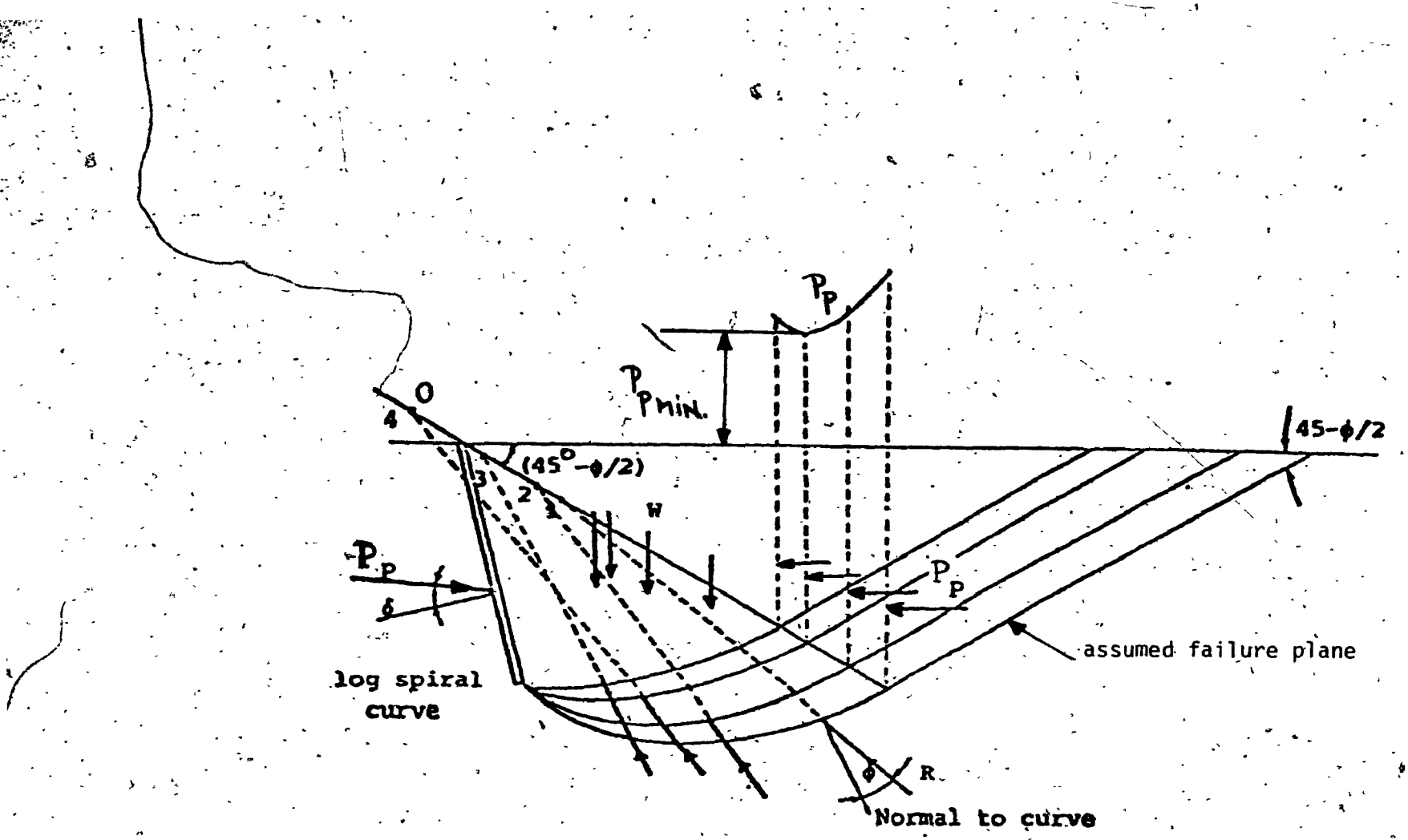

Figure 1.4: Passive Resistance by Logarithmic Spiral (Terzaghi,1948)

Caquot and Kérisel derived in 1948 solutions for the passive pressure acting on the face of a wall, showing that the wall friction angle δ depends on the direction of wall movement relative to the soil. The values of the passive earth pressure were obtained by integrating the differential equations governing the conditions of limiting equilibrium in a soil mass.

In 1975 Chen developed tables for passive pressure results by using limit analysis. By developing slip cone and velocity fields, the coefficients of passive pressure were calculated by equating the rate of work done (by external forces) to the rate of internal energy.

In spite of the common occurrence of the condition of layered soil, the subject was not really debated until late seventies. However no attempts were made to analyze a gravity retaining structure on layered soil.

The purpose of the present thesis is to present experimental and theoretical studies on the problem stated above.

CHAPTER 2

EXPERIMENTAL INVESTIGATION

2.1 General Description

The experimental set-up, as presented in Figure 2.1a was installed in the structural laboratory of Concordia University. The high ceiling was ideal for permitting the extension of the sand spreading support in the air above the holding tank in order to gain extra height. The entire apparatus was self supported and could be easily moved from one laboratory room to another.

The model tests were carried out with a duraluminum plate in a medium of sand. The purposes of these tests were:

(i) to verify the accuracy of the proposed theory for predicting passive earth pressures in layered cohesionless soils behind retaining walls.

(ii) to study the pressure distributions in the model retaining wall.

(iii) to study the effect of the layered sand on the passive earth pressure exerted on the retaining wall.

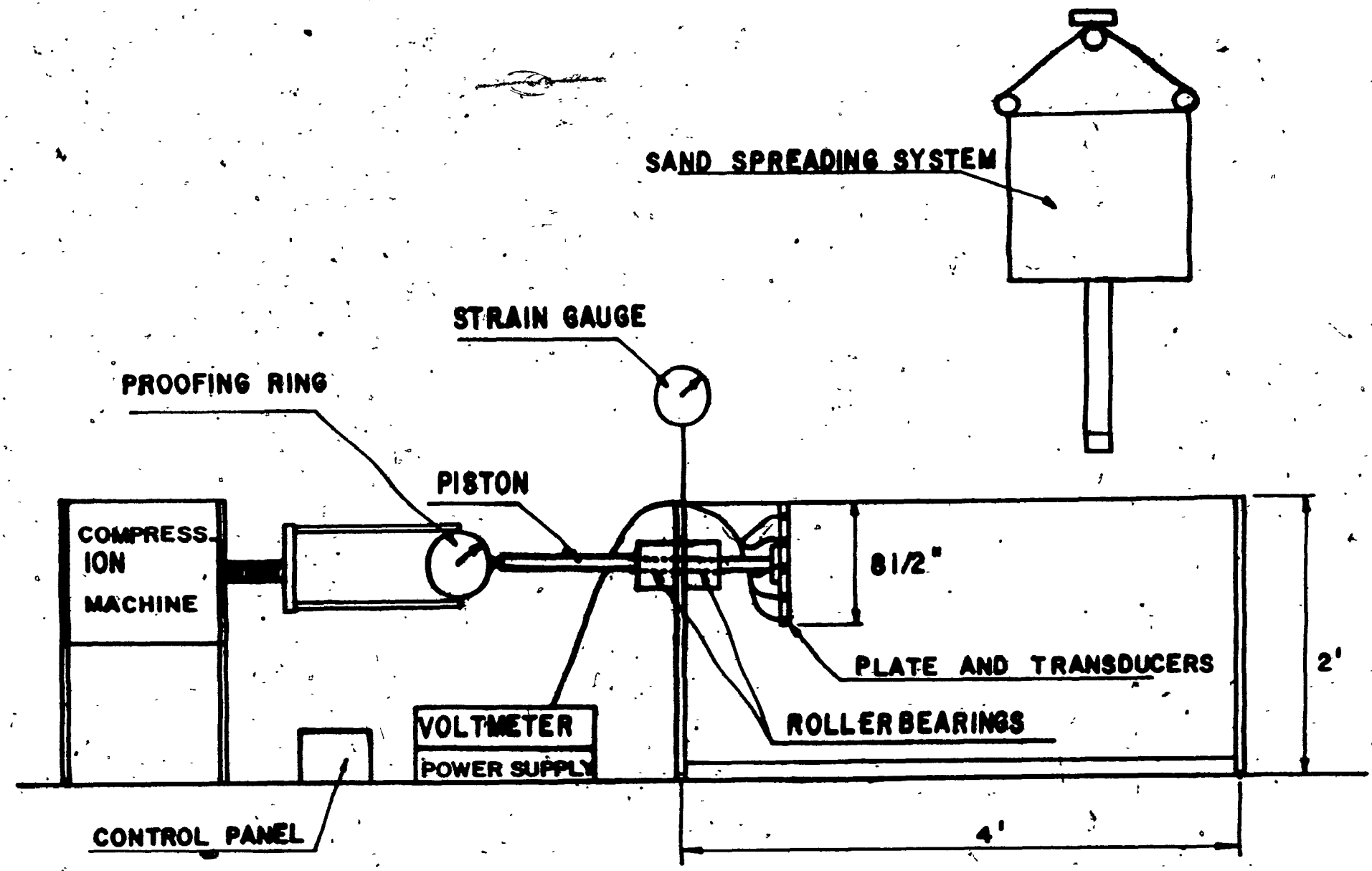

Figure 2.1 a: Sketch shows the experimental set-up

2.2 Experimental Set-up

2.2.1 Testing Tank

The apparatus is composed of a holding tank with sides made of plexiglass and ends and frame of steel (see Figure 2.1b). The plexiglass sides were reinforced with longitudinal metal angles after a first experiment showed that they deflect under the sand pressure. Inside the tank, a motor driven piston pushes a plate that simulates a vertical wall (see Figure 2.2). The piston was developed from an old compression test machine, taken apart and placed sideways in order to provide the driving force behind the plate. A multitude of gears was available that provided a wide selection of speeds for the piston, however only the slowest speed was used.

In order to measure the force by which the piston pushed the plate a proofing ring was installed between the piston and the plate. The plate, which is installed in the upper part of the tank is assuming the role of a retaining wall. The plate (see Figure 2.2), which is within the holding tank, is held horizontally and is fixed (would not rotate). The plate is installed at the end of a rod that is supported by two sets of roller bearings in order to minimize friction and to provide perfect horizontality.

Five pressure control points were chosen and pressure transducers were installed at those locations (see Figure 2.3), in order to monitor the pressure on the plate.

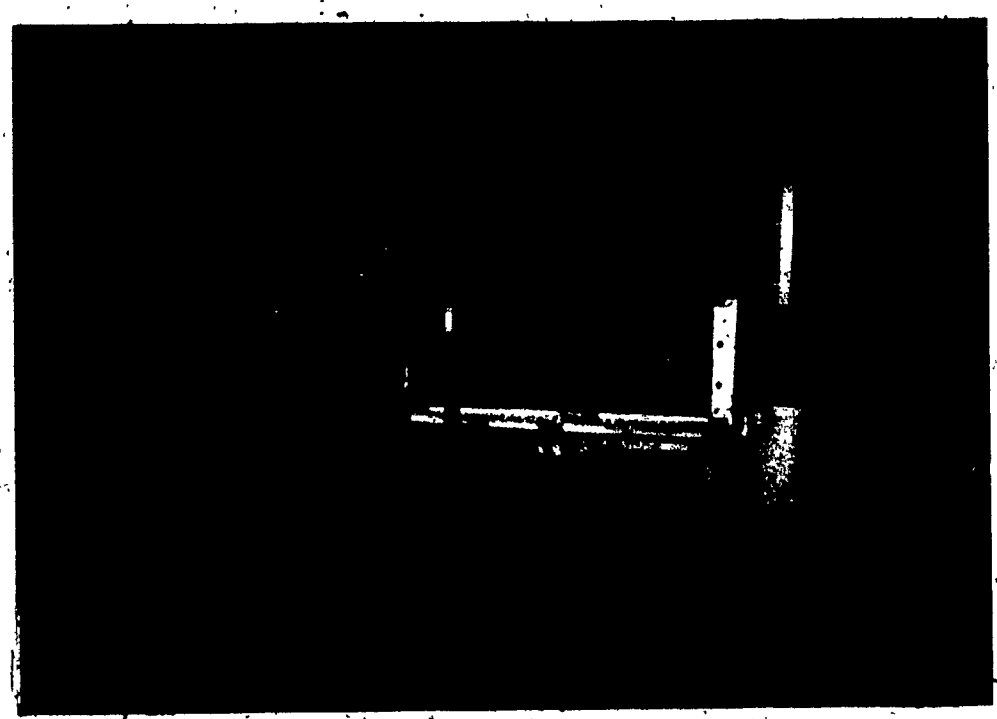

Figure 2.1b: Photographs show the experimental set-up

Figure 2.2: Photograph shows the plate and transducers

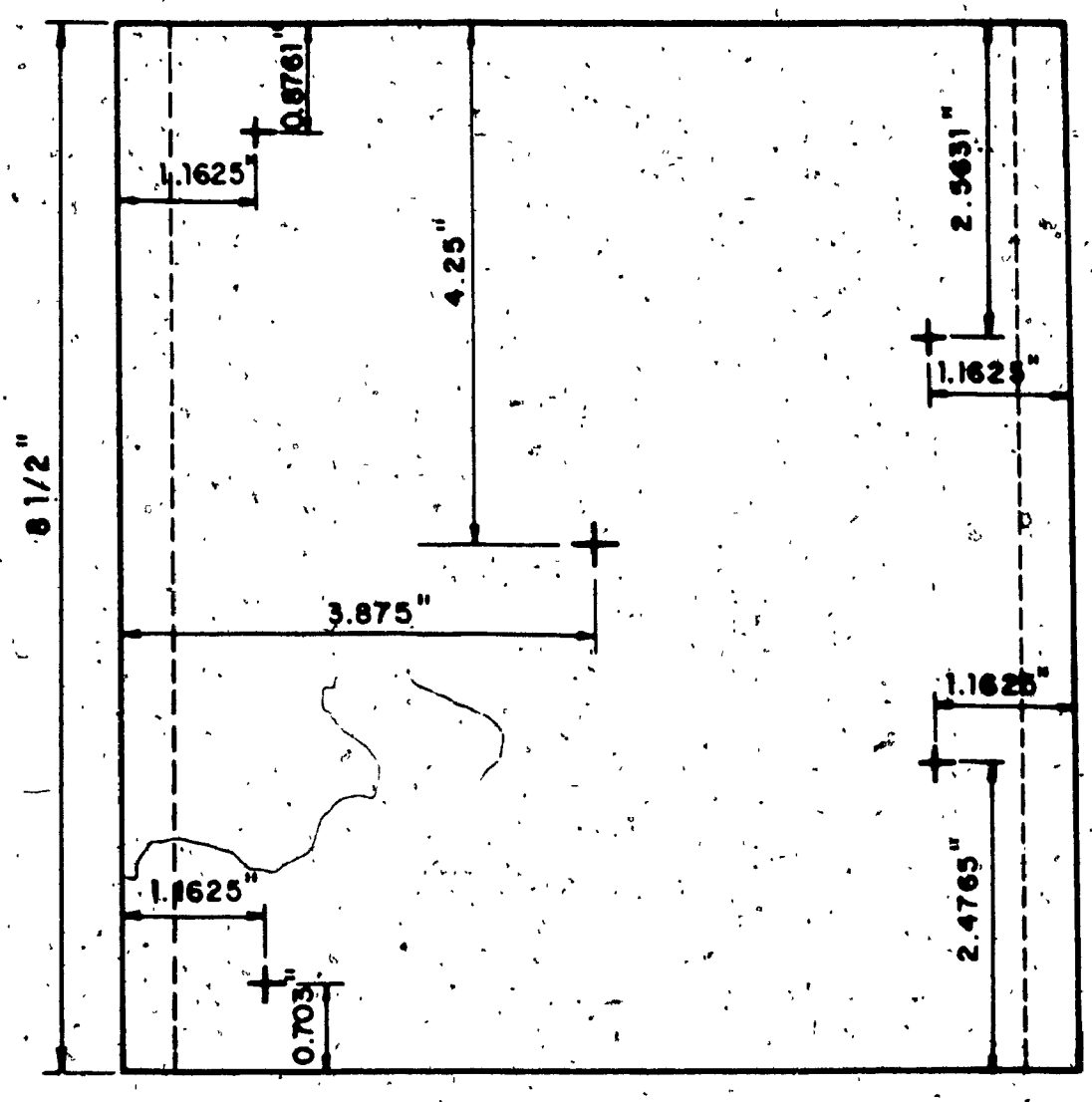

PLATE - FRONT VIEW

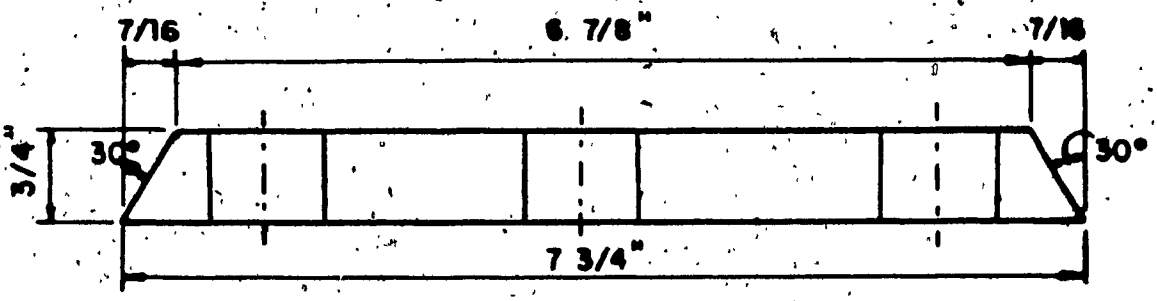

TOP VIEW

Figure 2.3: Plate details showing the locations of the transducers

The transducers were connected to a power supply source and to a voltmeter through a set of control buttons that permitted recalibration and individual readings for each transducer (see Figure 2.4).

2.2.2 Sand Spreading System

The sand spreading system, independent of the above described tank, was composed of a plastic bucket with a plastic tube exiting from its bottom (see Figure 2.5). The tube ends with a copper "T" head which has an opening to allow the sand to flow through without crowding. The opening width was twice the diameter of the largest grain size.

The capacity of the bucket allowed the spreading of a layer of sand 1-1/2" (inch) thick before refilling. After one such spreading the bucket was refilled and lifted an additional 1-1/2" (inch) to provide the same height of drop for the sand as for the previous layer (this is the case for homogeneous layer). Due to the controls available on the sand spreading system, the height of drop could be changed from zero to three feet, in increments of 1-1/2" (inch). A counterweight provided the stability necessary for the bucket not to overturn the system when held up high and full.

2.2.3 The Sand Spreading Technique

The sand was spread in 1 to 1-1/2" (inch) layers depending on the height that it was dropped from. The height of drop varied from the dense sand requirements to the loose sand ones. For dense sand the

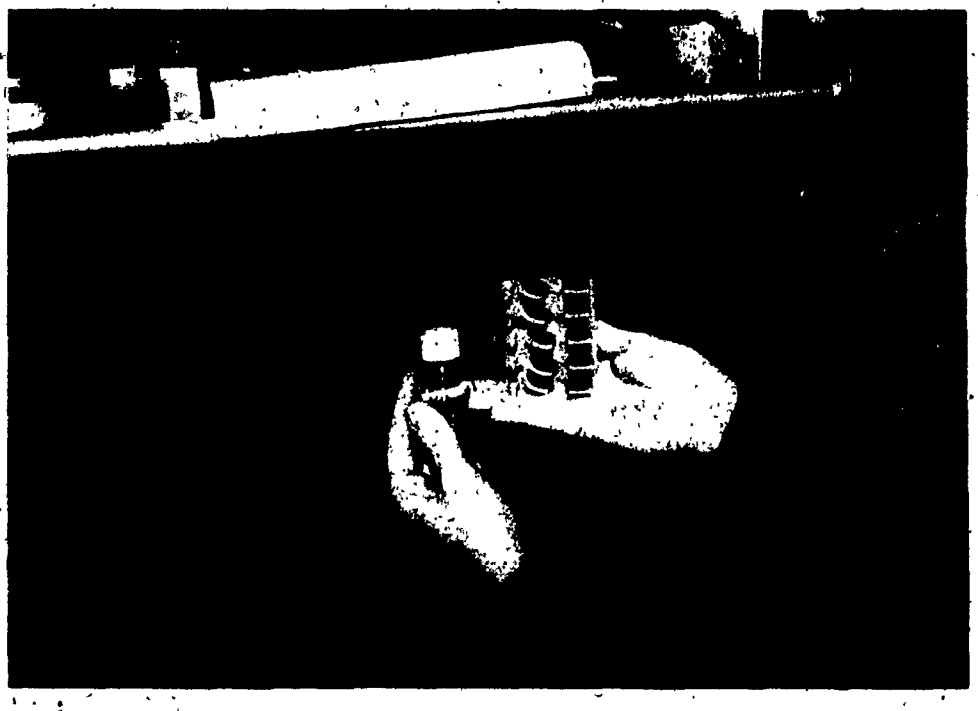

Figure 2.4: Photograph shows the control buttons

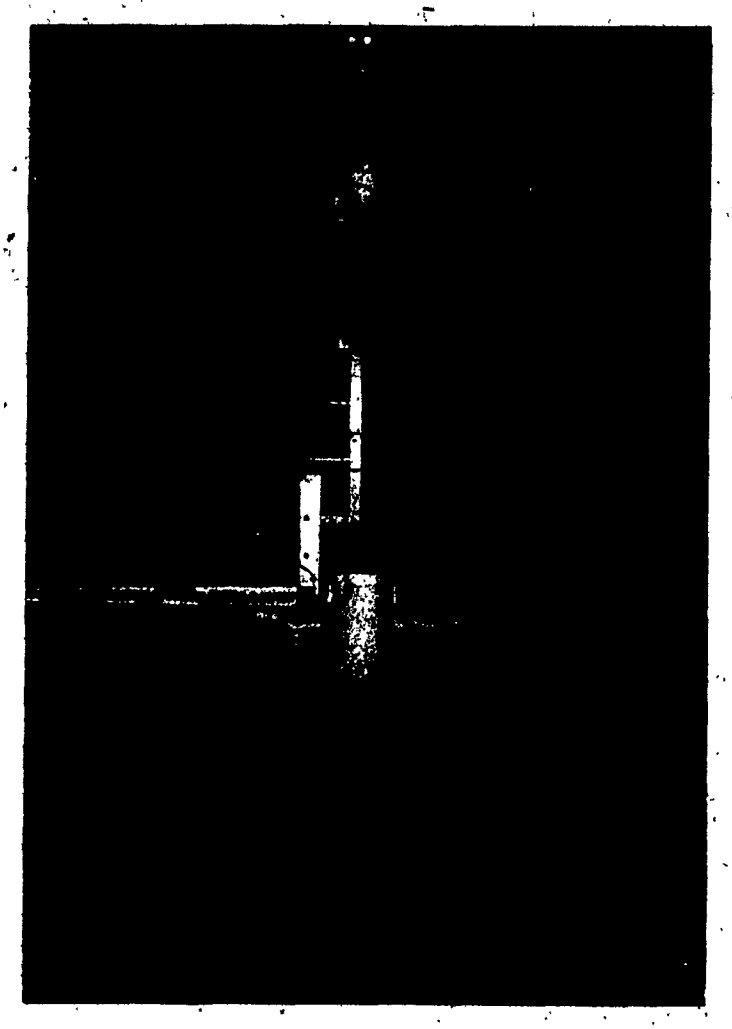

Figure 2.5: Photograph shows the sand spreading system

height of drop was 24" (inches), for medium sand the height of drop was 6" (inches) and for loose sand the height of drop was 1-1/2" (inches).

After each layer was placed (when the bucket was empty) a spray of ink and water mixture was used to mark an horizontal line which would make observation of the behaviour of the soil mass easier. After each spreading the bucket had to be raised by 1-1/2" (inch) to keep the height of drop constant for the next layer. When the tank was full, a transparent sheet of plastic was applied to the side of the tank. On it, the horizontal lines were traced and initialed. At the end of the test, the final position of the lines plus the failure lines were marked on paper.

This way, lifesize failure and behaviour lines were accurately obtained from the test.

2.2.4 Test Procedure

Before starting the experimental work and prior to final assembly of the apparatus, the five pressure transducers and the load cell had to be calibrated.

The calibration of the transducers was conducted using the apparatus seen in Figure 2.6.

A description of the calibration procedure follows:

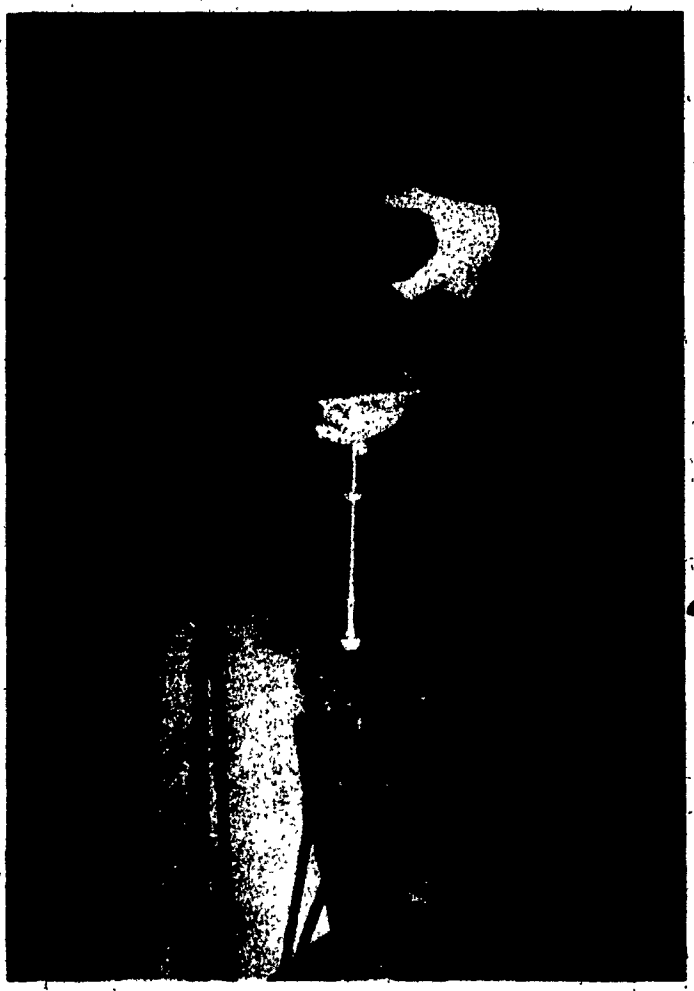

Figure 2.6: Photograph showing the calibration apparatus for transducers

One transducer at a time was introduced at the bottom of the tube. A column of sand of 6" was placed over the transducer. A piston with a plate at the other end was introduced in the tube over the sand column. A load of known weight was placed on the plate at the end of the piston and a reading was recorded by the transducer. With the help of the control buttons on the control panel (see Figure 2.4), a reading equal to the actual weight of the load was obtained. The procedure was repeated for different weights and all readings were recorded. The transducers were calibrated for a range from 0 to 35 psi.

After removing the sand from the tube the transducer should read zero. The procedure was repeated a few times for different loads for each transducer and after they were all calibrated, they were placed in their final positions in the plate and secured tightly.

Calibration curves were obtained for excitation versus pressure (see Figure 2.7).

In order to perform the calibration, the power source and the voltmeter were left on during the previous 24 hrs. A resistor of known value was installed for every transducer in order to verify the calibration of the transducers after every test and prior to starting a new one.

The load cell in the present experimental investigation served the following purposes:

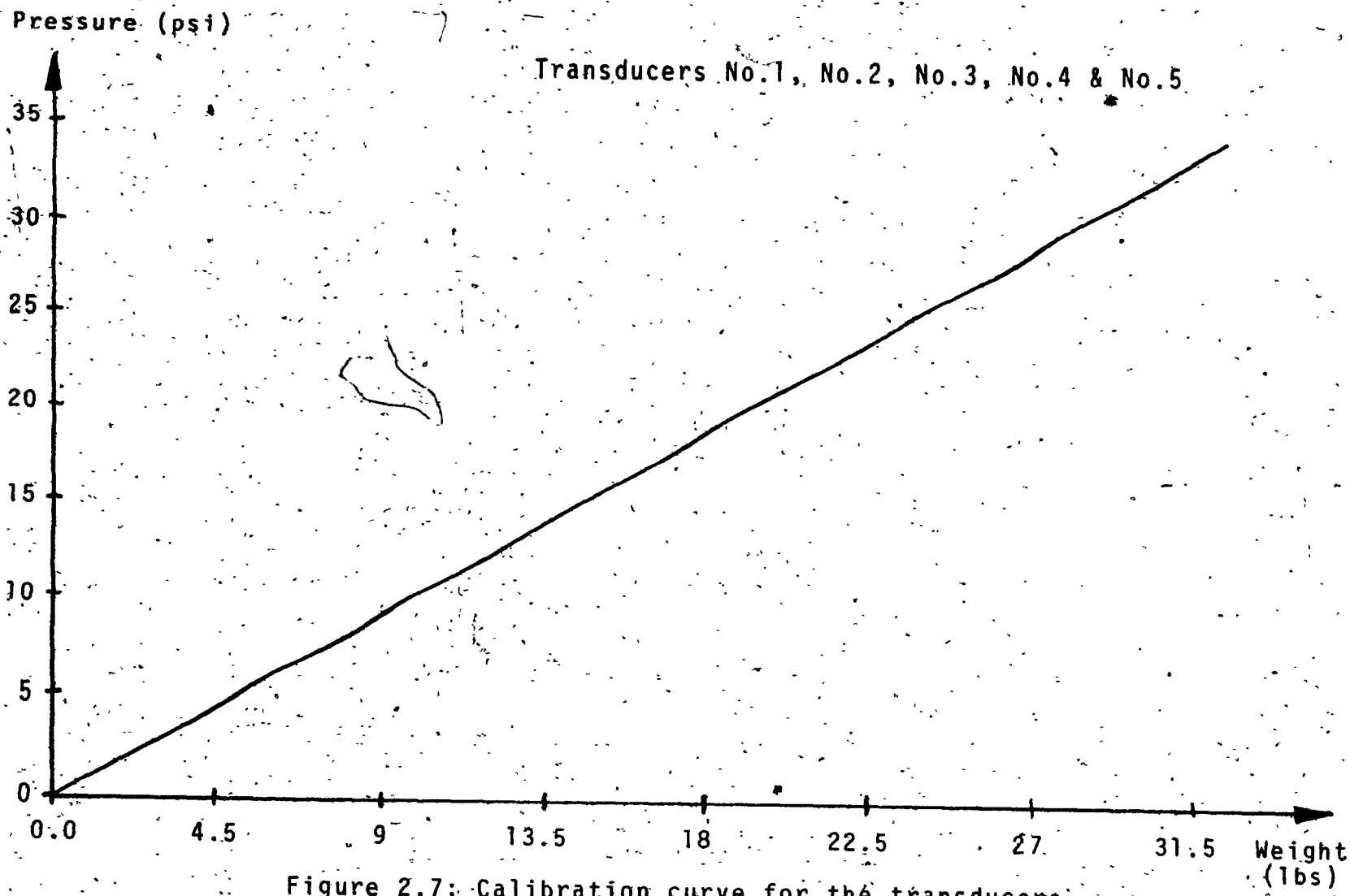

Figure 2.7: Calibration curve for the transducers

(i) to monitor for possible malfunctioning of the transducers and

(ii) to determine the frictional resistance produced in every test.

The calibration of the load cell was carried out by means of the stress control procedure. The curve obtained plots excitation versus load (see Figure 2.8).

Before spreading the sand, the transducers initial reading was taken to make sure that they were unchanged and did not need recalibration.

The test is started by applying power to the motor, which starts pushing the plate against the sand.

At the same displacement intervals (there is another gauge installed on the tank that measures the displacement of the wall) readings are taken for the total force applied to the wall, and the pressure indicated by each transducer. It takes three persons to conduct the test efficiently. Loading continues as long as the force gauge measures additional increments. When the force gauge readings start to decrease, failure is occurring and this is backed up by visual observations of the sand in the box. The failure lines are recorded as they occur on sheets of plastic placed over the side of the tank.

At the end of the test, after unloading, the transducers are checked to see if they read the same values as the initial values they

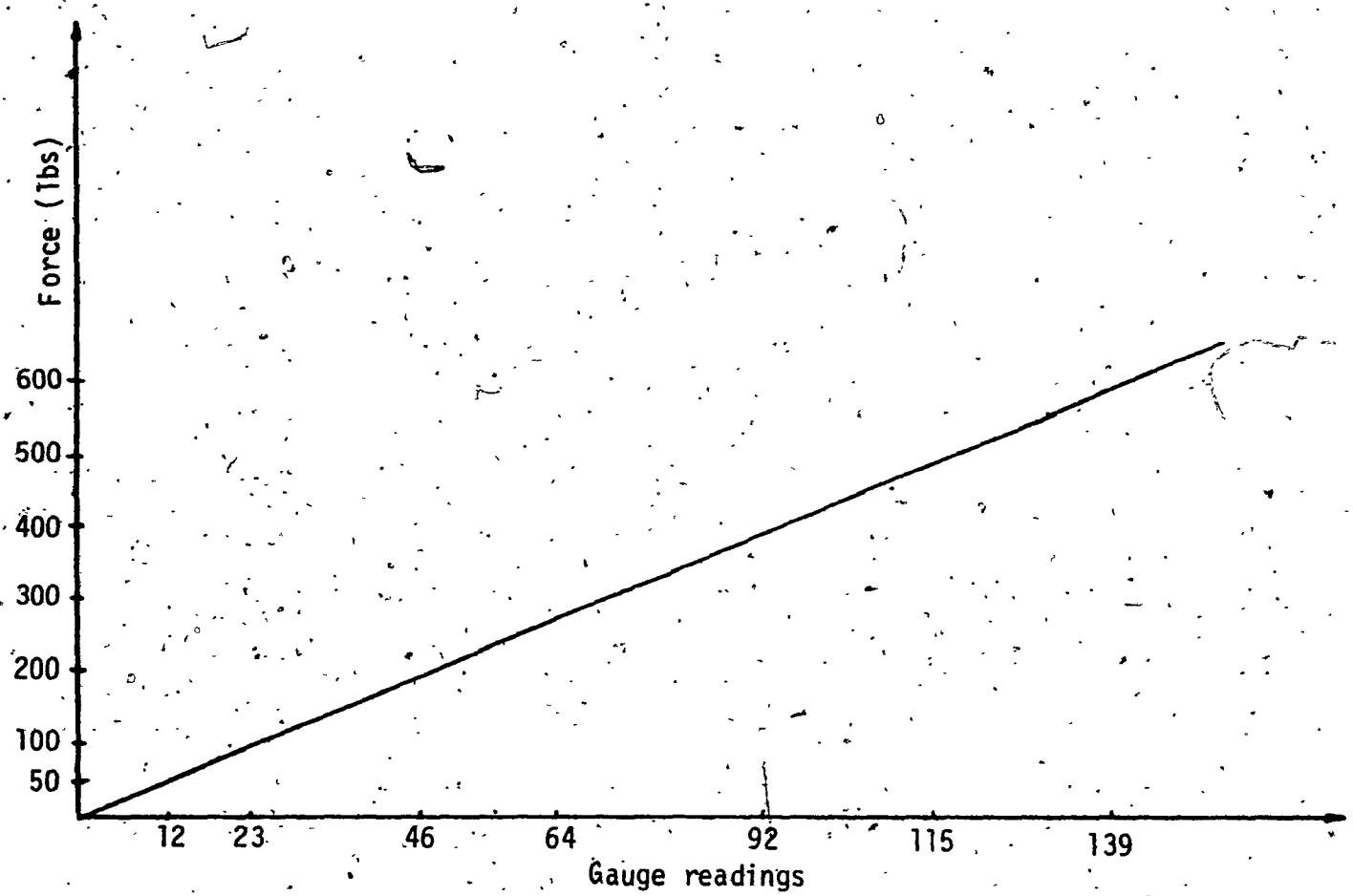

Figure 2.8: Load cell calibration curve

were reading before the test, and if everything is in order, the test is classified as successful.

2.3 Soil Properties

The sand used in this investigation is called "Morie Sand" and is imported from the U.S.A.. A detailed study of the physical properties of the sand used for the tests was given by Afram (1984). Only a summary description of some aspects of these properties will be given here.

The grain size distribution indicated a medium, uniform sand with a uniformity coefficient of 1.45. The measured minimum and maximum densities are 91.5 percent and 104.5 percent respectively.

The average value of the specific gravity of this sand was 2.662.

The test results showing the variation of the angle of friction with the relative density are shown in Figure 2.9.

2.4 Determination of Unit Weight

A good method for obtaining the density at any location in the test tank was to use small metal pots and place them at different levels in the sand. After each test the pots were removed then weighed and the density calculated.

It was determined that:

$\gamma_{\text{loose homogeneous sand}} = 95.2 \text{ lbs/ft}^3$,

$\gamma_{\text{medium homogeneous sand}} = 97.7 \text{ lbs/ft}^3$ and

$\gamma_{\text{dense homogeneous sand}} = 99.6 \text{ lbs/ft}^3$.

2.5 Relative Density

Table 2.1 presents the relative densities for loose, medium and dense homogeneous sands.

Using the relative densities from Table 2.1 we obtain from Figure 2.9 the corresponding angles of friction (direct shear tests):

R.D. = 31.3% for loose sand

ϕ = 37.5°

R.D. = 50% for medium sand

ϕ = 39°

R.D. = 64.6% for dense sand

ϕ = 42°

	R.D.	e_{max}	e_{min}	γ	G
Loose homog.	31.3%	.815	.590	95.2	2.662
Medium homog.	50.0%	.815	.590	97.7	2.662
Dense homog.	64.6%	.815	.590	99.6	2.662

Table 2.1: Relative densities for loose, medium and dense homogeneous sand

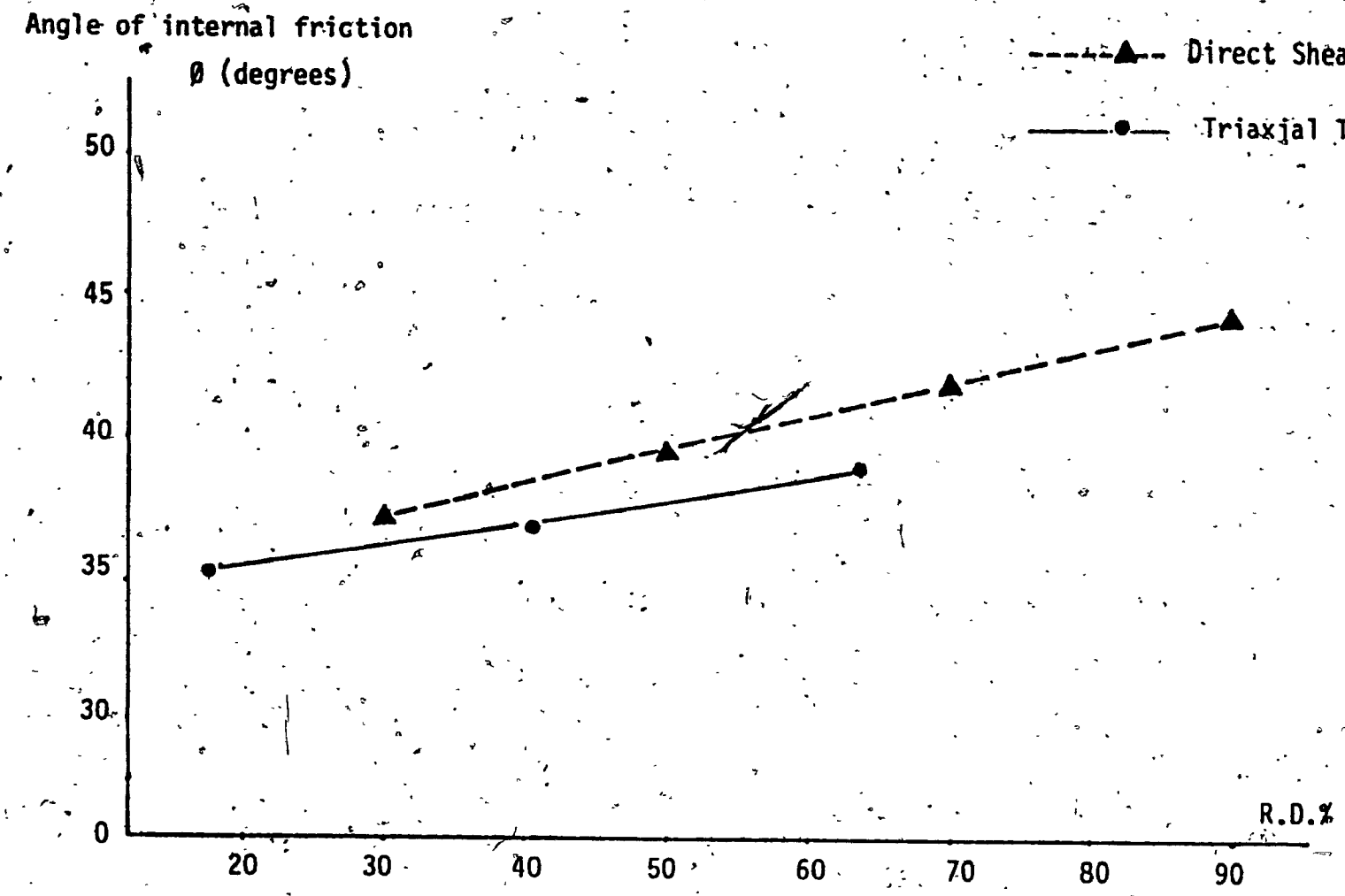

Figure 2.9: Angle of Internal Friction vs R.D. of Sand (Afram, 1984)

CHAPTER 3

EXPERIMENTAL RESULTS

The tests were divided in three groups depending on the condition of the soil behind the plate:

(i) homogeneous soil (loose, medium and dense)

(ii) weak layer overlying strong layer of sand (loose/dense, loose/medium and medium/dense)

(iii) strong layer overlying weak layer of sand (dense/medium, dense/loose and medium/loose)

The curves for the ultimate load on the retaining wall are shown in Figures 3.1 to 3.9. In addition to these, the transducer readings made feasible the drawing of curves which show the ultimate load per transducer with respect to the displacement of the plate (model retaining wall). Figures 3.10 to 3.18 represent the above mentioned curves.

The failure planes were traced off the glass side of the testing tank and are shown at a reduced scale in Figures 3.19 to 3.27.

The failure planes observed show that for the homogeneous conditions the present theory of calculating the passive earth pressure

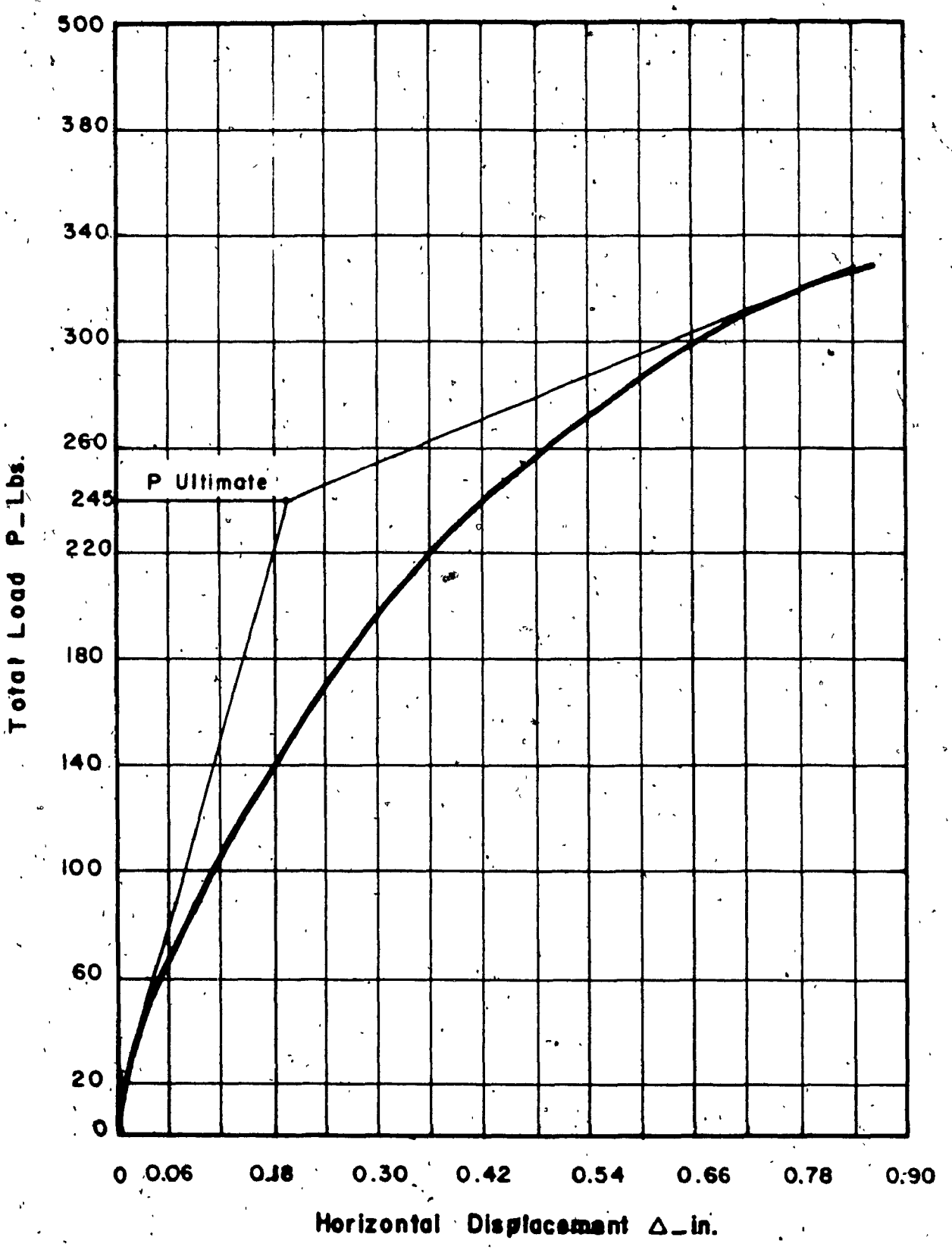

Figure 3.1: Load-settlement curve for loose homogeneous sand

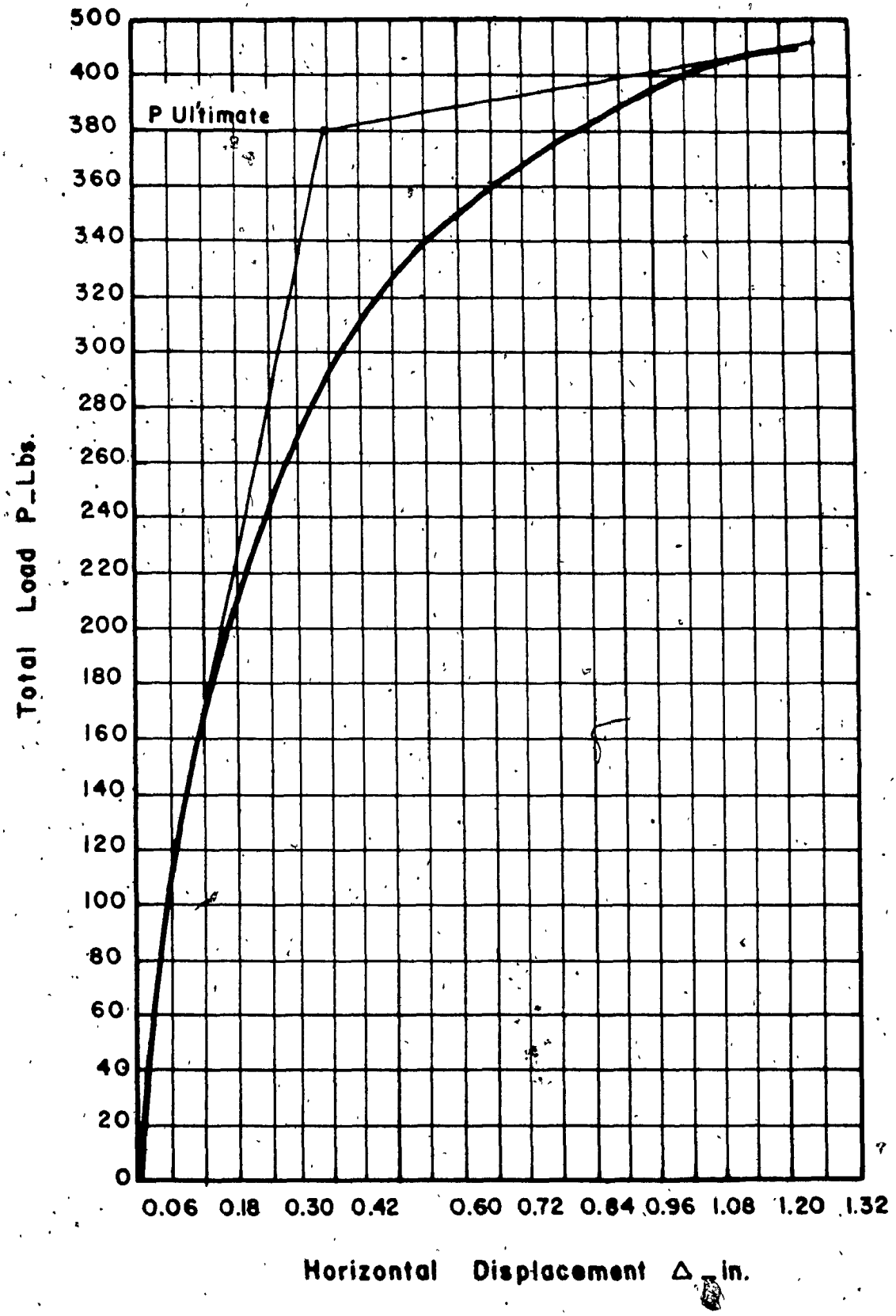

Figure 3.2: Load-settlement curve for medium homogeneous sand

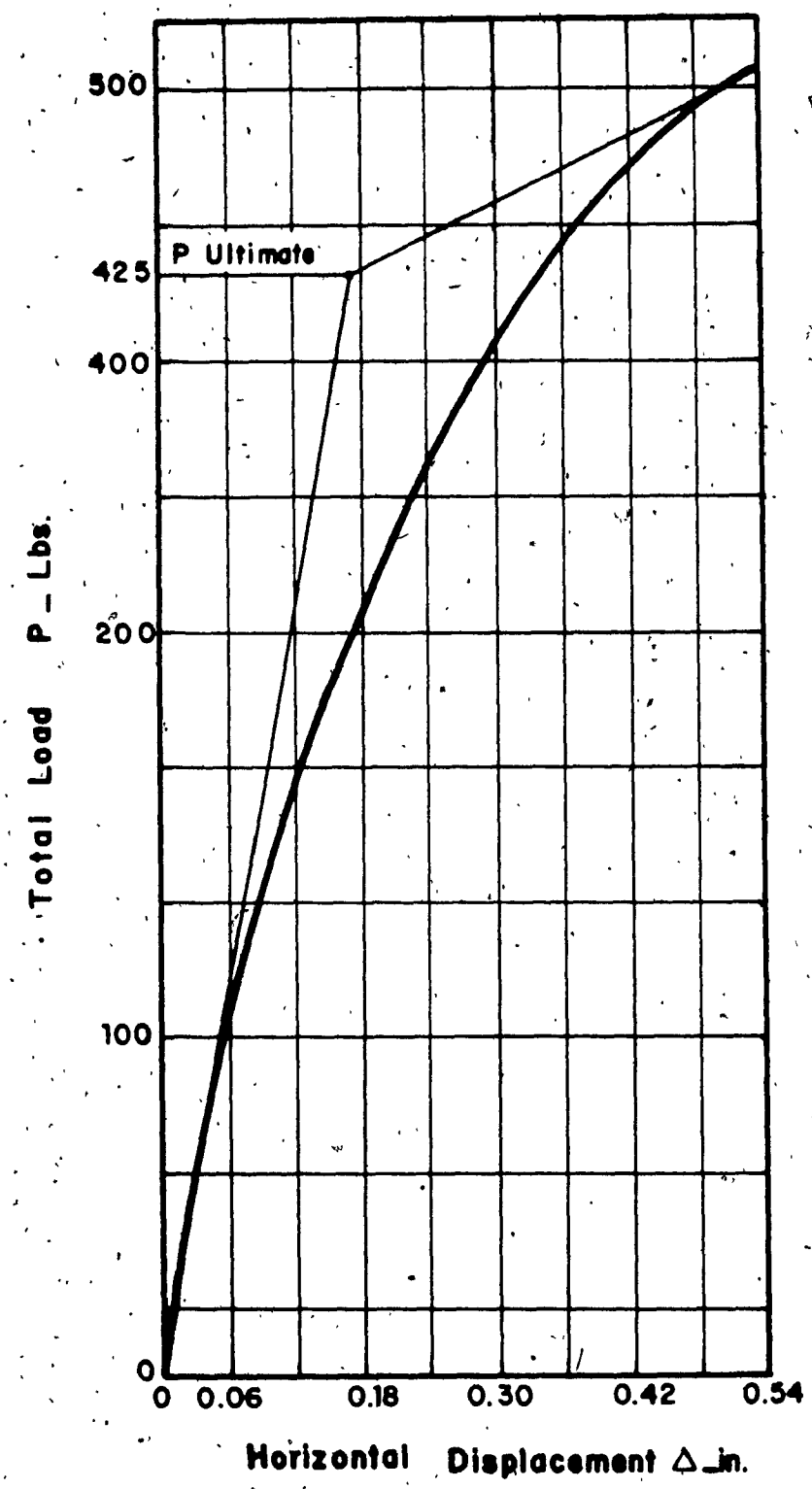

Figure 3.3: Load-settlement curve for dense homogeneous sand

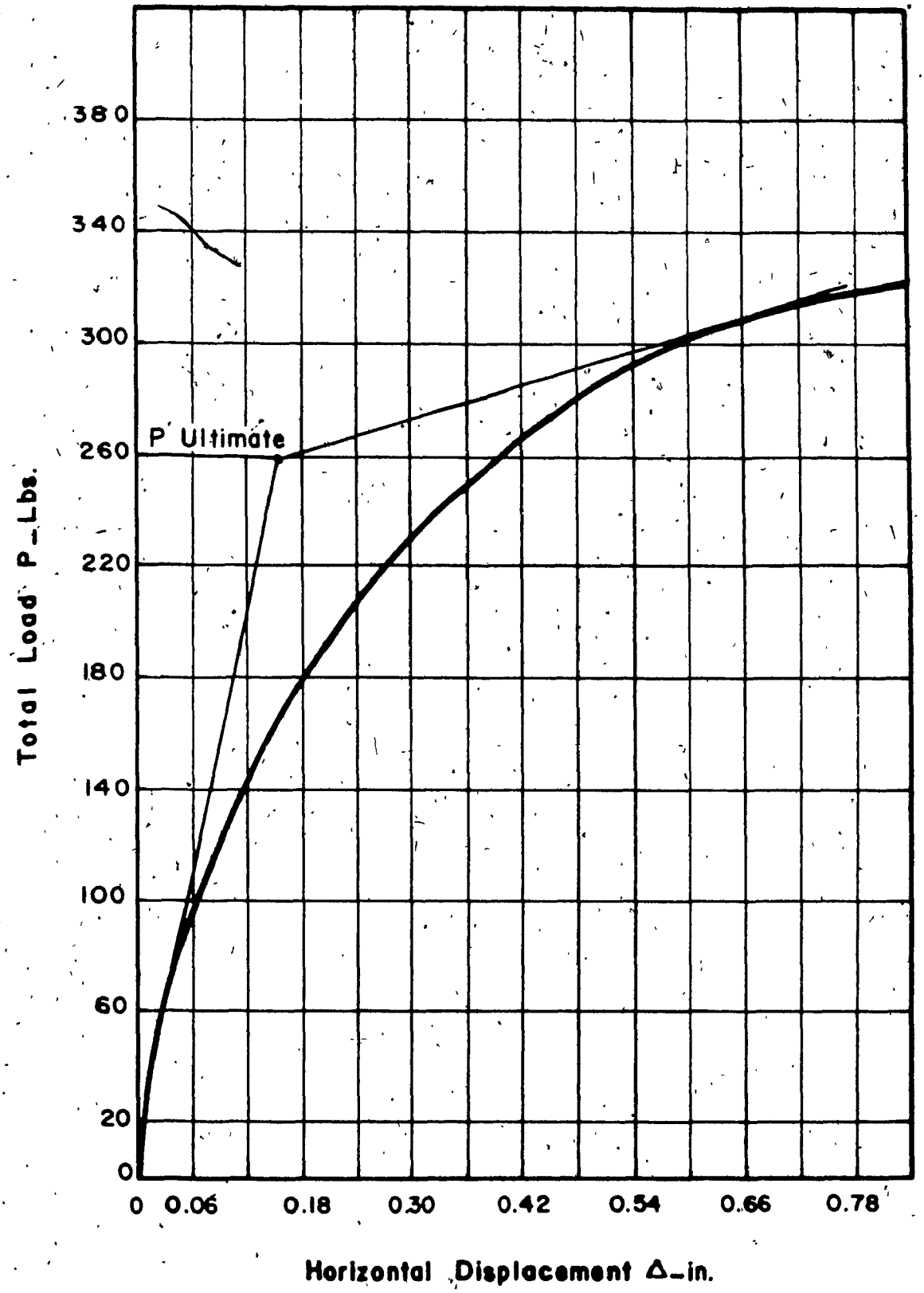

Figure 3.4: Load-settlement curve for loose overlying medium sand

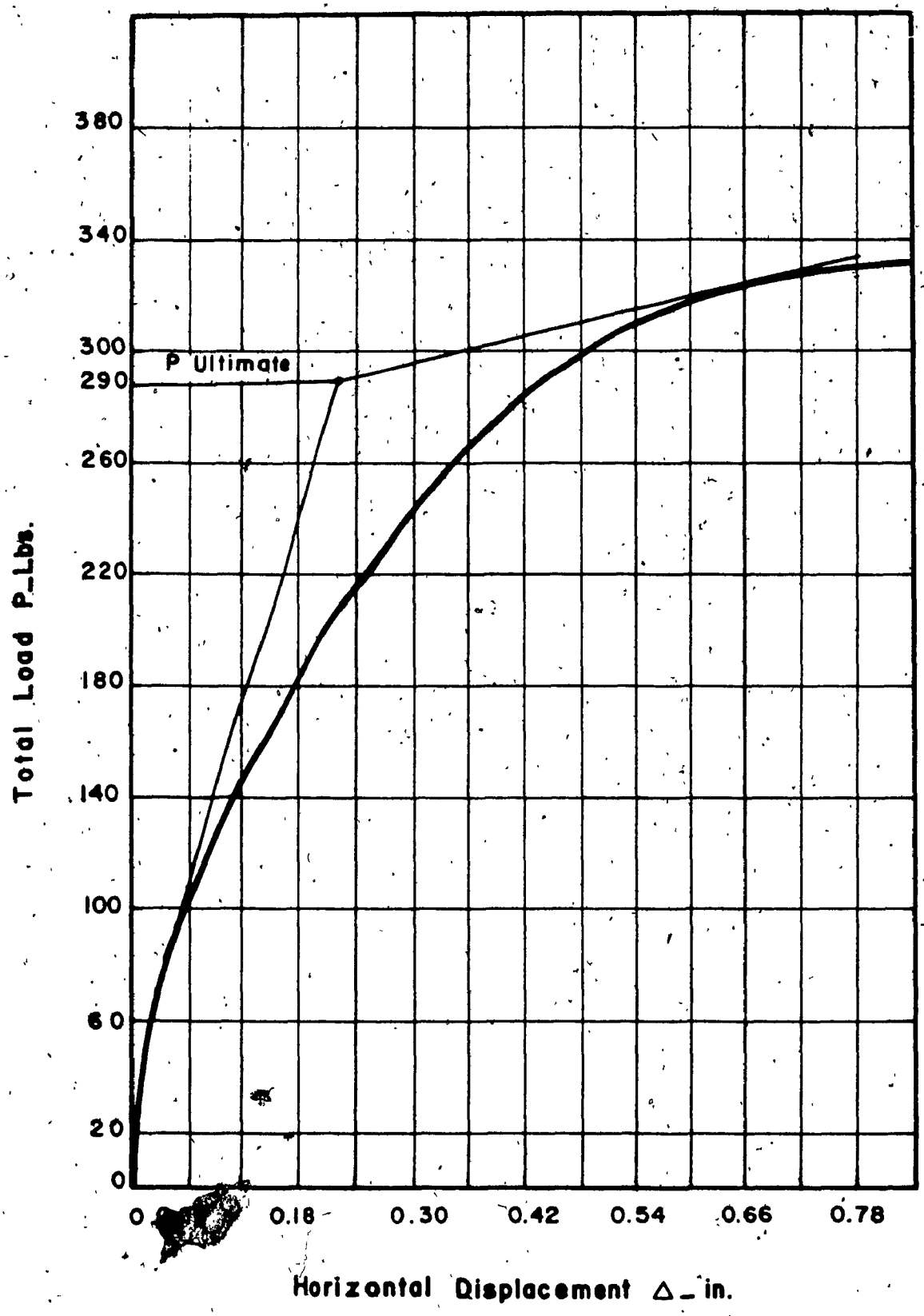

Figure 3.5: Load-settlement curve for loose overlying dense sand

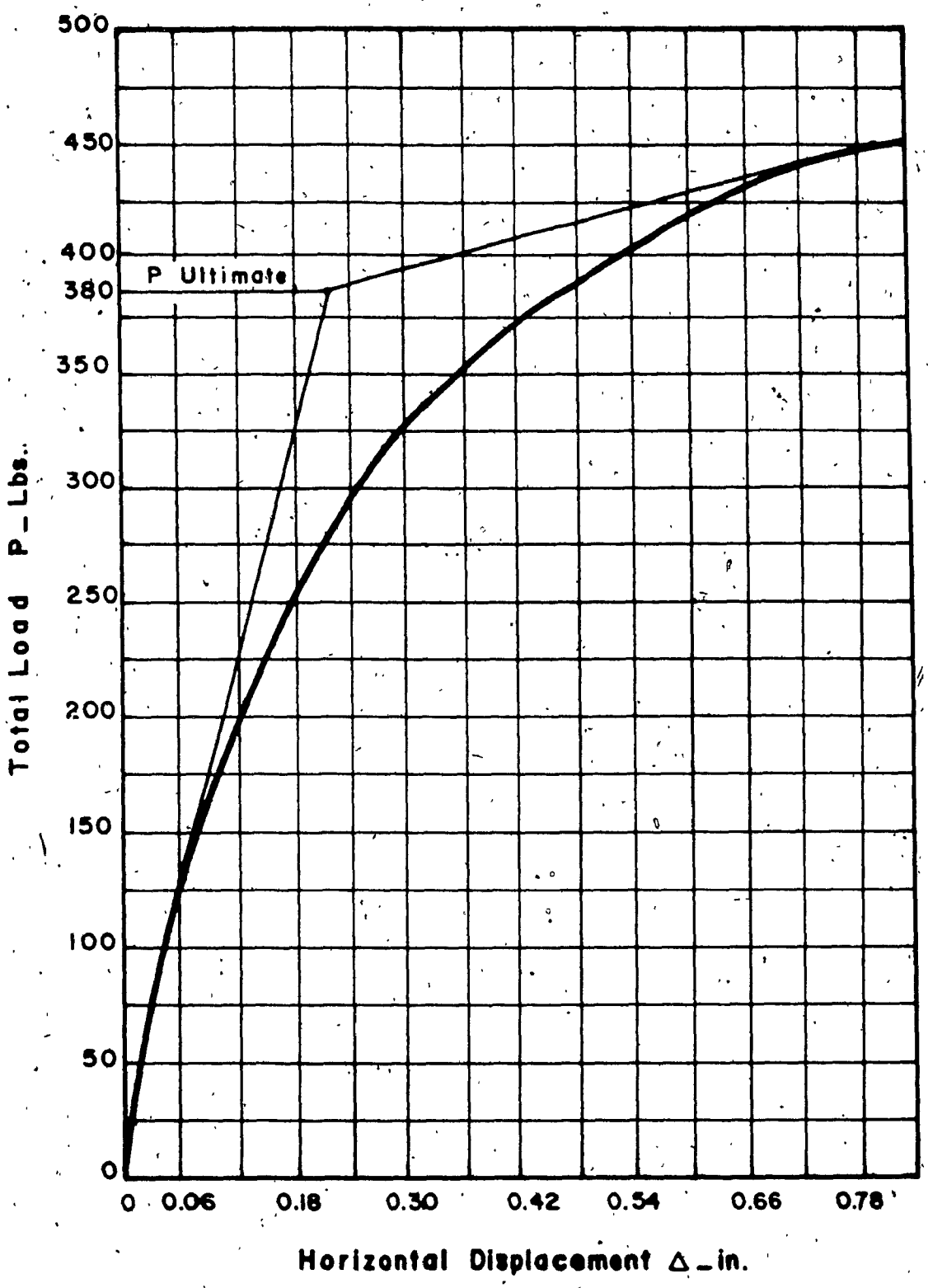

Figure 3.6: Load-settlement curve for medium overlying dense sand

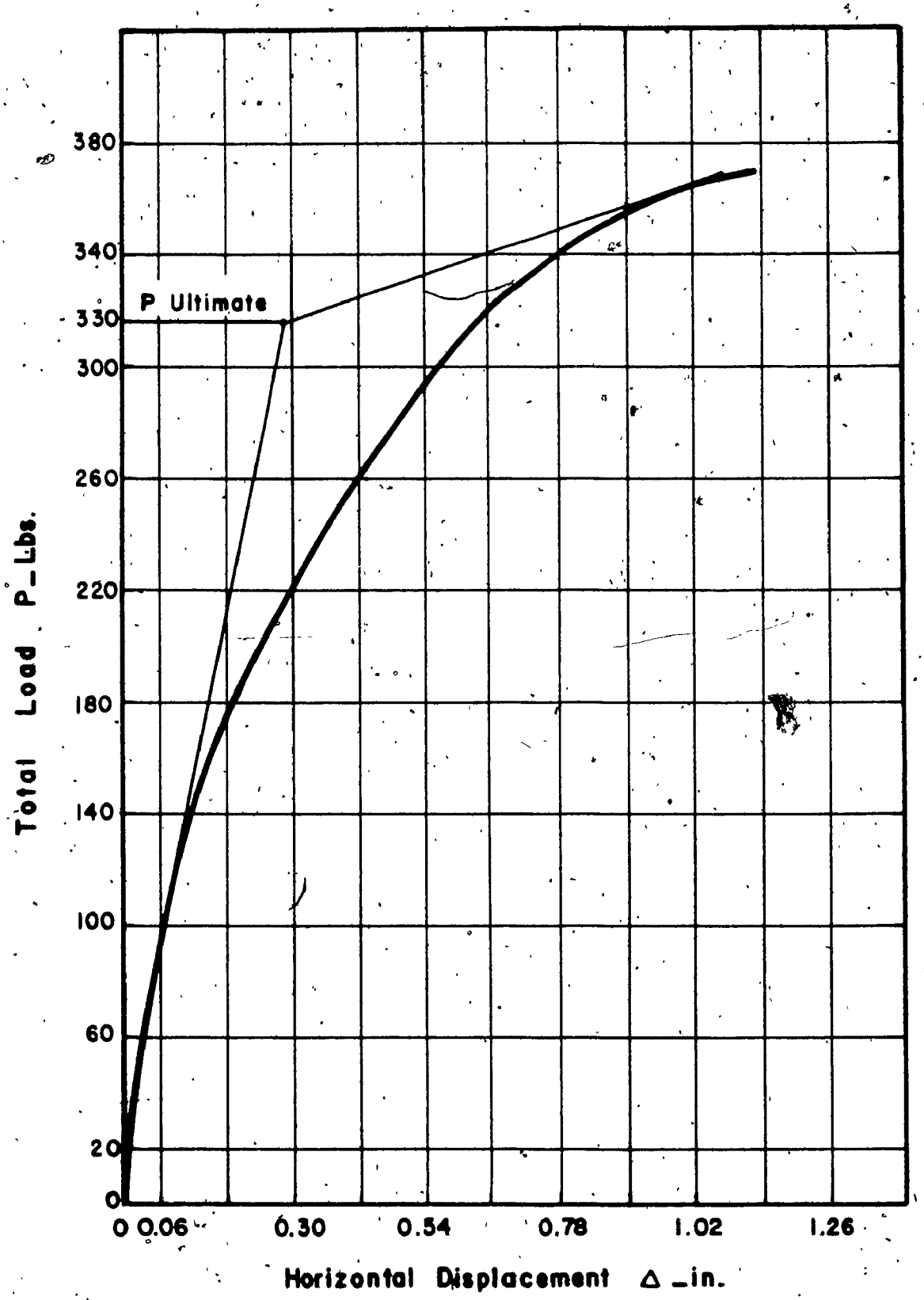

Figure 3.7: Load-settlement curve for medium overlying loose sand

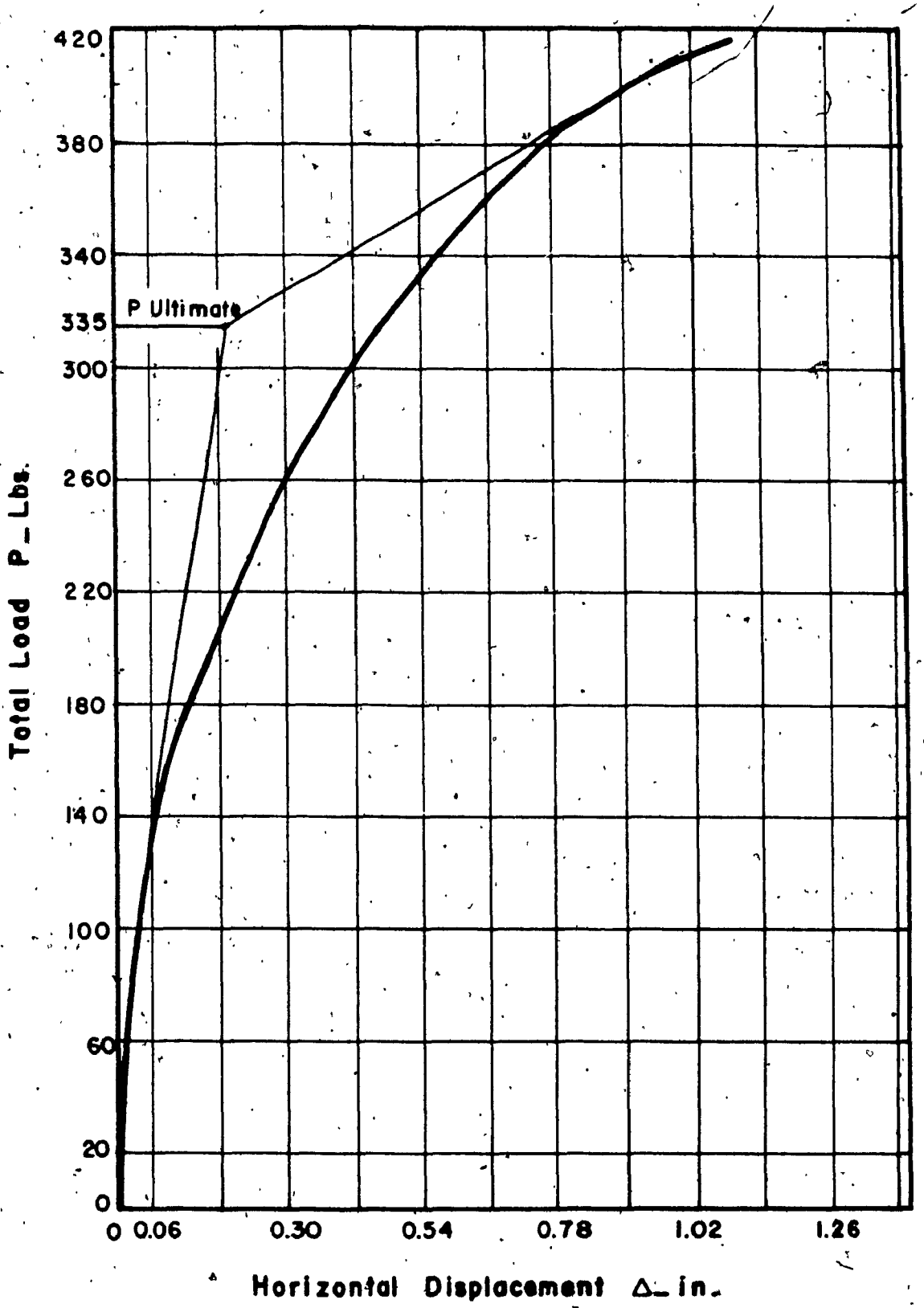

Figure 3.8: Load-settlement curve for dense overlying loose sand

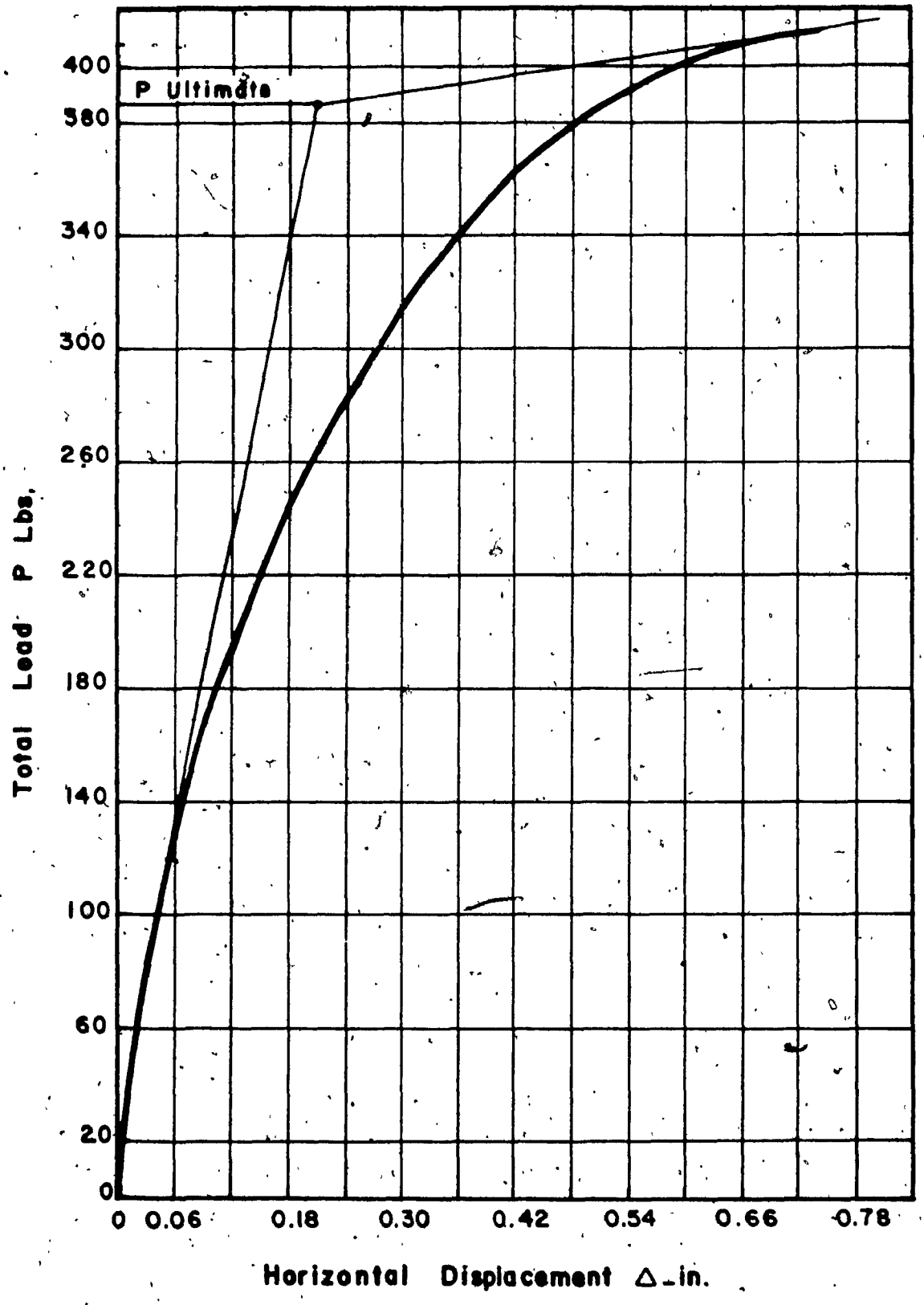

Figure 3.9: Load-settlement curve for dense overlying medium sand

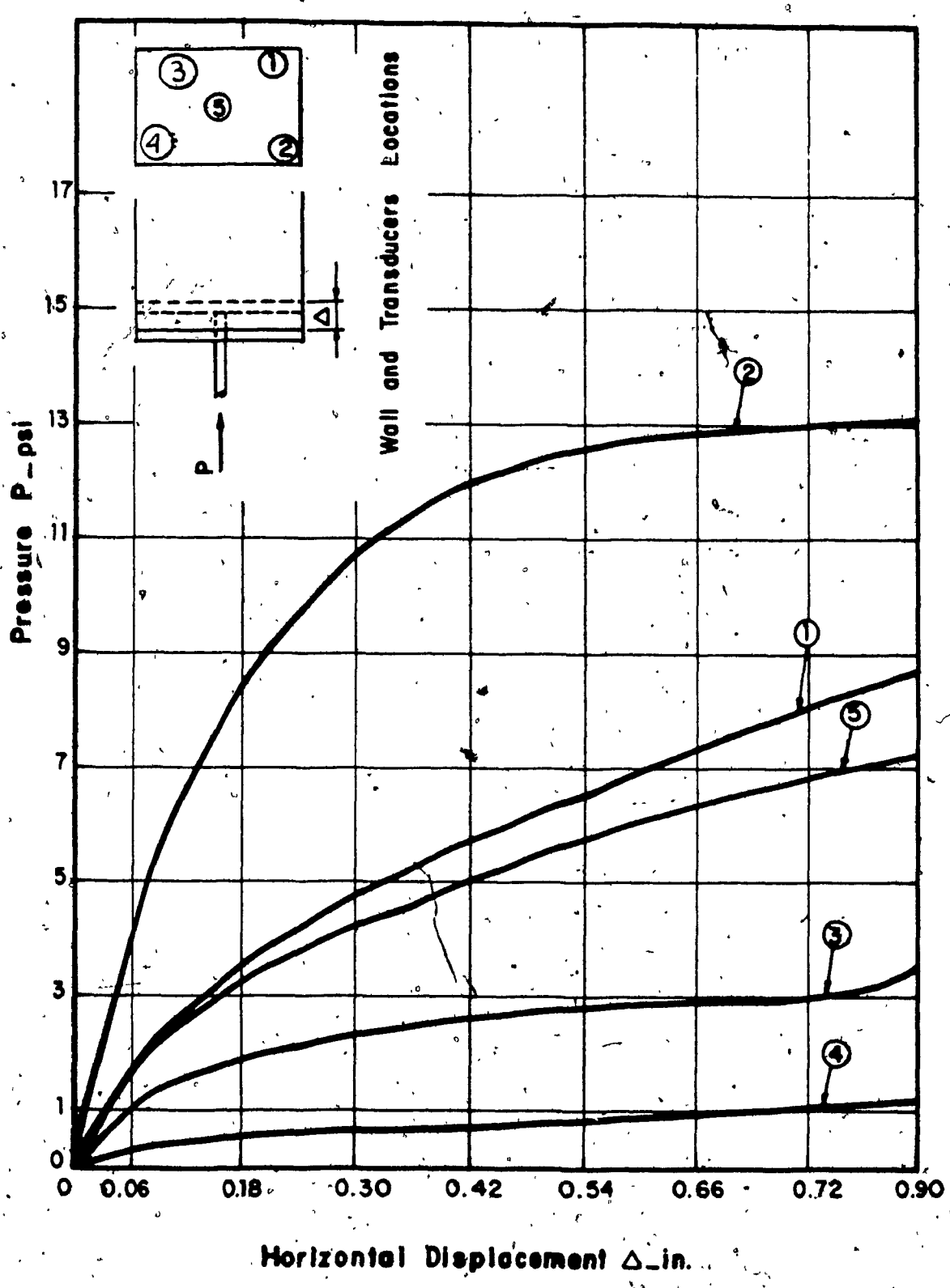

Figure 3.10: Load-settlement curves for each transducer for loose homogeneous sand

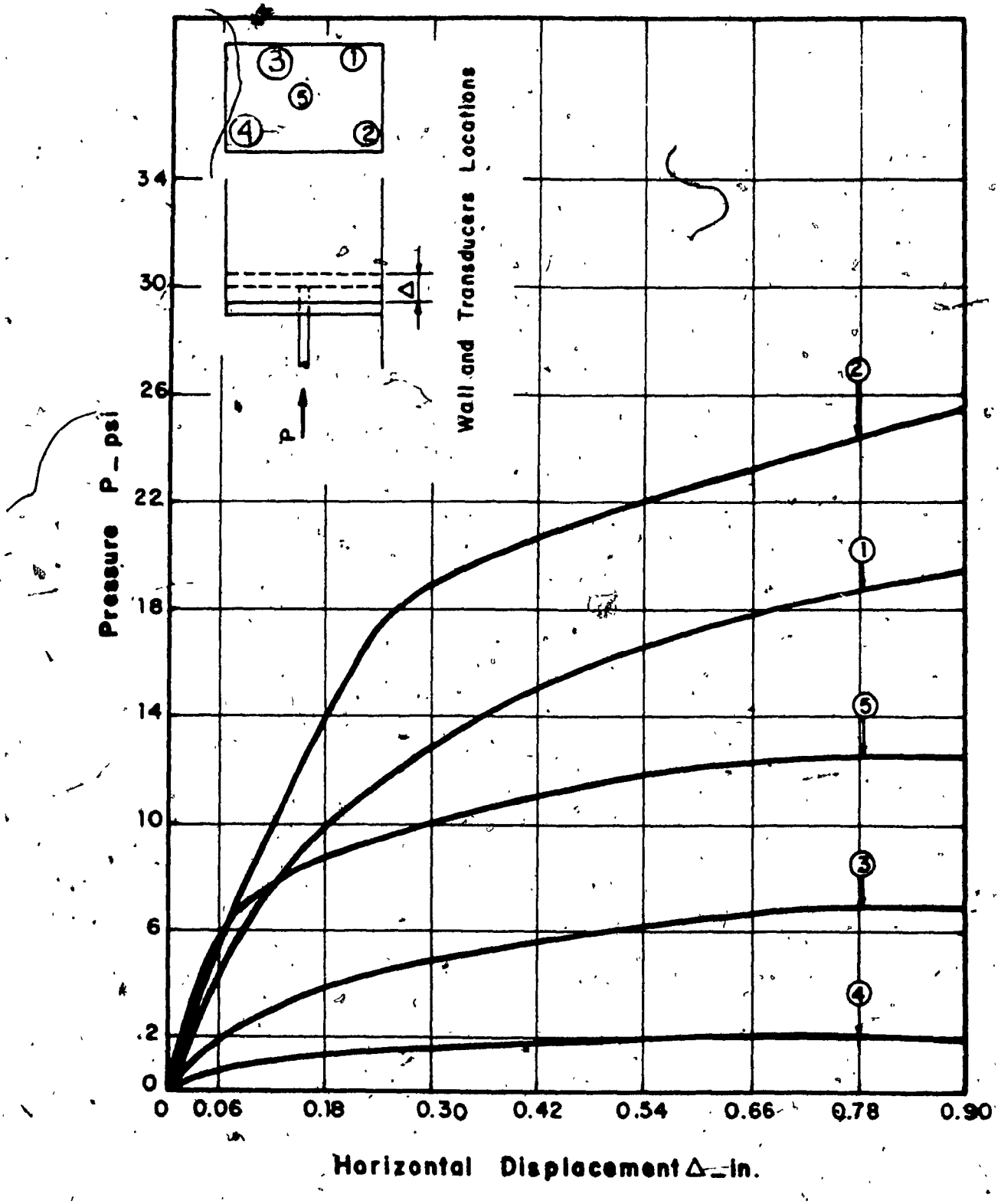

Figure 3.11: Load-settlement curves for each transducer for medium homogeneous sand

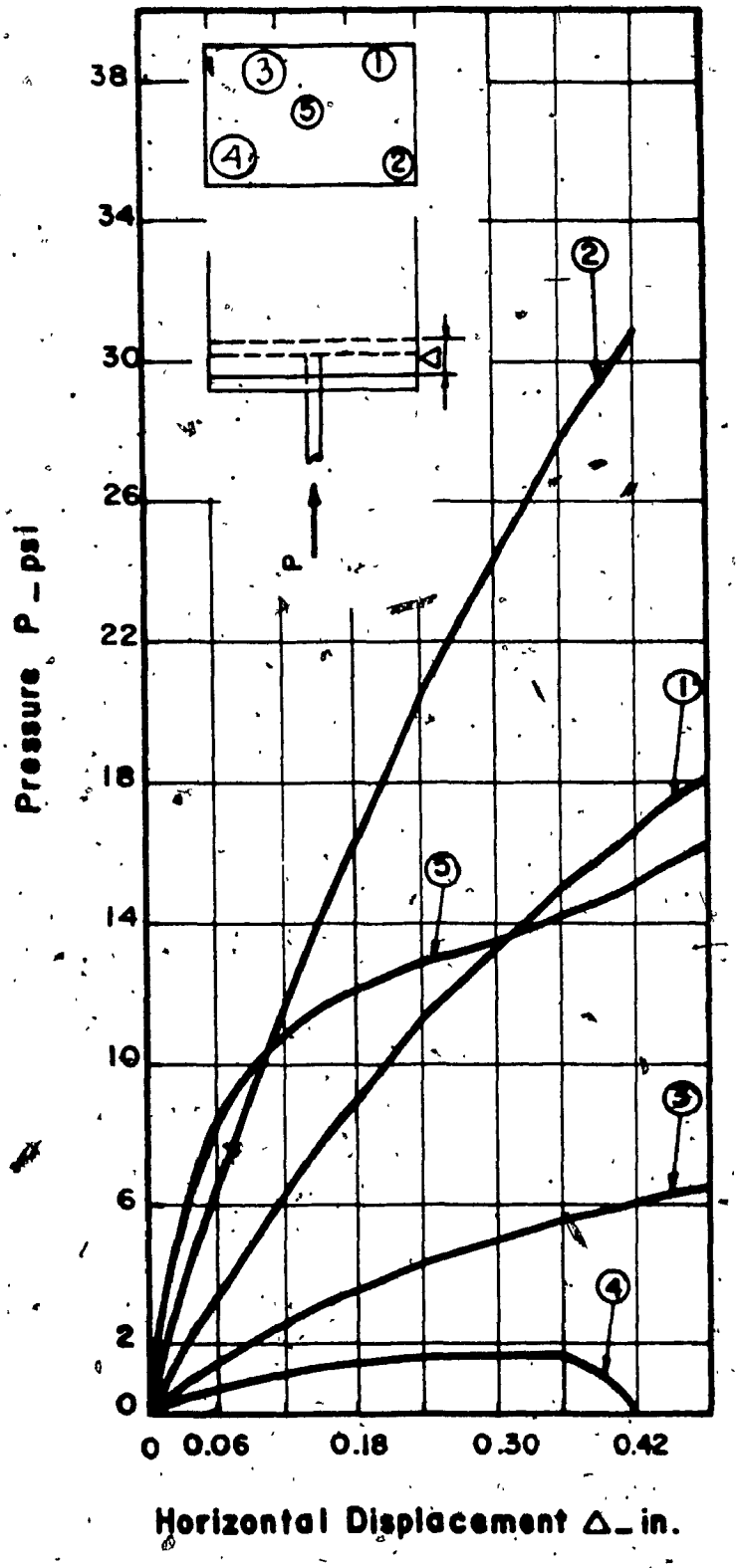

Figure 3.12: Load-settlement curves for each transducer for dense homogeneous sand

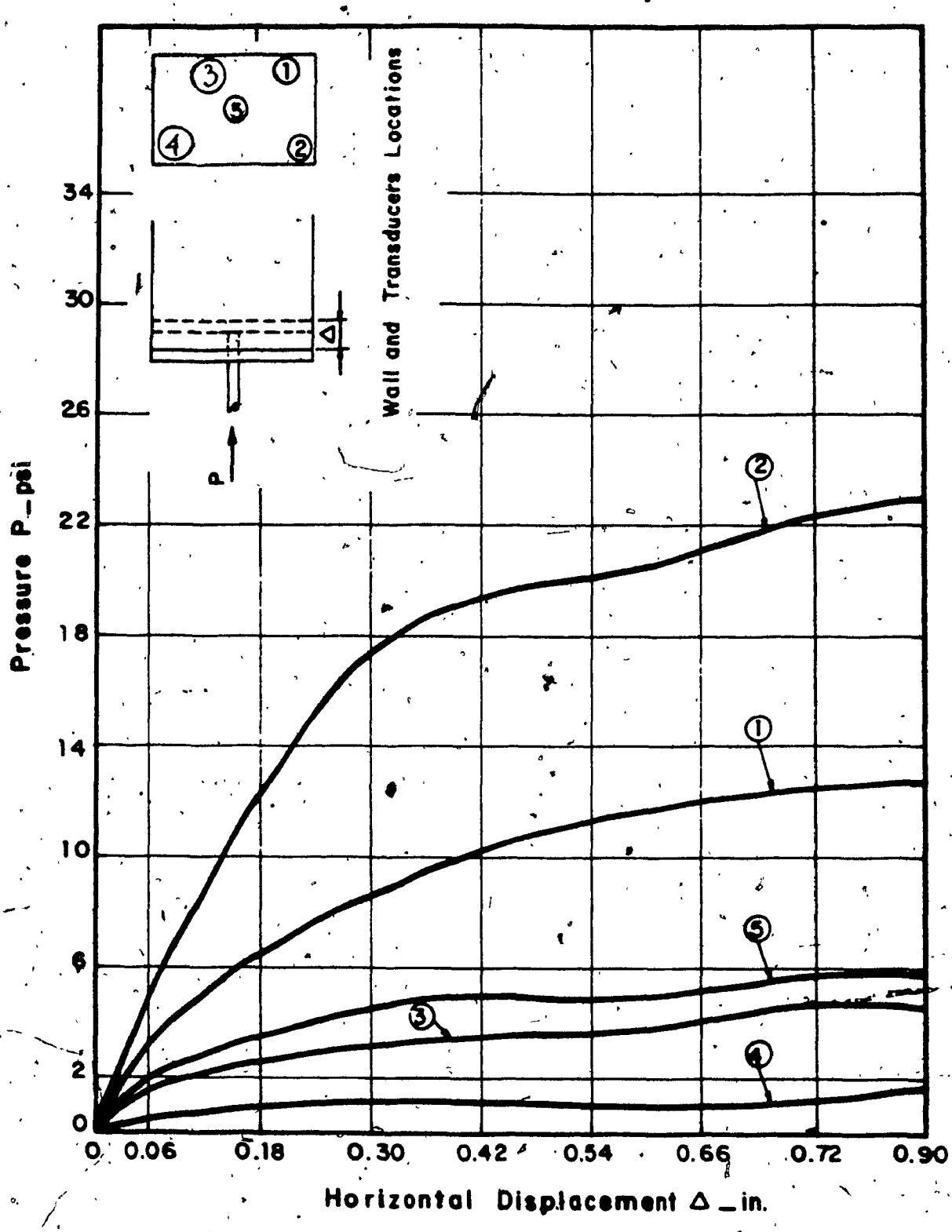

Figure 3.13: Load-settlement curves for each transducer for loose overlying medium sand.

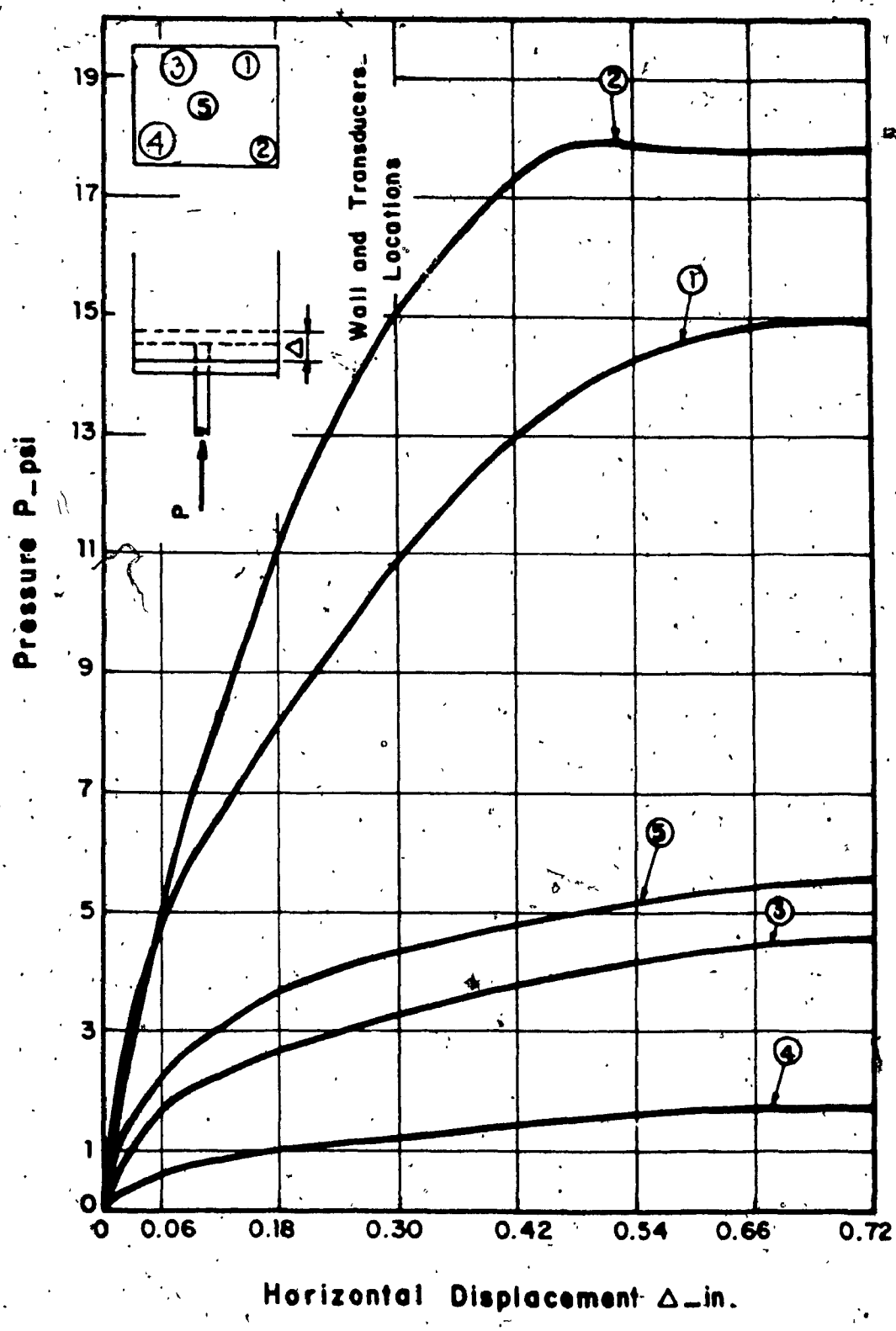

Figure 3.14: Load-settlement curves for each transducer for loose overlying dense sand

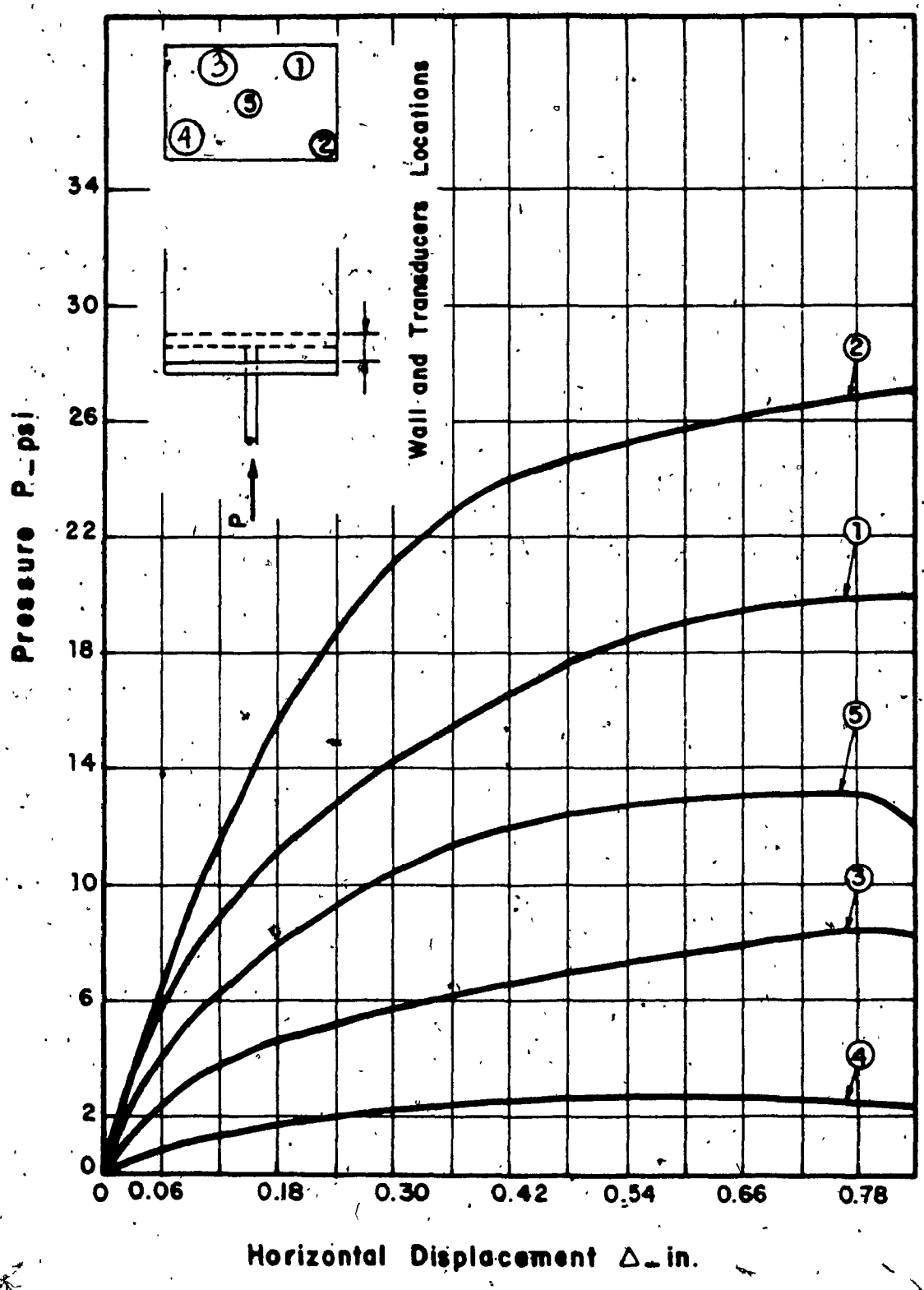

Figure 3.15: Load-settlement curves for each transducer for medium overlying dense sand

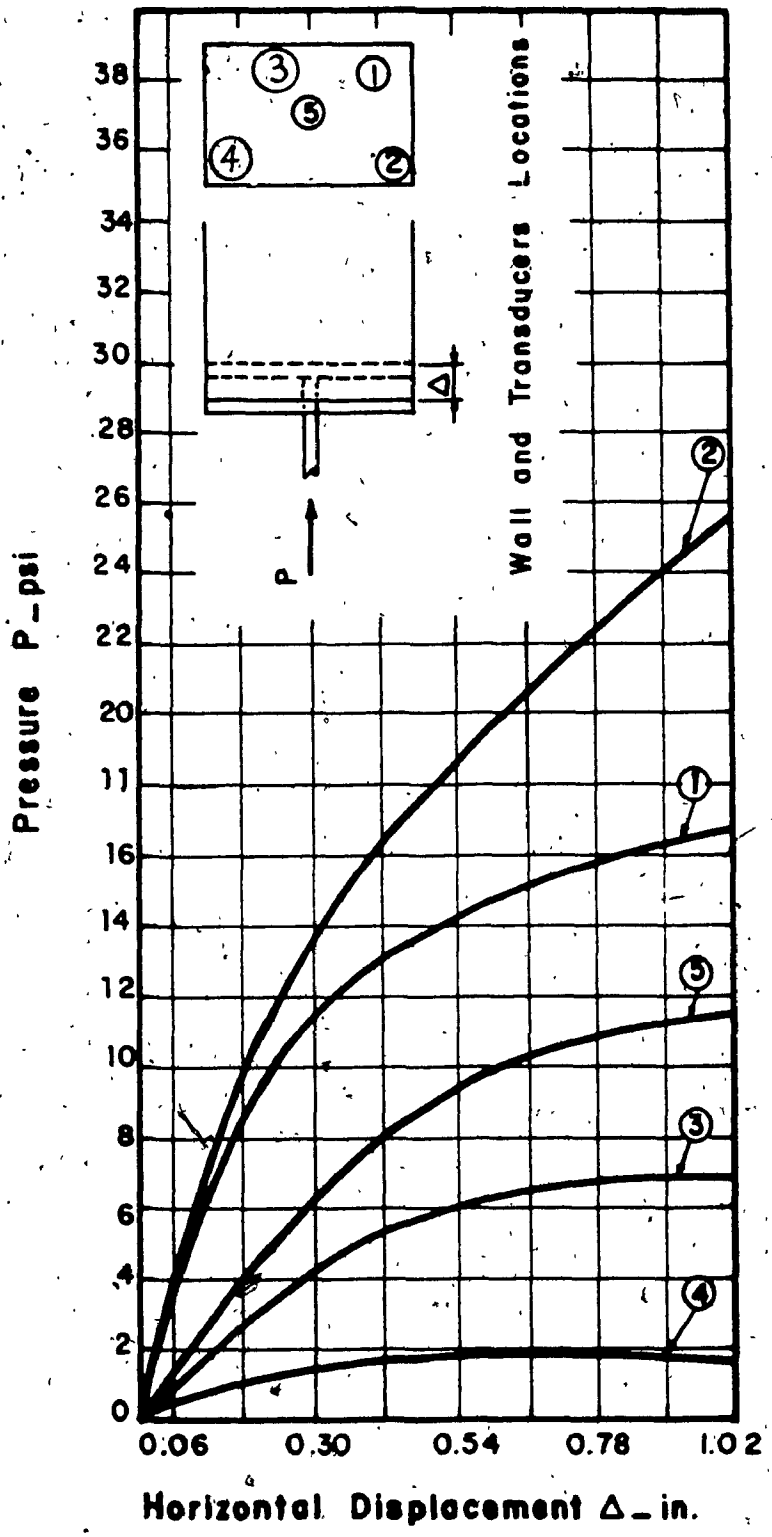

Figure 3.16: Load-settlement curves for each transducer for medium overlying loose sand

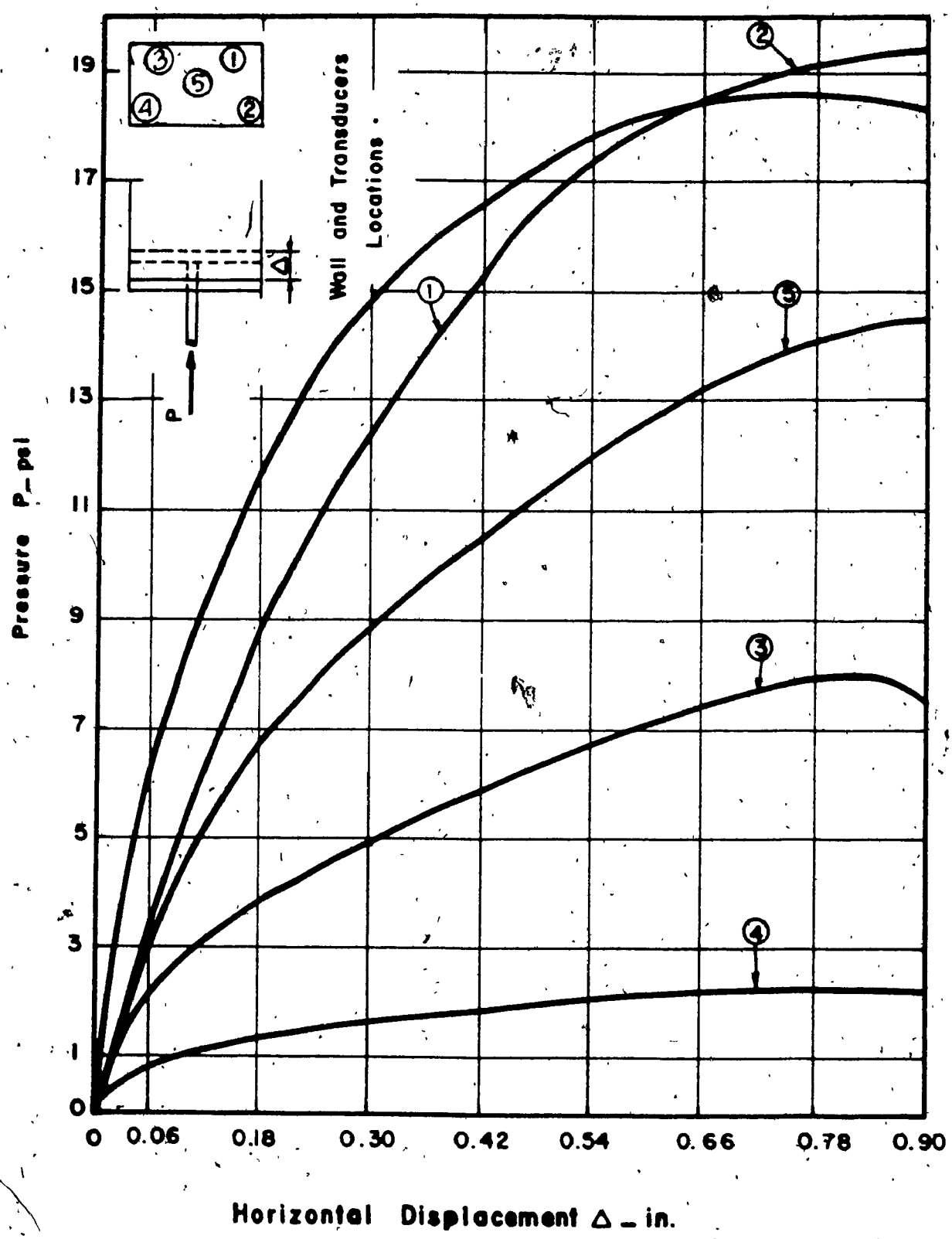

Figure 3.17: Load-settlement curves for each transducer for dense overlying medium sand

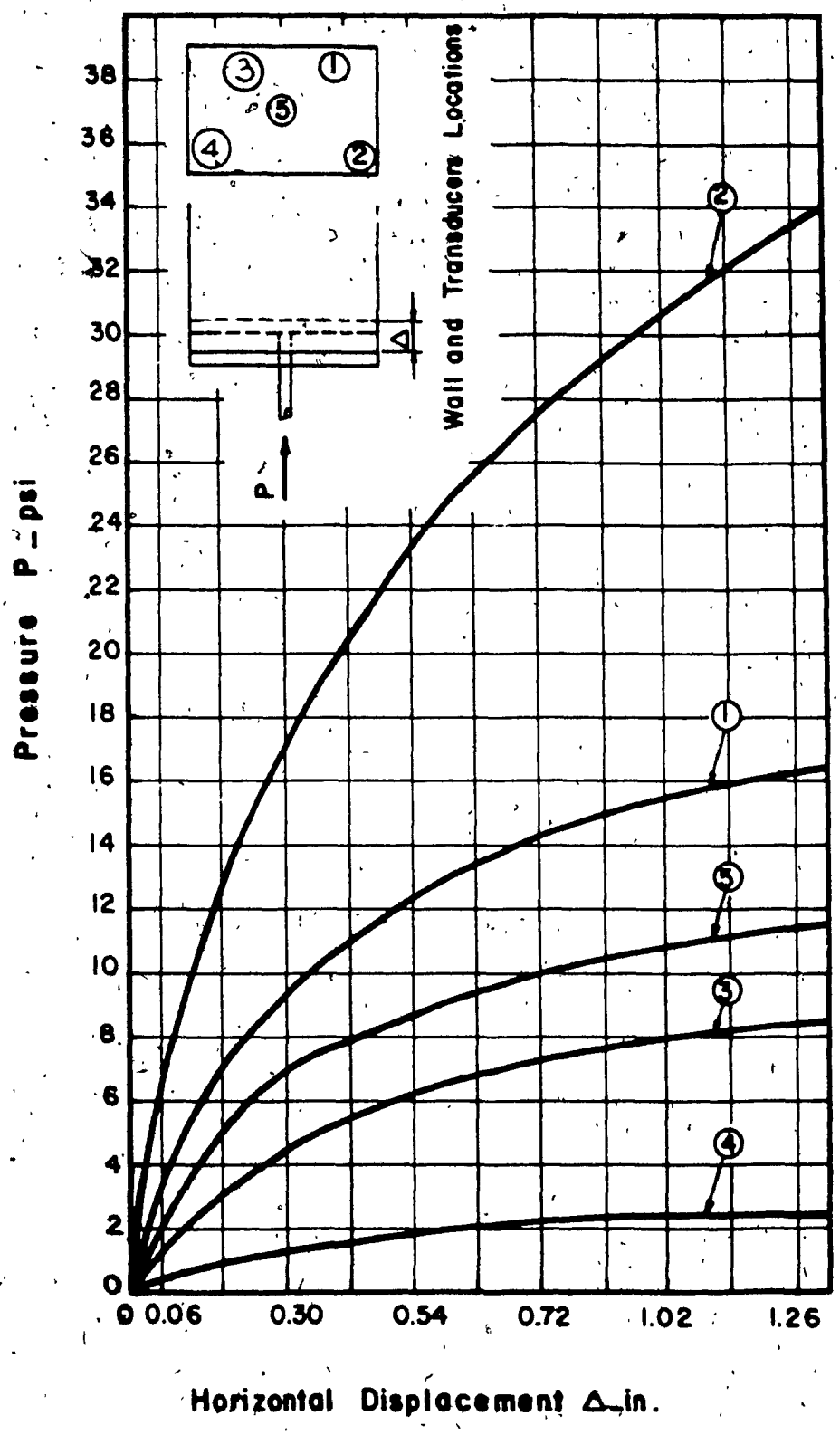

Figure 3.18: Load-settlement curves for each transducer for dense overlying loose sand

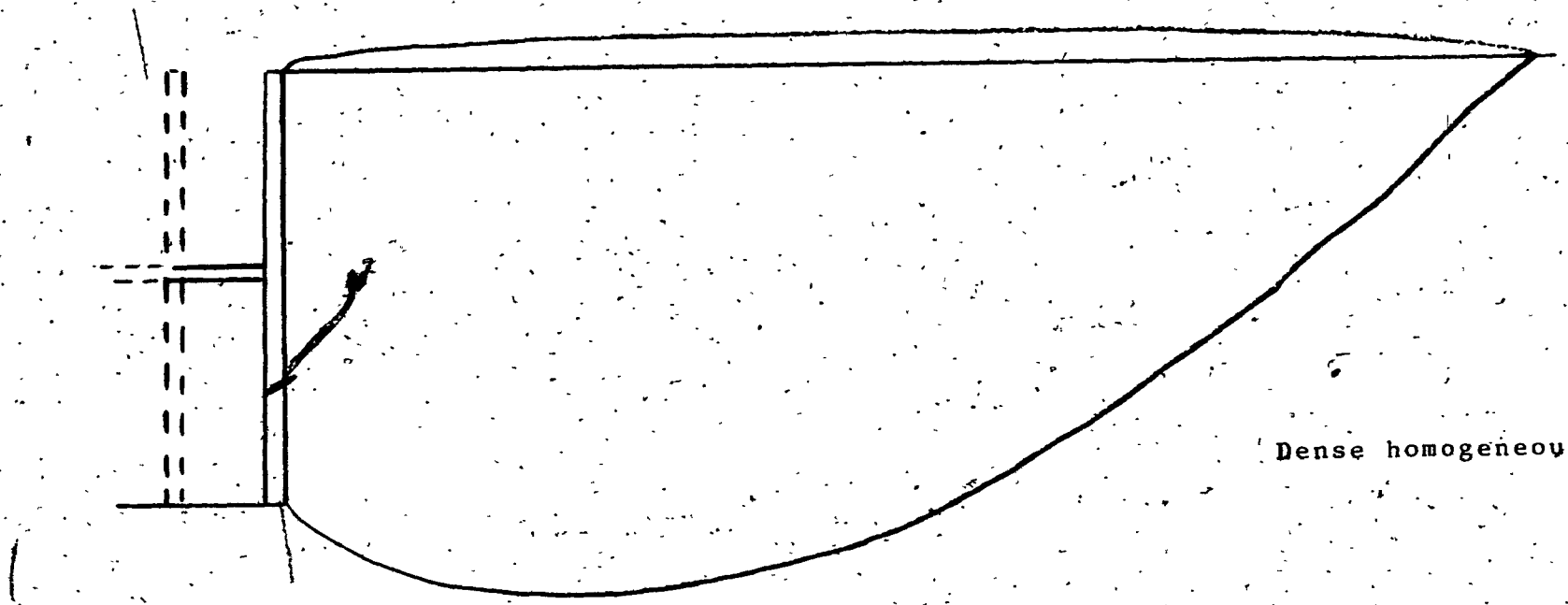

Figure 3.19: Actual failure plane for dense homogeneous sand
Scale 1":1

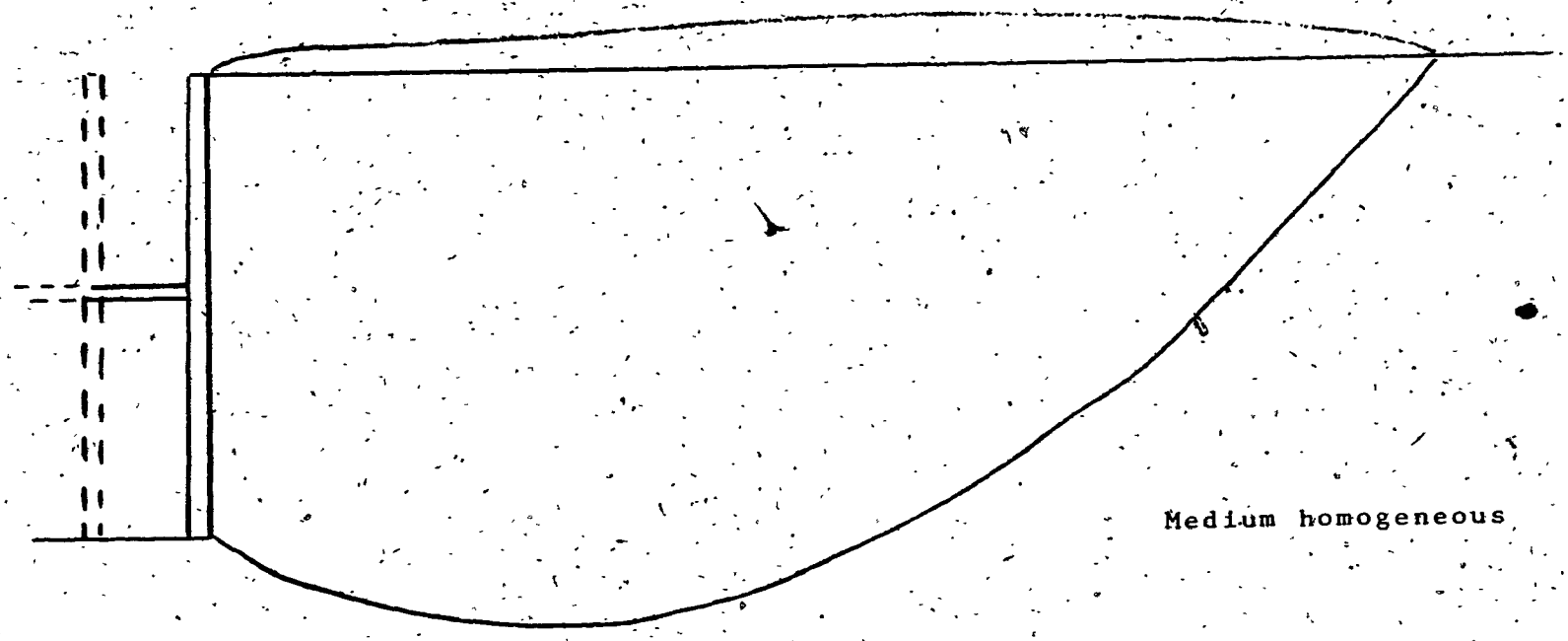

Figure 3.20: Actual failure plane for medium homogeneous sand
Scale 1":1

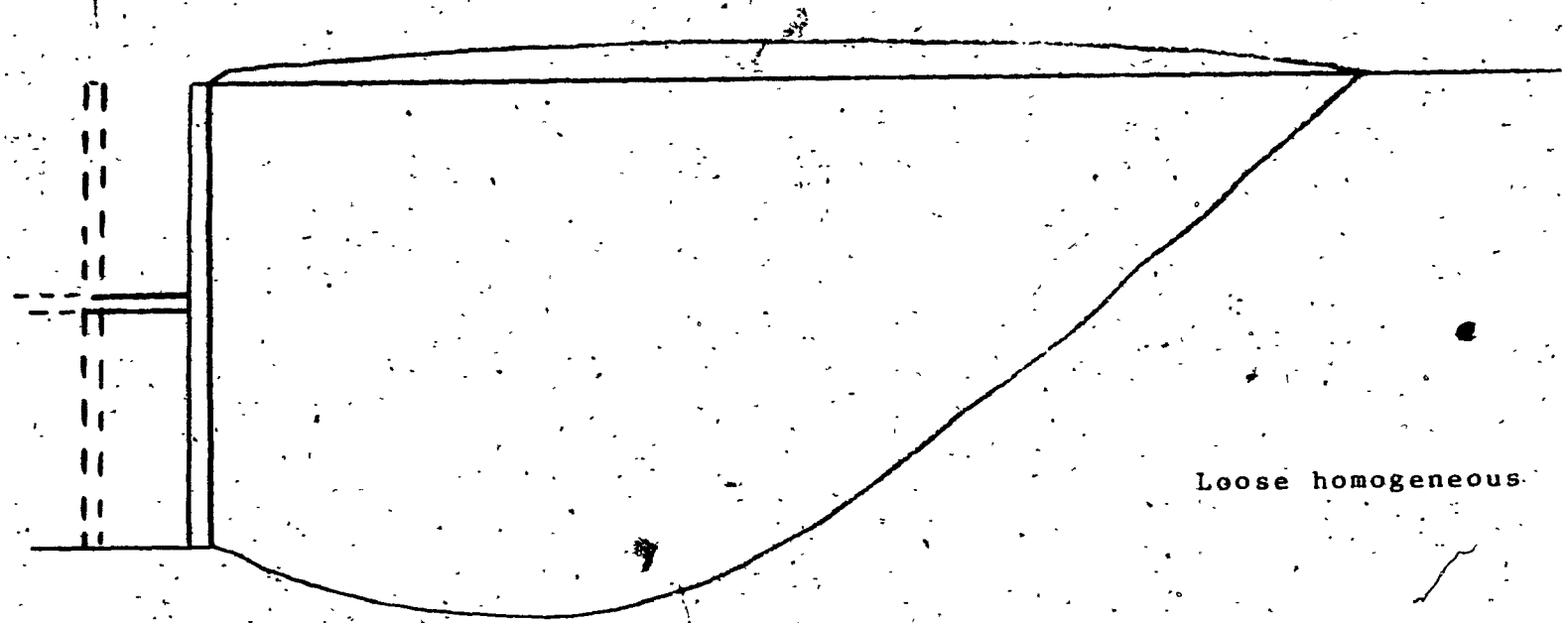

Figure 3.21: Actual failure plane for loose homogeneous sand
Scale 1":1

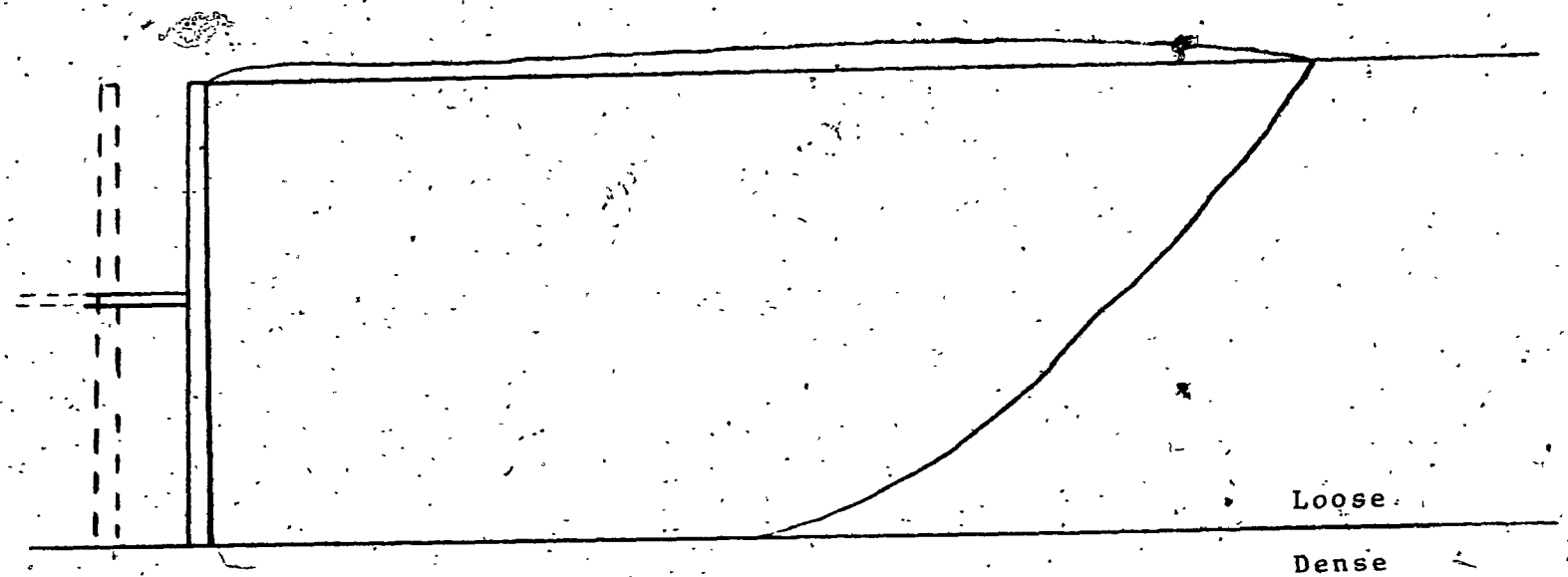

Figure 3.22: Actual failure plane for loose overlying dense sand
Scale ½":1

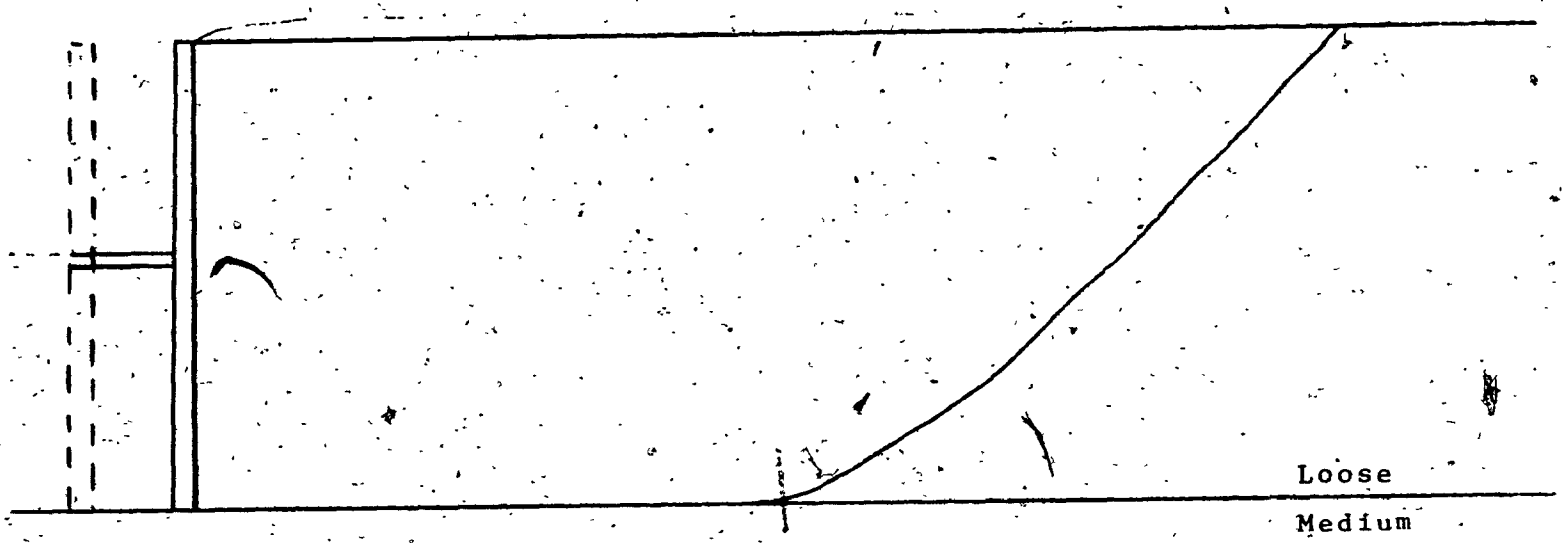

Figure 3.23: Actual failure plane for loose overlying medium sand
Scale ½":1

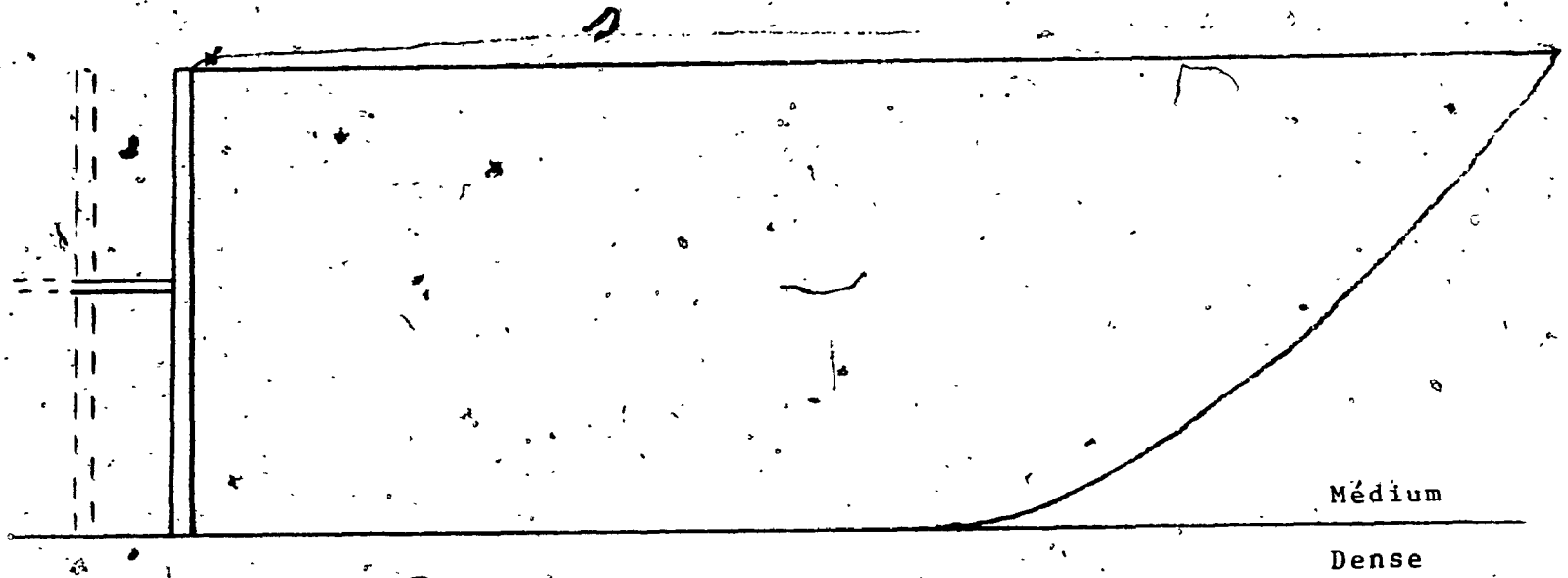

Figure 3.24: Actual failure plane for medium overlying dense sand
Scale 1":1

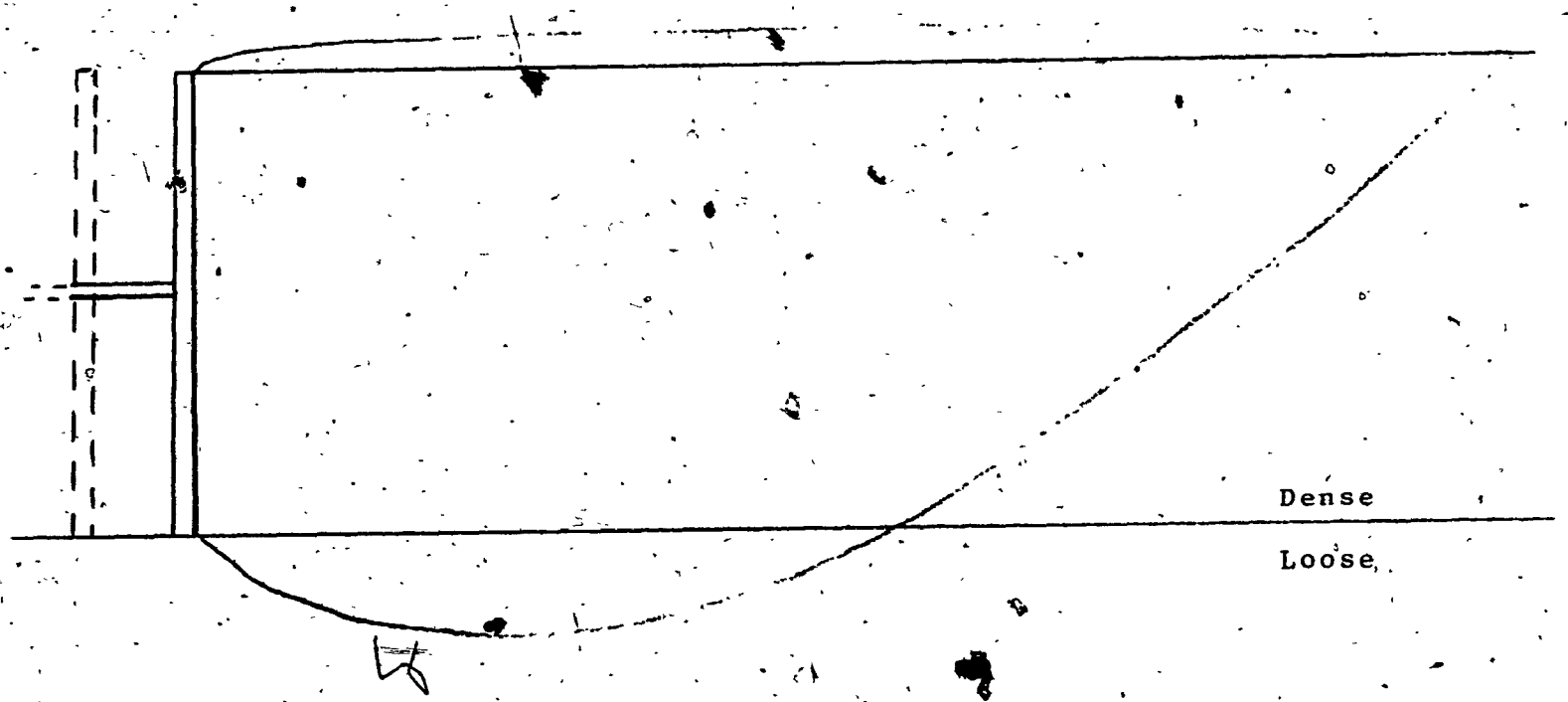

Figure 3.25: Actual failure plane for dense overlying loose sand
scale ½":1

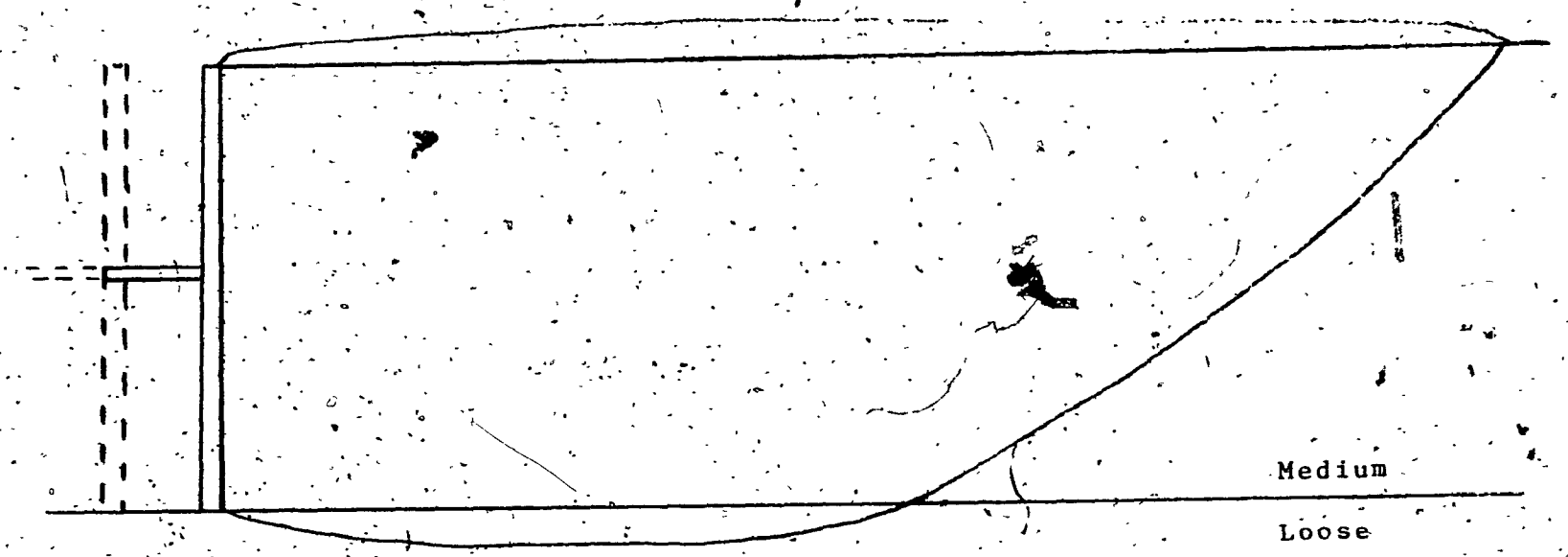

Figure 3.26: Actual failure plane for medium overlying loose sand
Scale 1":1

Figure 3.27: Actual failure plane for dense overlying medium sand
Scale 1":1

holds true (see Figures 3.19 to 3.21). However, once the soil behind the retaining wall is changed to a layered soil, the soil behaviour changes. For the case of the weak layer of soil over the strong layer of soil, the failure line follows the plane of separation of the two layers for a certain length after which it follows the known pattern of an oblique failure line towards the surface (see Figures 3.22 to 3.24). This is due to the lateral compaction of the weaker soil which reacts first.

For the case of the strong layer of soil over the weak layer of soil, it was observed that a certain part of the lower layer gets mobilized before an oblique failure plane starts to appear (see Figures 3.25 to 3.27). This is due to the vertical compaction of the weaker soil which reacts first.

In this present experimental investigation the value of the total passive earth pressure was calculated by integrating the pressure transducer readings on the face of the plate (model retaining wall). The integration was done by approximating the area below the pressure distribution curve with a summation of trapezoids.

The difference obtained between the load cell value and the total passive load equals the frictional resistance value of the apparatus, namely soil friction against the walls and that of the shaft through the ball bearings (see Table 3.1).

Test No.	Test description	Load Cell Reading (lbs) P_{total}	Integration of transducers (lbs) P_p	Frictional resistance value (lbs) P_f
1	dense homogeneous	425	390	35
2	medium homogeneous	380	340	40
3	loose homogeneous	245	220	25
4	dense / medium	390	350	40
5	dense / loose	335	300	35
6	medium / loose	330	290	40
7	medium / dense	380	345	35
8	loose / dense	290	250	40
9	loose / medium	260	230	30

Table 3.1: Calculation of frictional resistance value

CHAPTER 4

ANALYSIS OF RESULTS

4.1 General

The analysis was geared towards developing a technique to evaluate the passive earth pressure behind a retaining wall for layered cohesionless soil.

The experimental results for homogeneous sand were compared with the present theories for homogeneous cohesionless soil. The experimental results for layered soils were compared with the proposed theory and with present theories modified to suit layered soils.

4.2 Analysis of Test Results Using the Logarithmic Spiral Method

In order to analyze the test results by the logarithmic spiral method, Terzaghi's approach to the problem was used. For the homogeneous case the original method was used without any changes. For the weak overlying strong sand and strong overlying weak sand cases, the method was modified in order to accommodate the layered soil condition. Figure 4.1 represents a section through the retaining wall face (ab) in the case of homogeneous soil.

The location of point "d" is not known. The surface of sliding consists of a curved part "bd" and a plane part "de". Within the mass

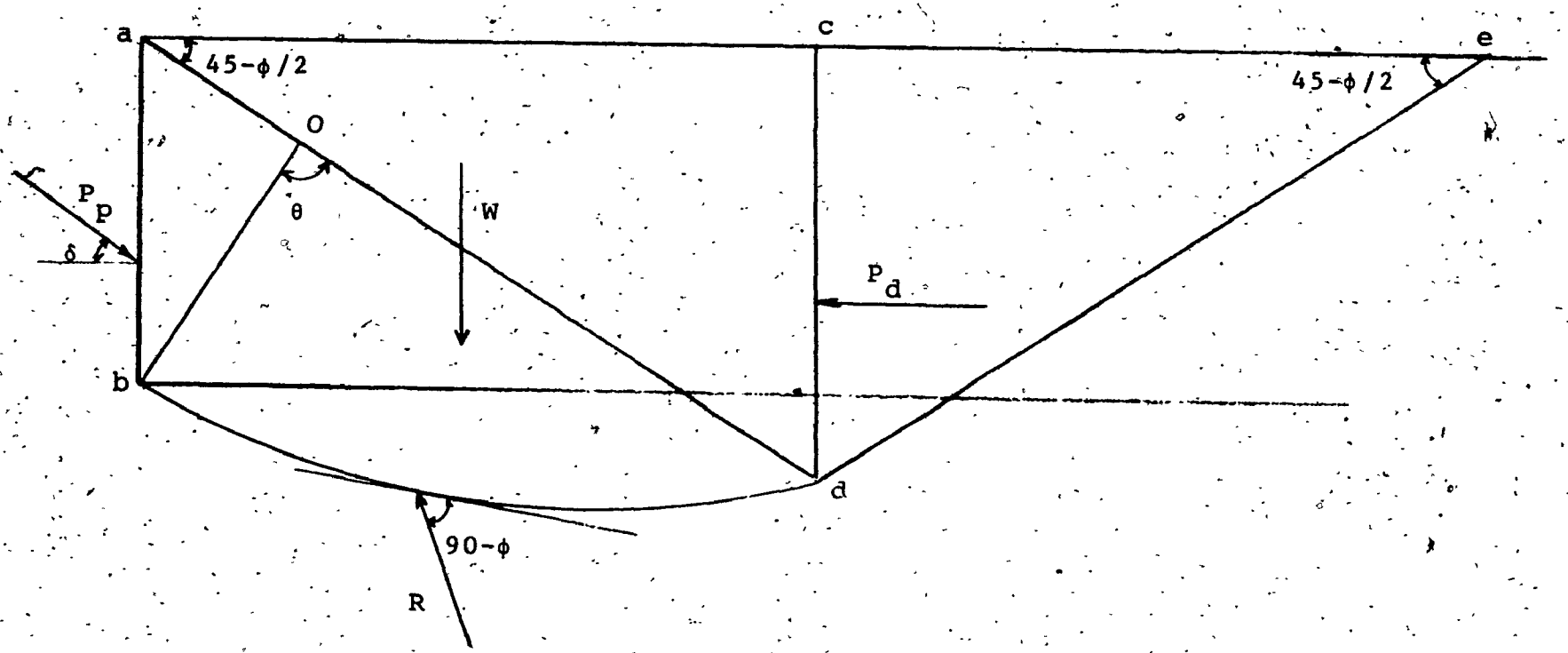

Figure 4.1: Logarithmic spiral method

of soil represented by the triangle "ade" the state of stress is the same as that in a semi-infinite deposit in a passive Rankine state.

The shearing stresses along vertical sections are equal to zero; i.e. the passive earth pressure P_d is acting horizontal on the vertical face "dc" at a depth of $2H_{dc}/3$ and is equal to:

$$P_d = (1/2)\ \gamma H^2_{dc} \tan^2(45+\phi/2) \qquad 4.1$$

The curve "bd" is part of a spiral whose center "O" is on the line "ad" and whose equation is:

$$r=r_o e^{\theta \tan\phi} \qquad 4.2$$

Any vector passing through the center "O" of the spiral intersects the corresponding tangent to the spiral at an angle $90-\phi$, and corresponds to the reaction R. The point of application of the passive earth pressure P_p on the face "ab" is located at a height of H/3 above point "b", and the force makes an angle "δ" with the horizontal. The body of soil "abdc" is acted upon by the weight "W", the horizontal force "P_d", the passive earth pressure "P_p" and the reaction "R". For the equilibrium condition to be satisfied the polygon of forces created by the above named vectors should close. In order to achieve this, the forces "W" and "P_d" are plotted in value and direction.

Afterwards, parallel lines to the reaction "R" and "P_p" are drawn and the polygon of forces is closed, resulting in a value for "P_p". This is

considered one trial and the value P_p is recorded.

A new position for point "d" is chosen and a new spiral will pass through points "b" and "d". The whole operation described above is repeated and the new value of "P_p" is recorded. After a few trials, the lowest recorded value for "P_p" is determined and that is the value of the passive earth pressure acting on the wall.

Figure 4.2 (a, b and c) shows the actual diagrams obtained for the three homogeneous tests carried out during the experimental work. For the case of layered soil, Figure 4.3 represents a section through the retaining wall face (ab).

The curve "bd" in this case is part of a spiral whose equation is:

$$r=r_o e^{\theta \tan \phi_2} \qquad 4.3$$

The reaction R is acting at an angle of $90-\phi_2$ to the tangent to the spiral.

Otherwise, all the forces remain the same as in the homogeneous case.

For the equilibrium condition to be satisfied the moment of all the forces about the center "O" must be equal to zero.

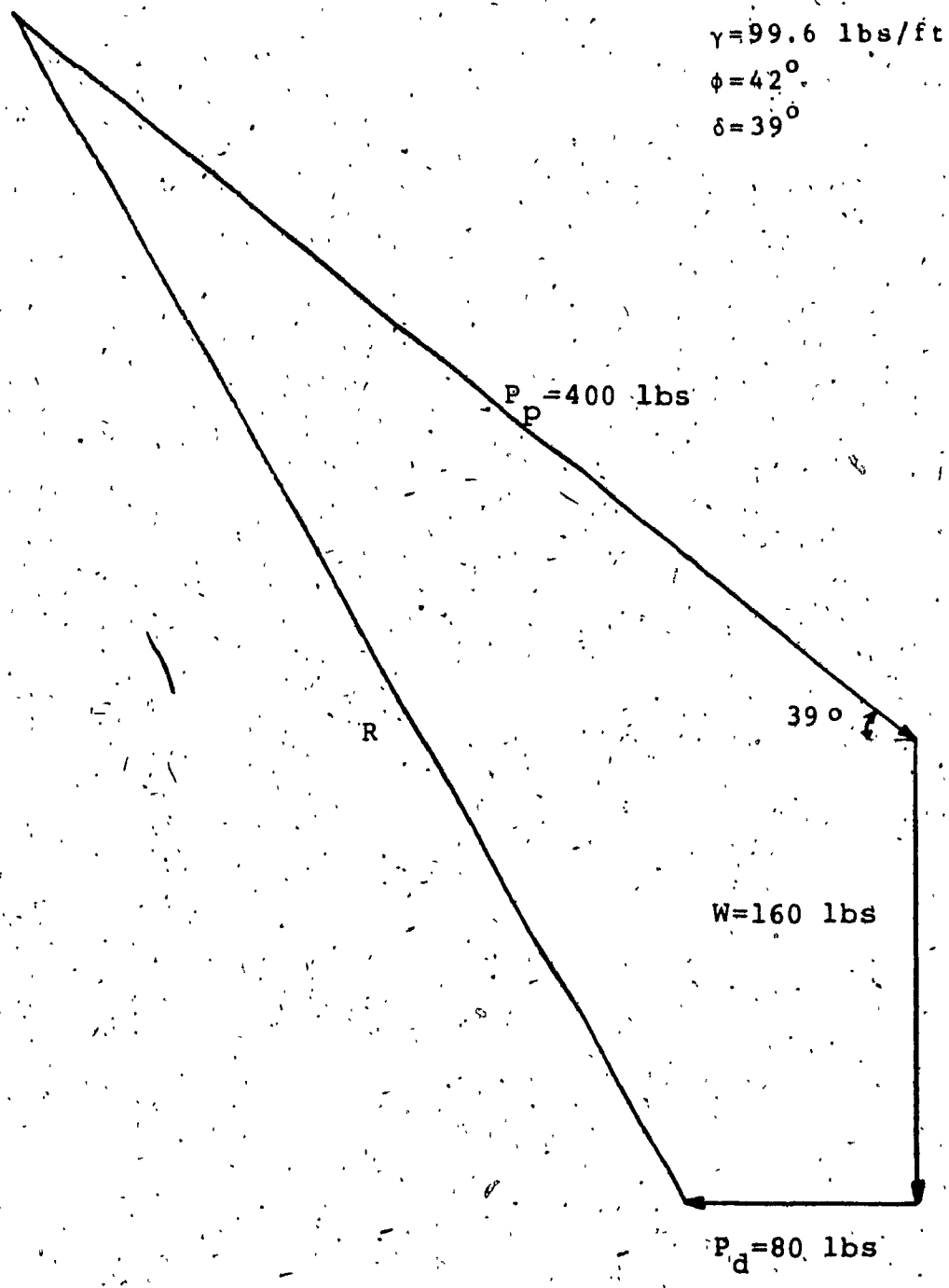

Figure 4.2a: Polygon of forces for dense homogeneous sand

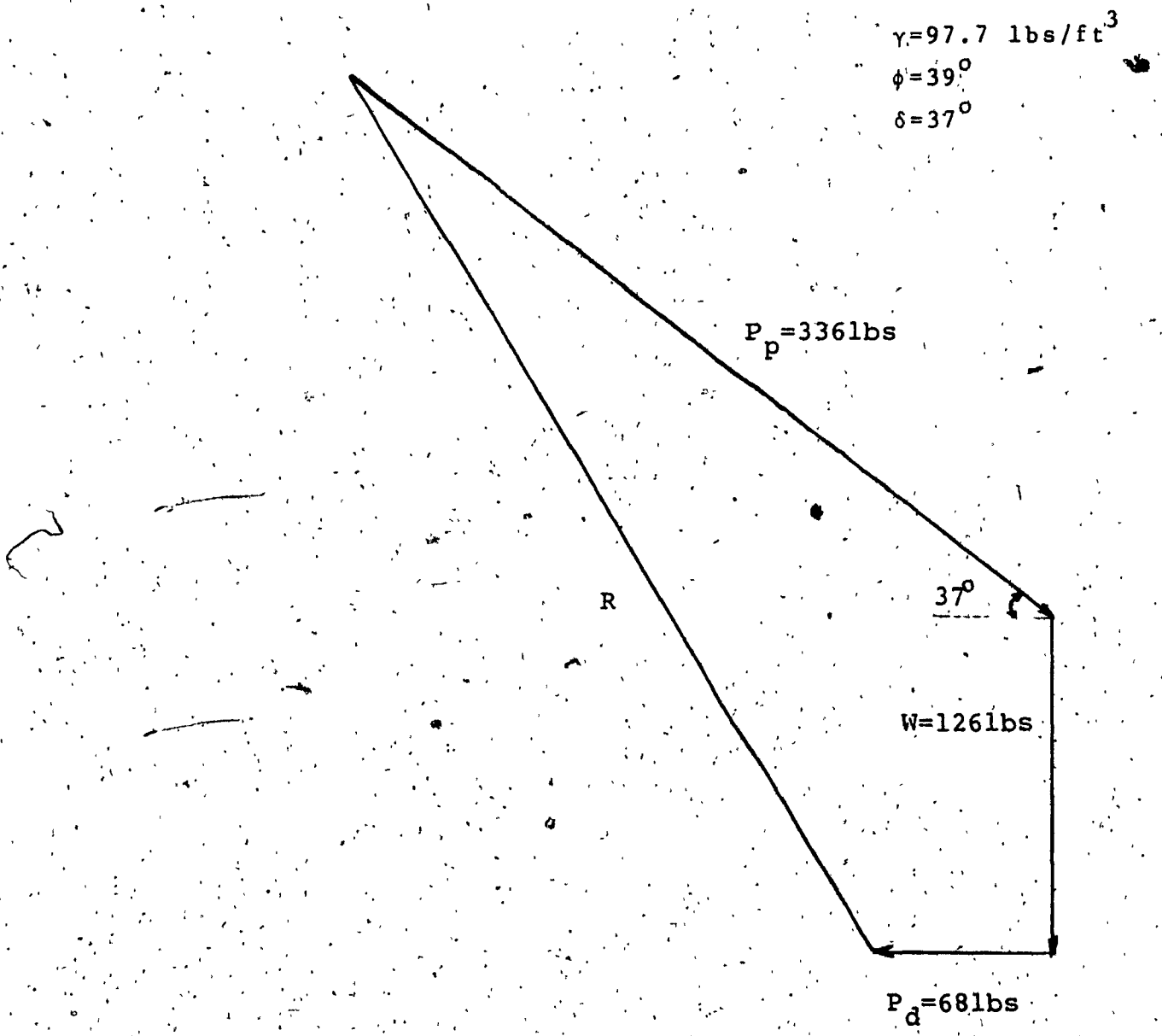

Figure 4.2b: Polygon of forces for medium homogeneous sand

$\gamma = 95.2$ lbs/ft^3
$\phi = 37.5^{o}$
$\delta = 32^{o}$

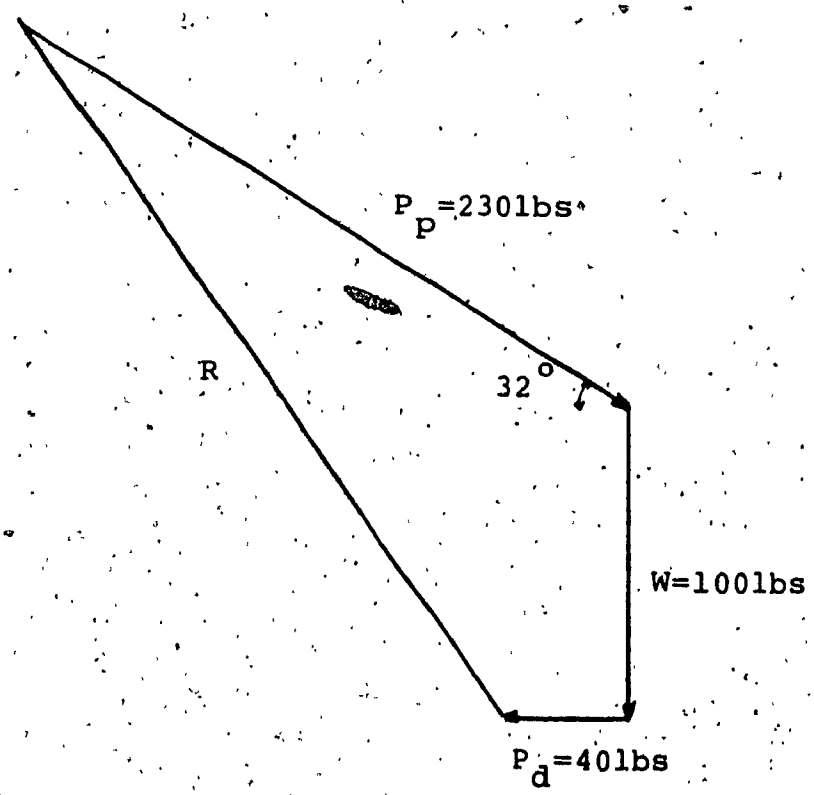

Figure 4.2c: Polygon of forces for loose homogeneous sand

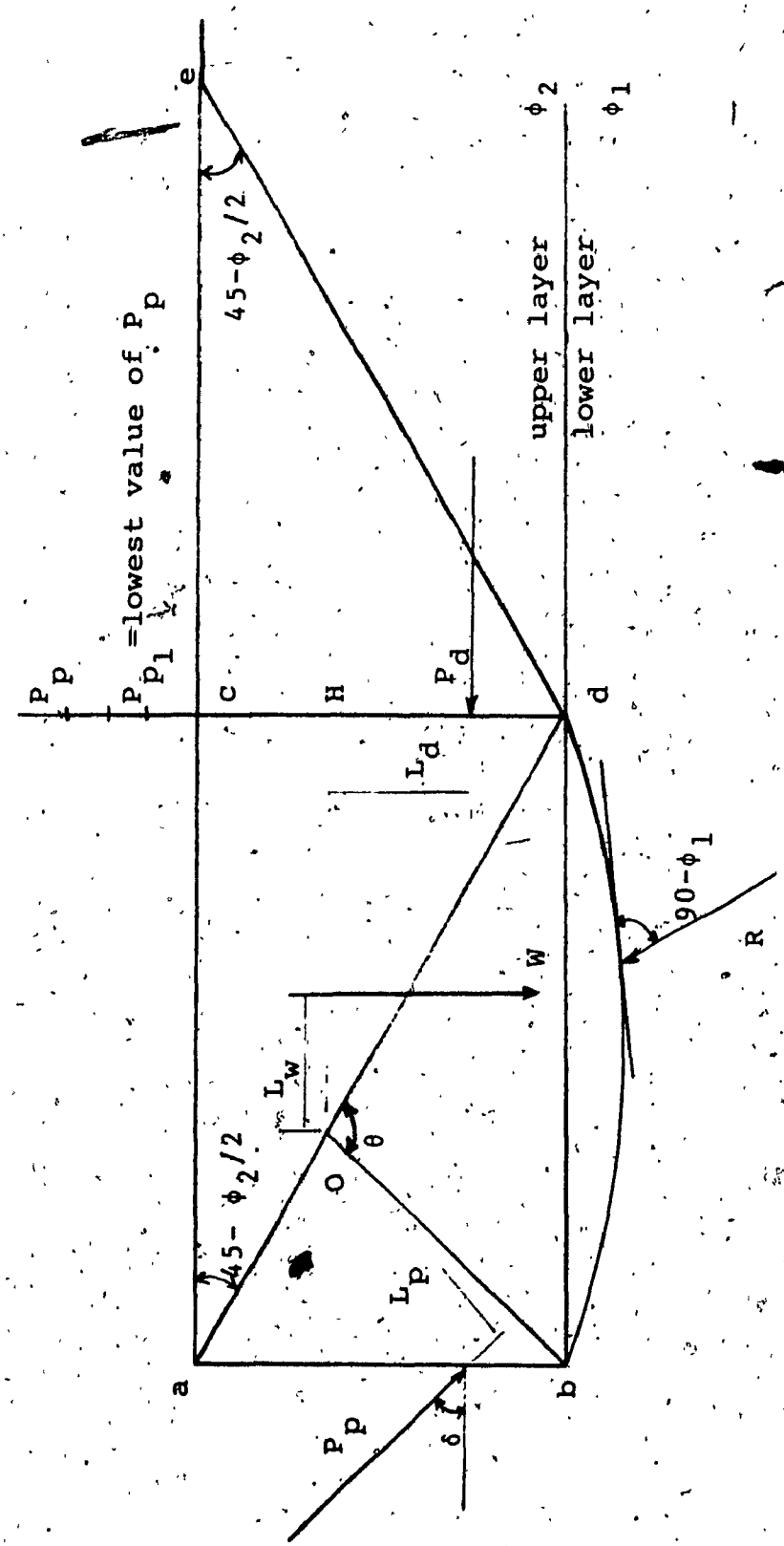

Figure 4.3: Logarithmic spiral method for layered sand

Therefore:

$$P_p \cdot L_p + W \cdot L_w + P_d \cdot L_d = 0 \qquad 4.4$$

and

$$P_p = -(1/L_p)(W \cdot L_w + P_d \cdot L_d) \qquad 4.5$$

where

P_p = passive earth pressure

W = weight of soil

P_d = passive earth pressure according to Rankine

L_p = arm of the passive earth force

L_w = arm of the weight force

L_d = arm of the passive earth force according to Rankine

A few trials have to be executed in order to determine the lowest value of P_p.

An example is explained below for a strong/weak case of layered soil and tables for the other cases follow.

Choosing the dense/loose test we have:

γ dense = 99.6 lb/ft^3	H = .71 ft	γ loose = 95.2 lb/ft^3
ϕ dense = 42°	width = .64 ft	ϕ loose = 37.5°

$$P_d = (1/2)\gamma_{dense} H^2 \tan^2(45 + \frac{\phi_{dense}}{2}) =$$

$$= (.5)(99.6)(.71)^2\tan^2(45+21) = 126 \text{ lbs/ft of wall}$$

$$P_d = 126 \cdot \text{width} = 126 \cdot (.64) = 80 \text{ lbs}$$

First trial

Establishing the spiral:

$r_o = 0.67$ ft $\theta = 85° = 0.46\ \pi$ rad

$W = \text{Area}_{abdc} \cdot \text{Width} \cdot \text{dense} - \text{Area}_{bdb} \cdot \text{Width} \cdot \text{loose}$

$\text{Area}_{abdc} = \text{Area}_{aob} + \text{Area}_{adc} + \text{Area}_{obd}$

$\text{Area}_{\overset{\frown}{bdb}} = \text{Area}_{\overset{\frown}{obd}} - \text{Area}_{obd}$

$\text{Area}_{aob} = 0.14 \text{ ft}^2$

$\text{Area}_{adc} = 0.55 \text{ ft}^2$

$$\text{Area}_{\overset{\frown}{obd}} = \frac{r_o^2(e^{2\theta\tan\phi_2}-1)}{4\tan\phi_2} = 1.33 \text{ ft}^2$$

$\text{Area}_{obd} = 0.78 \text{ ft}^2$

$\text{Area}_{abdc} = 0.14+0.55+1.33 = 2.02 \text{ ft}^2$

$W = (2.02)(\text{Width})(99.6)-(1.33-0.78)(\text{Width})(95.2) = 95$ lbs

$P_p = -(1/L_p)(W \cdot L_w + P_d \cdot L_d) = -(1/L_p)(95 \cdot L_w + 80 \cdot L_d)$

$L_p = 0.29$ ft

$L_w = 0.67$ ft

$L_d = 0.42$ ft

$P_p = -(1/0.29)(95 \cdot 0.67 + 80 \cdot 0.42) = 333.27$ lbs

Second trial

r_o = 0.75 ft θ = 90° = π/2 rad

The whole sequence of operations is repeated and another value for P_p is obtained. Specifically P_p = 518.8 lbs.

Table 4.1 shows the mathematical approach to obtaining the minimum value for P_p.

The value of the lowest passive earth pressure is P_p = 333.27 lbs.

It compares favourably to the test value of 300 lbs., at 11% error. In the tables 4.2 and 4.3 the values of passive earth pressures in the remaining combination of strong/weak layered soils were determined.

4.3 Analysis of Test Results Using Method of Slices

The test results were also analyzed by means of the method of slices suggested by Shields in 1973.

For the case of slice 2 in Figure 4.4, the summation of the forces in the horizontal, X, direction will yield:

$$E+dE-E-R\sin(\alpha+\phi) = 0$$

where:

c = u = 0

E and E+dE = horizontal forces

Trial No.	1 $1/L_p$ ft^{-1}	2 W lbs	3 L_w ft	4 2 x 3 WxL_w	5 P_d lbs	6 L_d ft	7 5 x 6 $P_d xL_d$	8 1 x (4+7) P_p lbs	9 Minimum P_p lbs
1	3.45	95	.666	63.3	80	.416	33.3	333.27	333.27
2	3.69	208	.5	104	80	.458	36.6	518.8	----
3	3.42	190	.4	87	80	.416	33.3	411.4	----
4	3.53	185	.438	81	80	.438	35	409.5	----

Table 4.1: Calculation of the passive earth pressure for dense overlying loose sand

Trial No.	1 $1/L_p$ ft^{-1}	2 W lbs	3 L_w ft	4 2 x 3 WxL_w	5 P_d lbs	6 L_d ft	7 5 x 6 $P_d x L_d$	8 1 x (4+7) P_p lbs	9 Minimum P_{p_d} lbs
1	3	190	.458	87	80	.416	33.3	360.9	360.9
2	3.69	210	.5	105	80	.458	36.6	522.8	-----
3	4	180	.446	80	80	.438	35	460	-----
4	3.53	200	.438	87.5	80	.45	36	435.9	-----

Table 4.2: Calculation of the passive earth pressure for dense overlying medium sand

Trial No.	1 $1/L_p$ ft^{-1}	2 W lbs	3 L_w ft	4 2 x 3 WxL_w	5 P_d lbs	6 L_d ft	7 5 x 6 P_dxL_d	8 1 x (4+7) P_p lbs	9 Minimum P_p lbs
1	4	150	.416	62.5	69	.416	29	366	-----
2	3.5	160	.375	60	69	.391	27	304.5	304.5
3	4	170	.375	63.8	69	.391	27	363	-----
4	3.43	180	.392	70.5	69	.4	27.6	336.3	-----

Table 4.3: Calculation of the passive earth pressure for medium overlying loose sand

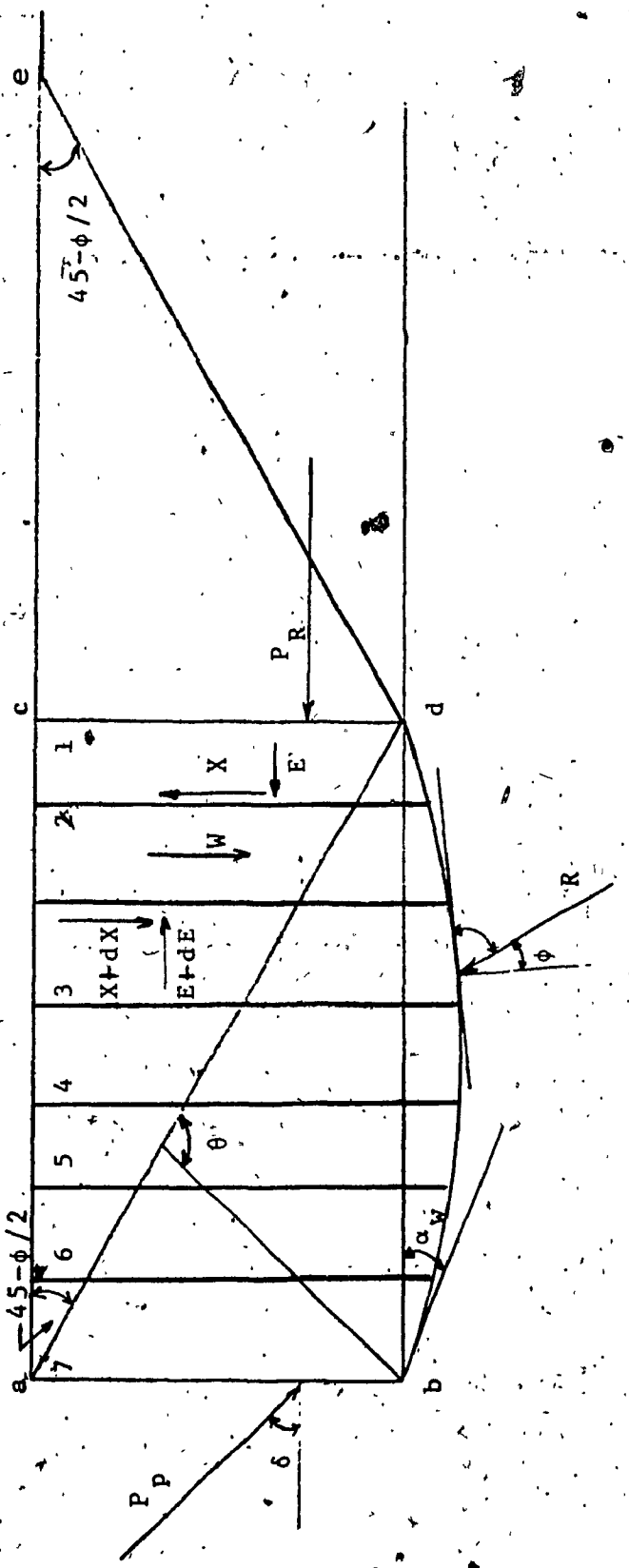

Figure 4.4: The method of slices

R = resultant of tangential and normal forces on the plane of failure

α = inclination of the plane of failure to the horizontal

ϕ = internal friction angle

Hence,

$$dE - R\sin(\alpha+\phi) = 0 \qquad 4.7$$

For the vertical, Y, direction:

$$W+X+dX-X-R\cos(\alpha+\phi) = 0 \qquad 4.8$$

where: W = weight of the slice
X and X+dX = shear forces on the sides of the slice

Therefore,

$$W+dX = R\cos(\alpha+\phi) \qquad 4.9$$

For layered sand conditions the value of the weight W is a proportionate combination of the weights of the respective layers within the slice.

Therefore,

$$dE = \frac{W + dX}{\cos(\alpha+\phi)} \sin(\alpha+\phi) = W+dX \tan(\alpha+\phi) \qquad 4.10$$

The new term that Shields brings in, different from Terzaghi is the angle at which the logarithmic spiral will leave the bottom of the wall. That angle, α_w is

$$\alpha_w = (1/2)(\arccos(\cos(\phi-\delta) - \sin(\phi-\delta)/\tan\phi) - \phi - \delta) \qquad 4.11$$

Therefore, knowing the angle of internal friction ϕ and the roughness of the wall δ, the failure surface can be precisely established.

The soil edge cde is in a passive Rankine state and the value of the passive force P_R acting at height H_R is:

$$P_R = (1/2)\gamma H_R^2 \tan^2(45+\phi/2) \qquad 4.12$$

and

$$dE = \Sigma(W+dX)(\tan(\alpha+\phi)) \qquad 4.13$$

Therefore

$P_p = P_R + \Sigma(W+dX)\cdot\tan(\alpha+\phi)$ where X=o at CD

and $X+dX = P_p\tan\delta$ at the wall

and

$P_p = P_R+\Sigma W\tan(\alpha+\phi)+dX\tan(\alpha+\phi)$

at the wall $\alpha=\alpha_w$ and $dX = P_p\tan\delta$

Hence

$$P_p = P_R+\Sigma(W\tan(\alpha+\phi) + P_p\tan\delta\tan(\alpha_w+\phi) \qquad 4.14$$

and

$$P_p(1-\tan\delta\tan(\alpha_w+\phi) = P_R+\Sigma(W\tan(\alpha+\phi)) \qquad 4.15$$

Therefore

$$P_p = \frac{P_R+\Sigma W\tan(\alpha+\phi)}{1-\tan\delta\tan(\alpha_w+\phi)} \qquad 4.16$$

and

$$P_R = (.5)\gamma H^2\tan^2(45+\phi/2)$$

Hence

$$P_p = \frac{(1/2)\gamma H^2 \tan^2(45+\phi/2)+\Sigma W\tan(\alpha+\phi)}{1-\tan\delta\tan(\alpha_w+\phi)} \qquad 4.17$$

Tables 4.4 to 4.6 represent the homogeneous cases.

For the layered soils condition the equation 4.11 should be modified to:

$$\alpha_w = (1/2)(\arccos(\cos(\phi_{weak}-\delta) \\ -s[illegible]_{weak}-\delta)/\tan\phi_{weak})-\phi_{weak}-\delta) \qquad 4.18$$

and equation 4.17 should be modified to:

$$P_p = \frac{(1/2)\gamma_{\substack{upper\\layer}} H^2 \tan^2(45+\phi_{\substack{upper\\layer}})+\Sigma W\tan(\alpha+\phi_{strong})}{1-\tan\delta\tan(\alpha_w+\phi_{\substack{lower\\layer}})} \qquad 4.19$$

Tables 4.7 to 4.12 show the calculations according to the above changes to the original formulae.

After analysing the results, the following empirical theory can be formulated. For the case of a layered soil condition behind the retaining wall the only time a correction should be made to the existing theory is for a strong/weak layers condition.

Slice No.	1 P_R lbs	2 w_i lbs	3 α_i deg.	4 ϕ_i deg.	5 $\tan(\alpha_i+\phi_i)$	6 2 x 5 $w_i\tan(\alpha_i+\phi_i)$	7 Σ 6 $\Sigma w_i\tan(\alpha_i+\phi_i)$	8 $1-\tan\delta$ x x $\tan(\alpha_w+\phi)$	9 1 + 7/8 P_p lbs
1		14	-18	37.5	.354	4.96			
2		17.5	-16	37.5	.394	6.9			
3		23.3	-3	37.5	.687	16			
4		23.3	+6	37.5	.949	22.12			
5		21	+12	37.5	1.17	24.57			
6		17.5	+22	37.5	1.7	29.75			
	62.6						104.3	.802	207.85

$\delta = 32^\circ$ $\phi_{loose} = 37.5^\circ$ $\alpha_w = -20^\circ$

Table 4.4: Calculation of the passive earth pressure for loose homogeneous sand

Slice No.	1 P_R lbs	2 w_i lbs	3 α_i deg.	4 ϕ_i deg.	5 $\tan(\alpha_i+\phi_i)$	6 2 x 5 $w_i\tan(\alpha_i+\phi_i)$	7 Σ 6 $\Sigma w_i\tan(\alpha_i+\phi_i)$	8 $1-\tan\delta$ x x $\tan(\alpha_w+\phi)$	9 1 + 7/8 P_p lbs
1		17.5	-20	39	.344	6.03			
2		21	-6	39	.65	13.64			
3		24	+5	39	.965	23.2			
4		27	+15	39	1.37	37.2			
5		26	+22	39	1.8	46.8			
6		22.75	+25	39	2.5	46.63			
Total	69						173.5	.87	280

$\delta = 37^o$ $\phi_{medium} = 39^o$ $\alpha_w = 29.5^o$

Table 4.5: Calculation of the passive earth pressure for medium homogeneous sand

Slice No.	1 P_R lbs	2 w_i lbs	3 α_i deg.	4 ϕ_i deg.	5 $\tan(\alpha_i+\phi_i)$	6 2 x 5 $w_i\tan(\alpha_i+\phi_i)$	7 Σ 6 $\Sigma w_i\tan(\alpha_i+\phi_i)$	8 $1-\tan\delta$ x x $\tan(\alpha_w+\phi)$	9 1 + 7/8 P_p lbs
1		16.5	-17	42	.466	7.7			
2		21	-5	42	.754	15.8			
3		23.9	0	42	.9	21.5			
4		28	18	42	1.73	48.4			
5		29.4	21	42	1.96	57.6			
6		23.3	24.5	42	2.3	53.6			
	80.4						204.6	.835	341.5

$\delta=39^\circ$ $\phi=42^\circ$ $\alpha_w=-30^\circ$

Table 4.6: Calculation of the passive earth pressure for dense homogeneous sand

Slice No.	1 P_R lbs	2 w_i lbs	3 α_i deg.	4 ϕ_i deg.	5 $\tan(\alpha_i+\phi_i)$	6 2 x 5 $w_i\tan(\alpha_i+\phi_i)$	7 Σ 6 $\Sigma w_i\tan(\alpha_i+\phi_i)$	8 $1-\tan\delta$ x x $\tan(\alpha_w+\phi)$	9 $1+A/8$ P_p lbs
1		15	-25	42	.305	4.6			
2		19.2	- 6	42	.726	14.02			
3		20.1	4	42	1.04	21			
4		20	11	42	1.32	26.4			
5		19.7	18	42	1.73	34.1			
6		18	23.5	42	2.2	39.6			
	80						139.72	.835	265

$\delta=39^o$ $\phi_{dense}=42^o$ $\phi_{loose}=37.5^o$ $\alpha_w=-30.5^o$

Table 4.7: Calculation of the passive earth pressure for dense overlying loose sand

Slice No.	1 P_R lbs	2 w_i lbs	3 α_i deg.	4 ϕ_i deg.	5 $\tan(\alpha_i+\phi_i)$	6 2 x 5 $w_i\tan(\alpha_i+\phi_i)$	7 Σ 6 $\Sigma w_i\tan(\alpha_i+\phi_i)$	8 $1-\tan\delta$ x x $\tan(\alpha_w+\phi)$	9 1 + 7/8 P_p lbs
1		21	-28	42	.25	5.25			
2		24	-18	42	.45	10.8			
3		29	5	42	1.07	30.45			
4		29.5	11	42	1.33	39.2			
5		29	21	42	1.96	56.8			
6		27.5	24	42	2.25	61.9			
	80.5						204.4	.827	345

$\delta=39^\circ$ $\phi_{dense}=42^\circ$ $\phi_{medium}=39^\circ$ $\alpha_w=-30^\circ$

Table 4.8: Calculation of the passive earth pressure for dense overlying medium sand

Slice No.	1 P_R lbs	2 w_i lbs	3 α_i deg.	4 ϕ_i deg.	5 $\tan(\alpha_i+\phi_i)$	6 2 x 5 $w_i\tan(\alpha_i+\phi_i)$	7 Σ 6 $\Sigma w_i\tan(\alpha_i+\phi_i)$	8 $1-\tan\delta$ x x $\tan(\alpha_w+\phi)$	9 1 + 7/8 P_p lbs
1		17.5	-26	39	.23	4.03			
2		21.6	-11	39	.53	11.45			
3		23.7	0	39	.81	19.20			
4		25	6	39	1.0	25			
5		23.6	18	39	1.54	36.34			
6		21	25	39	2.05	43.15			
	69						139.07	.87	240

$\delta=37^o$ $\phi_{medium}=39^o$ $\phi_{loose}=37.5^o$ $\alpha_w=-30.5^o$

Table 4.9: Calculation of the passive earth pressure for medium overlying loose sand

Slice No.	1 P_R lbs	2 w_i lbs	3 α_i deg.	4 ϕ_i deg.	5 $\tan(\alpha_i+\phi_i)$	6 2 x 5 $w_i\tan(\alpha_i+\phi_i)$	7 Σ 6 $\Sigma w_i\tan(\alpha_i+\phi_i)$	8 $1-\tan\delta$ x x $\tan(\alpha_w+\phi)$	9 1 + 7/8 P_p lbs
1		10.75	0	37.5	.767	8.25			
2		10.25	0	37.5	.767	8.25			
3		10.25	0	37.5	.767	8.25			
4		10.25	0	37.5	.767	8.25			
5		10.25	0	37.5	.767	8.25			
6		10.25	0	37.5	.767	8.25			
	62.6						49.5	.437	256

$\delta=32^\circ$ $\phi_{loose}=37.5^\circ$ $\phi_{dense}=42^\circ$ $\alpha_w=0^\circ$

Table 4.10: Calculation of the passive earth pressure for loose overlying dense sand

Slice No.	1 P_R lbs	2 w_i lbs	3 α_i deg.	4 ϕ_i deg.	5 $\tan(\alpha_i+\phi_i)$	6 2 x 5 $w_i\tan(\alpha_i+\phi_i)$	7 Σ 6 $\Sigma w_i\tan(\alpha_i+\phi_i)$	8 $1-\tan\delta$ x x $\tan(\alpha_w+\phi)$	9 1 + 7/8 P_p lbs
1		10.75	0	37.5	.767	8.25			
2		10.75	0	37.5	.767	8.25			
3		10.25	0	37.5	.767	8.25			
4		10.25	0	37.5	.767	8.25			
5		10.25	0	37.5	.767	8.25			
6		10.25	0	37.5	.767	8.25			
	62.6						49.5	.494	226.3

$\delta=32^\circ$ $\phi_{loose}=37.5^\circ$ $\phi_{medium}=39^\circ$ $\alpha_w=0^\circ$

Table 4.11: Calculation of the passive earth pressure for loose overlying medium sand

Slice No.	1 P_R lbs	2 w_i lbs	3 α_i deg.	4 ϕ_i deg.	5 $\tan(\alpha_i+\phi_i)$	6 2 x 5 $w_i\tan(\alpha_i+\phi_i)$	7 Σ 6 $\Sigma w_i\tan(\alpha_i+\phi_i)$	8 $1-\tan\delta$ x x $\tan(\alpha_w+\phi)$	9 1 + 7/8 P_p lbs
1		13	0	39	.81	10.5			
2		13	0	39	.81	10.5			
3		13	0	39	.81	10.5			
4		13	0	39	.81	10.5			
5		13	0	39	.81	10.5			
6		13	0	39	.81	10.5			
	69						63	.389	338.6

$\delta=37^\circ$, $\phi_{medium}=39^\circ$ $\phi_{dense}=42^\circ$ $\alpha_w=0^\circ$

Table 4.12: Calculation of the passive earth pressure for medium overlying dense sand

In this case, it was observed that the value of the passive earth pressure is lower than the value of the passive earth pressure determined by means of the existing theories.

Therefore,

$$P_{p\ \frac{\text{strong}}{\text{weak}}} < P_{p\ \text{strong homogeneous}} \qquad 4.20$$

A constant was introduced in order to transform the inequality into an equality.

$$P_{p\ \frac{\text{strong}}{\text{weak}}} = \lambda \cdot P_{p\ \text{strong homogeneous}} \qquad 4.21$$

Empirically it was determined from the tests that the value of λ corresponds to:

$$\lambda = \frac{k_{p\ \text{weak homogeneous}}}{k_{p\ \text{strong homogeneous}}} \qquad 4.22$$

where k_p is the coefficient of passive earth pressure for the respective soil condition.

Hence:

$$P_{p\ \frac{\text{strong}}{\text{weak}}} = \frac{k_{p\ \text{weak homogeneous}}}{k_{p\ \text{strong homogeneous}}} \cdot P_{p\ \text{strong homog.}} \qquad 4.23$$

and

$$(1/2)\gamma H^2 k_{p\ \frac{strong}{weak}} = \frac{k_{p\ weak}}{k_{p\ strong}} (1/2)\gamma H^2 k_{p\ strong} \qquad 4.24$$

The conclusion is therefore that:

$$k_{p\ \frac{strong}{weak}} = k_{p\ weak\ homogeneous} \qquad 4.25$$

For the case of a weak/strong layer of sand the following reasoning applies, based on the test results and observations:

$$P_{p\ \frac{weak}{strong}} = P_{p\ weak\ homogeneous} \qquad 4.26$$

and

$$(1/2)\gamma H^2 k_{p\ \frac{weak}{strong}} = (1/2)\gamma H^2 k_{p\ weak\ homogeneous} \qquad 4.27$$

Hence,

$$k_{p\ \frac{weak}{strong}} = k_{p\ weak\ homogeneous} \qquad 4.28$$

Comparing equations 4.25 and 4.28 we have

$$k_{p\ \frac{strong}{weak}} = k_{p\ weak\ homogeneous} = k_{p\ \frac{weak}{strong}} \qquad 4.29$$

and the general conclusion for layered soils condition is that the value of the coefficient of passive earth pressure to be used when calculating

the passive earth pressure should be

$$K_p \text{ layered soil} = K_p \text{ weaker layer} \qquad 4.30$$

In order to verify the theory presented, the computer program developed by Hanna & Foriero (1985) for the particular case of an anchor plate (when it acts as a retaining wall) was used.

As an input data, the angle of internal friction of the weakest layer was used in order to determine the value of the coefficient of passive earth pressure K_p with which to calculate the passive earth pressures for layered soils conditions.

Using the computer results of the coefficient of passive earth pressure thus obtained and the test results we can prove that the proposed theory holds true.

The computer program is presented in the appendix of the thesis.

For example, in the case of dense/medium soil which is a strong layer overlying a weak layered soil condition, the passive earth pressure that resulted from the tests was 350 lbs.

Actual theories would have come up with 390 lbs., the same as for the dense homogeneous case.

Using the formula in equation 4.23,

$$P_{p\ \frac{\text{strong}}{\text{weak}}} = \frac{k_p \text{ weak homog.}}{k_p \text{ strong homog.}} \cdot P_p \text{ strong homog.}$$

gives:

$$P_{p\ \frac{\text{dense}}{\text{medium}}} = \frac{k_p \text{ medium homog.}}{k_p \text{ dense homog.}} \cdot P_p \text{ dense homog.}$$

$$= \frac{k_p \text{ medium homog.}}{k_p \text{ dense homog.}} \cdot (1/2)(\gamma_{dense})H^2 \cdot \text{width} \cdot k_p \text{ dense homog.}$$

$$= (21.76)(1/2)(99.6)(8.5/12)^2(7.65/12) = 346.6 \text{ lbs}$$

Actual value for this particular test was 350 lbs., a difference of only 1% but overall much more conservative than the value present theories would have resulted in.

A summation of all results and comparisons is presented in Table 4.13a and 4.13b.

A comparison of the experimental values of K_p for layered cohesionless soils versus theoretical values is presented in Figures 4.5a and 4.5b.

Test No.	Material	Present Test Results	Logarithmic Spiral Terzaghi	Method of slices Shields	Computer Program Hanna & Foriero	Proposed Theory
1	dense homogeneous	390	400	341	399.8	----
2	medium homogeneous	340	336	280	354.7	----
3	loose homogeneous	220	230	207	210.1	----
4	dense / medium	350	360.9	345	----	346.6
5	dense / loose	300	333.27	265	----	220
6	medium / loose	290	304.5	240	----	215
7	loose / medium	230	----	226.3	229.3	210.1
8	medium / dense	345	----	338.6	378.8	340
9	loose / dense	250	----	256	247.7	210.1

Table 4.13a: Passive earth pressures (lbs)

Test No.	Material	Present Test Results	Logarithmic Spiral Terzaghi	Method of slices Shields	Computer Program Hanna & Foriero	Proposed Theory
1	dense homogeneous	24.48	25.11	21.4	25.1	----
2	medium homogeneous	21.76	21.5	17.92	22.7	----
3	loose homogeneous	13.8	15.11	13.6	13.8	----
4	dense / medium	21.97	22.66	21.66	----	21.76
5	dense / loose	18.83	20.92	16.64	----	13.8
6	medium / loose	20.95	19.49	15.36	----	13.8
7	loose / medium	15.11	----	14.86	15.06	13.8
8	medium / dense	22.08	----	21.67	24.24	21.76
9	loose / dense	16.42	----	16.81	16.27	13.8

Table 4.13b: Coefficients of passive earth pressures

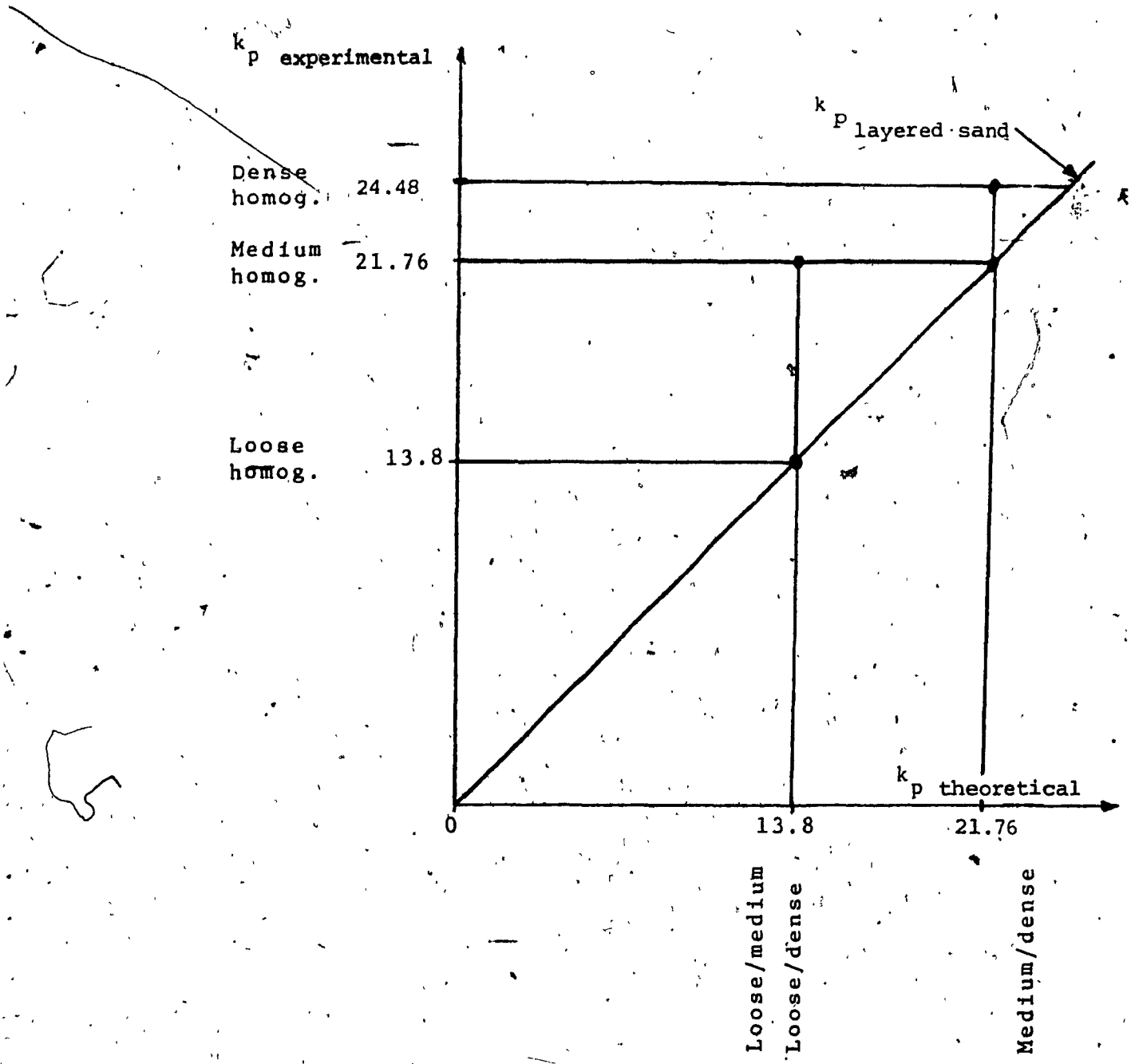

Figure 4.5a: k_p experimental vs. k_p theoretical for weak/strong sand layers

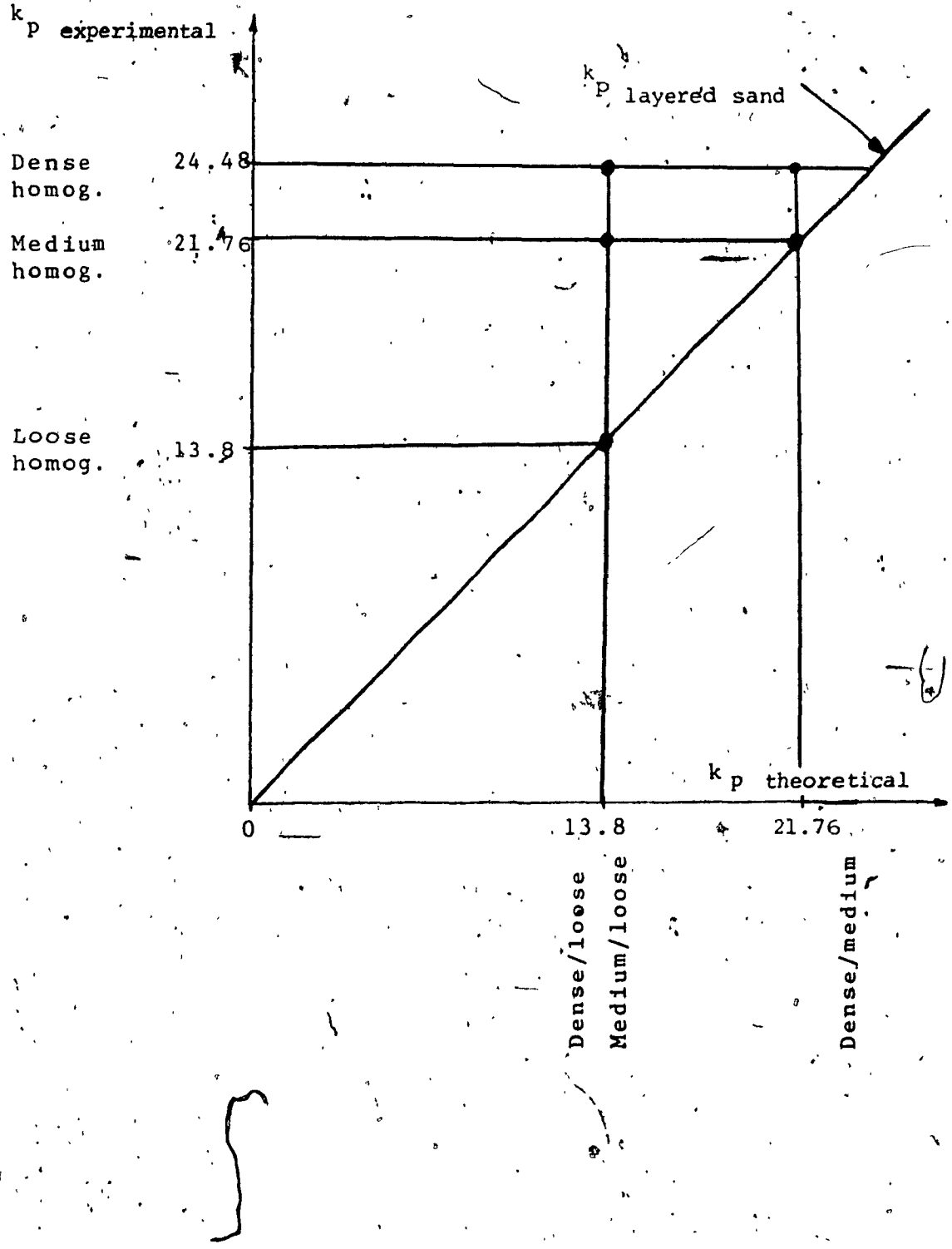

Figure 4.5b: k_p experimental vs. k_p theoretical for strong/weak sand layers

In order to use the proposed theory, Tables 4.5a and 4.5b should be used for the layered soils conditions.

For a weak layer overlying a strong layer of sand, from Table 4.5a, under k_p theoretical, the value of k_p should be chosen such as to correspond to the value of k_p homogeneous of the weak layer. As an example, for a loose layer overlying a dense layer of sand, the value of $k_p = 13.8$ from the k_p theoretical values should be chosen (presently in practice the same value of $k_p = 13.8$ would be used).

For a strong layer overlying a weak layer of sand, from Table 4.5b, under k_p theoretical, the value of k_p should be chosen such as to correspond to the value of k_p homogeneous of the weak layer. As an example, for a dense layer overlying a medium layer of sand, the value $k_p = 21.76$ from the k_p theoretical values should be chosen (presently in practice the value of $k_p = 24.48$ from the k_p experimental values would be used).

4.4 Discussion

From Table 4.13a the passive earth pressures exerted on the model retaining wall can be compared for the same types of soil configurations (i.e. homogeneous, strong overlying weak sand and weak overlying strong sand) according to the different methods of analysis used.

The results show that for the homogeneous sand the logarithmic spiral method and the computer program provided the best results while the method of slices resulted in lower values.

For the strong overlying weak sand the results are mixed, but again the logarithmic spiral resulted in the closest values to the actual passive earth pressures measured during the tests. For this type of soil configuration, the computer program could not be used due to a restriction in the value of the angle of friction of sand against the wall which should not be greater than the angle of internal friction of the sand.

For the case of weak overlying strong sand, the analytical results agreed very well with the test results. In this case the logarithmic spiral method could not be used due to the actual failure planes observed during the test and which showed that the failure plane occurred at the intersection of the two sand layers and was continued with an oblique plane through the upper layer.

In general, the method of slices provided lower values for the passive earth pressures than the logarithmic spiral method and than the computer program method. The reason should be due to the limitations imposed on the construction of the spiral that represents the failure plane; only one such spiral can be constructed and in actual conditions it is not possible to obtain a perfect spiral. Due to pockets of nonhomogeneity even in homogeneous soil, the actual failure plane may deviate and the best fitting curve to represent the real failure plane will be another spiral with a larger angle.

Although the proposed theory seems to be on the lower side when compared to the actual test results it results in very close values to

the method of slices results which is a recognized method for calculating the coefficients of passive earth pressures and passive earth pressures.

CHAPTER 5

CONCLUSIONS

The conclusions drawn from the present test study help establish a formula for obtaining the passive earth pressure behind a retaining wall when layered soil conditions exist behind the wall. We recommend that for a layered soil condition behind the wall the value of the passive earth pressure should be calculated on the basis of the following equality:

$$K_{p,\ \text{layered soil}} = K_{p\ \text{weaker layer}} \qquad 5.1$$

During the experimental work it was observed that for layered sands the passive earth pressure exerted on a retaining wall depends on the properties of the weaker layer of sand.

For the case of a weak layer overlying a strong layer of sand, after applying a force to the retaining wall, a phenomenon of horizontal compaction in the direction of the applied force occurs in the weaker (upper) layer and it was observed that the failure plane occurs at the interface between the weak and the strong layer finishing in an oblique plane through the weak (upper) layer.

For the case of the strong layer overlying a weak layer of sand, after applying a force to the retaining wall, a phenomenon of vertical compaction in a direction perpendicular to the direction of the applied force occurs in the weak (lower) layer and it was observed that the

failure plane is similar to the one occurring in homogeneous sand.

It is recommended that additional work be performed on determining the passive earth pressures behind retaining walls for the condition of a strong overlying a weak layer of sand, as the behaviour of the weak layer (vertical compaction and horizontal shear at the same time) is very complex and a three-dimensional analysis of this subject should be attempted.

For the homogeneous cases, any of the already existing theories of mass approval should be used as they are close in values.

REFERENCES

1 - Afram, A. (1984). "Pullout Capacity of Battered Piles in Sand", M. Engr. Thesis, Concordia University, Montreal, Canada.

2 - Bauer, E.G. (1970). "A Historical Review of the Determination of Earth Pressures on Retaining Structures".

3 - Belidore, B.F., 1729. "La Science des Ingénieurs." Paris, (1st edition), 1813 ed. edited by Navier.

4 - Bishop, A.W., "The use of the Slip Circle in the Stability Analysis of Slopes," Geotechnique, London, England, Vol. 5, No. 1, Mar., 1955, pp. 7-18.

5 - Caquot, A., and Kerisel, J., "Tables for the Calculation of Passive Pressure, Active Pressure and Bearing Capacity of Foundations, Gauthier-Villars, Paris, France, 1948.

6 - Casbarian, A.O.P. (1967). "Ultimate Lateral Resistance of Anchor Plates in Cohesionless Soils", Third Pan-American Conf. on Soil Mech. and Found., Caracus, Venezuela, Vol. II, Div. 4.

7 - Chen, W.F. (1975), "Limit Analysis and Soil Plasticity", Elsevier Scientific Publishing Company, New York, N.Y. pp. 341-398.

8 - Coulomb, C.A., 1776. "Essai sur une Application des Règles des Maximis et Minimis à quelques Problèmes de Statique", Mémoire Académie Royale des Sciences, 7, Paris.

9 - Fellenius, W., 1927. "Erdstatische Berechnungen mit Reigung und Koheasion und unter Annahme Kreiszylindrischer Gleitflaechen": Wilh. Ernst, Berlin.

10 - Gauthey, E.M., 1816. "Oeuvres". Published by Navier, Traité des la Construction des Ponts. 1:1809-1818, Paris.

11 - Graham, J., "Calculation of Passive Pressure in Sand," Canadian Geotechnical Journal, Vol. 8, No. 4, Nov., 1971, pp. 566-579.

12 - Hannah, A.M. and Foriero, A. (1986), "Pullout Capacity of Continuous Anchor Plates".

13 - Hansen, J, Brinch. 1953. "Earth pressure calculation". The Danish Technical Press, Copenhagen.

14 - James, R.G., and Bransby, P.L., "Experimental and Theoretical Investigations of a Passive Earth Problem," Geotechnique, London, England, Vol. 20, No. 1, Mar., 1970, pp. 17-38.

15 - Janbu, N., "Earth Pressure and Bearing Capacity Calculations by Generalized Procedure of Slices," Proceedings of the 4th International Conference, International Society of Soil Mechanics and Foundation Engineering, Vol. 2, 1957, pp. 207-213.

16 - Kostyukov, V.D. (1967). "Distribution of the Density of Sand in the Sliding Wedge in Front of Anchor Plates", Soil Mech. and Found. Engr., No. 1, pp. 12-13.

17 - Mayniel, E., 1808. "Traité Expérimental, Analytique et Pratique de la Poussée des Terres et Murs de Revêtement". p. 316, Paris.

18 - Mises, R. von, 1913. "Mechanik der festen Körper im plastisch-deformablen Zustand". Nachr. Ges. d. Wiss. zu Goettingen.

19 - Müller-Breslau, H., 1906. "Erddruck auf Stuetzmauern". Berlin, 159 pp.

20 - Nadai, A., 1928. "Plasticitaet und Erddruck". Handbuch der Physik. VI, Ch. 6.

21 - Odquist, F., 1934. "Plasticitetsteori med Tillampningar. Ingeniør vetenskapsakademien", Stockholm.

22 - Ohde, J., 1938. "Zur Theorie des Erddruckes unter besdonderer Berücksichtigung der Erddruckverteilung". Die Bautechnik 16, No. 10/11, 13, 19, 35, 37, 42, 53/54.

23 - Peck, R.B., 1969. "Deep excavation and tunneling in soft ground". Proc. Int. Conf. on Soil Mech. and Fdn. Eng., Vol:III

24 - Prandtl, L., 1920. "Ueber die Haerte plastischer Koerper". Nachr. der Ges. der Wiss., Goettingen.

25 - Rankine, W.J.M., 1857. "On the stability of loose earth". Trans. Royal Soc., London, Vol. 147.

26 - Rendulic, L., 1935. "Ein Beitrag zur Bestimmung der Gleitsicherheit". Bauingenieur, Heft 19/20.

27 - Shields, D.H., and Tolunay, A.Z., "Passive Pressure Coefficients for Sand by the Terzaghi and Peck Method," Canadian Geotechnical Journal, Vol. 9, No. 4, Nov., 1972.

28 - Shields, D.H., and Tolunay, A.Z., "Passive Pressure Coefficients by the Method of Slices", Journal of the Soil Mechanics and Foundations Division, Dec. 1973.

29 - Terzaghi, K., and Peck, R.B., "Soil Mechanics in Engineering Practice, 2nd ed., John Wiley and Sons, Inc., New York, N.Y., 1967, pp. 212-217.

30 - Terzaghi, K. (1948). "Theoretical Soil Mechanics in Engineering Practice", Wiley, New York.

31 - Tschebotarioff, G.D. (1973). "Foundations, Retaining and Earth Structures - Second Edition", pp. 536-542.

32 - Vernant, B. de Saint, 1870. "Comptes Rendus". 70, 73, 74, Gauthier-Villard, Paris.

APPENDIX

```
      PROGRAM THE4
      SYSTEM INTRINSIC RAND1
      INTEGER Z
      REAL X(3),B(3),M,P,L(3),R
      REAL N(3),AU(3),A(3)
      PI=3.1415927
      ALPHA=90.0
9.01  DISPLAY 'PHY='
8.1   ACCEPT PHY
10    D=0.0
11    H=0.50
11.1  DISPLAY 'DELTA='
12    ACCEPT DELTA
13    DO 78 IB=1,20
14    F=1.5
15    DO 1 I=1,3
16    B(I)=0.0
17    A(I)=45.0
18 1  N(I)=90.0
19    M=0.78
20    DO 19 J=1,12
21    Z=30
22    DO 3 II=1,2
23    DO 4 K=1,3
24    IF (A(K)-N(K)/F+J.LT.B(K)) GO TO 50
25    GO TO 60
26 50 L(K)=B(K)
27    GO TO 65
28 60 L(K)=A(K)-N(K)/F+J
29 65 IF (A(K)+N(K)/F+J.ST.N(K)) GO TO 90
30    GO TO 90
31 90 AU(K)=N(K)-L(K)
32    GO TO 100
33 90 AU(K)=A(K)+N(K)/F+J-L(K)
34 100 CONTINUE
34.1  DO 107 IW=1,20000
34.2 107 CONTINUE
35    ZZZ=RAND1
36    YYY=RAND(ZZZ)
37    X(K)=L(K)+YYY*AU(K)
38 4  CONTINUE
39    R1=ALPHA+X(2)-X(1)
40    R2=PHY+X(2)+ALPHA
41    R3=X(3)+2*PHY+ALPHA-X(1)
42    R4=D+H*SIN(ALPHA*PI/180.0)
43    R5=H*SIN(X(1)*PI/180.0)+SIN(X(2)*PI/180.0)
44    R6=SIN(R1*PI/180.0)
45    IF((R4-R5/R6).LE.0.0) GO TO 3
46    IF ((PHY+X(2)).LE.(90.0-ALPHA)) GO TO 3
47    IF (X(2).GE.X(3)) GO TO 3
48    IF (SIN(R1*PI/180.0).GE.0.999) GO TO 3
49    IF (SIN(R1*PI/180.0).LE.0.001) GO TO 3
50    IF (SIN(R2*PI/180.0).GE.0.999) GO TO 3
51    IF (SIN(R2*PI/180.0).LE.0.001) GO TO 3
52    IF (SIN(R3*PI/180.0).GE.0.999) GO TO 3
53    IF (SIN(R3*PI/180.0).LE.0.001) GO TO 3
53.01 IF (ABS(TAN(DELTA*PI/180.0)/TAN(R2*PI/180.0)+1.0).LE.0.001)
53.02 *GO TO 3
53.1  CALL FCN(PI,ALPHA,PHY,D,H,DELTA,X,P)
54    IF (P.LE.0.0) GO TO 3
55    IF (P.LT.M) GOTO 200
56    GO TO 3
57 200 CONTINUE
58    M=P
59    DO 11 I=1,3
60    A(I)=X(I)
61 11 CONTINUE
62 3  CONTINUE
63 19 CONTINUE
64    WRITE(6,300) M
65 300 FORMAT(1H,E20.8)
66    WRITE(6,302) A(1),A(2),A(3)
67 302 FORMAT(1H,3F16.7)
68 78 CONTINUE
69    STOP
70    END
```